

**Molecular Determinants and Consequences of Specificity in  
Histone 2A Ubiquitination**

Michael Uckelmann

ISBN: 978-90-75575-48-4

Publisher: Het Nederlands Kanker Instituut - Antoni van Leeuwenhoek Ziekenhuis

Printing: Gildeprint

Layout and cover design: Michael Uckelmann (cover modified from PDB entry 1KX5)

Copyright © 2017 Michael Uckelmann. All rights reserved.

The research described here was supported by KWF (Koningin Wilhelmina Fonds), NWO (Nederlandse Organisatie voor de Wetenschappelijk Onderzoek) and the ERC (European Research Council)

**Molecular Determinants and Consequences of Specificity in Histone  
2A Ubiquitination**

Moleculaire determinanten en gevolgen van specificiteit bij de ubiquitinatie  
van histone 2A

Proefschrift

ter verkrijging van de graad van doctor aan de  
Erasmus Universiteit Rotterdam  
op gezag van de  
rector magnificus

Prof.dr. H.A.P. Pols

en volgens besluit van het College voor Promoties.  
De openbare verdediging zal plaatsvinden op

Wednesday 7 Februari 2018 om 11:30

door

Michael Uckelmann  
geboren te Rheda-Wiedenbrück, Duitsland

**Promotiecommissie:**

**Promotor:** Prof.dr. T.K. Sixma

**Overige leden:** Prof.dr. C.P. Verrijzer

Prof.dr. J. Jonkers

Dr.ir. J.A.F. Marteiijn

**Copromotor** Prof.dr. W. Vermeulen



## Table of contents

<b>Chapter 1</b>	General introduction	7
<b>Chapter 2</b>	Histone ubiquitination in the DNA damage response	27
<b>Chapter 3</b>	USP48 restrains resection by site specific cleavage of the BRCA1 ubiquitin mark from H2A	53
<b>Chapter 4</b>	The nucleosome acidic patch plays a critical role in RNF168-dependent ubiquitination of H2A	89
<b>Chapter 5</b>	Strategies to stabilize RING E3 ligase-target complexes for structural analysis	113
<b>Chapter 6</b>	General discussion	129
<b>Addendum</b>	Summary	140
	Samenvatting	141
	Curriculum vitae	143
	PhD portfolio	144
	List of publications	145
	Acknowledgements	146



# Chapter 1

## General introduction

## General background

The genomic integrity of a cell is constantly challenged by environmental and endogenous factors. High energy radiation, endogenous free radicals and replication stress are common causes of DNA damage that result in a wide variety of lesions that need to be repaired<sup>1</sup>. Double strand breaks (DSBs) are among the most toxic of possible lesions and faithful repair is crucial for cellular survival and protection from disease, in particular from cancer<sup>1,2</sup>. Two major pathways (and sub-pathways therein) are responsible for the repair of DSBs, homologous recombination (HR), commonly thought of as error-free, and error-prone non-homologous end joining. Repair by homologous recombination mechanisms are preferred in late S- and G2-phase where a sister chromatid is present and gene conversion (GC), one of the HR-mechanisms, is the most accurate form of DNA damage repair<sup>3</sup>.

The balance between the pathways needs to be tightly controlled to maintain genomic stability and the pathway choice needs to be made with respect to the given situation<sup>3-5</sup>. One important factor in initiating DNA repair and determining repair pathway choice are chromatin modifications, in particular posttranslational modifications (PTM) of histones<sup>6</sup>.

Whereas the genomic code is inherently static and protected from change, the chromatin itself, the complex of histone proteins and DNA, is inherently dynamic, constantly remodeled, with the histones acting as molecular signposts to guide and control chromatin biology. Histones can get modified by a variety of PTMs such as phosphorylation, acetylation, ubiquitination or methylation, among many more, and their functional consequences are just as diverse<sup>7</sup>. The importance of histone modification in the response to DNA DSBs is well established<sup>1,8,9</sup> though the exact molecular details and mechanisms of signaling are not very well understood for most of these PTMs. The newly emerging paradigm of crosstalk between histone modification, where signals are integrated over several different PTMs, adds another layer of complexity to the field<sup>9-11</sup>. Site specific ubiquitination of histone H2A has in recent years emerged as one of the central PTMs regulating the DNA damage response. The molecular determinants for site-specific ubiquitination and deubiquitination of H2A are the subject of this thesis.

## Ubiquitination

Ubiquitination, the modification of a target protein lysine with ubiquitin, a small 76 amino acid protein, is a major regulatory PTM in eukaryotes. Three classes of enzymes are involved in protein ubiquitination reactions: ubiquitin activating enzymes (E1), ubiquitin conjugating enzymes (E2) and ubiquitin ligases (E3). The E1 activates the ubiquitin C-terminus in an ATP dependent step and transfers the activated ubiquitin to its active site cysteine. Ubiquitin is

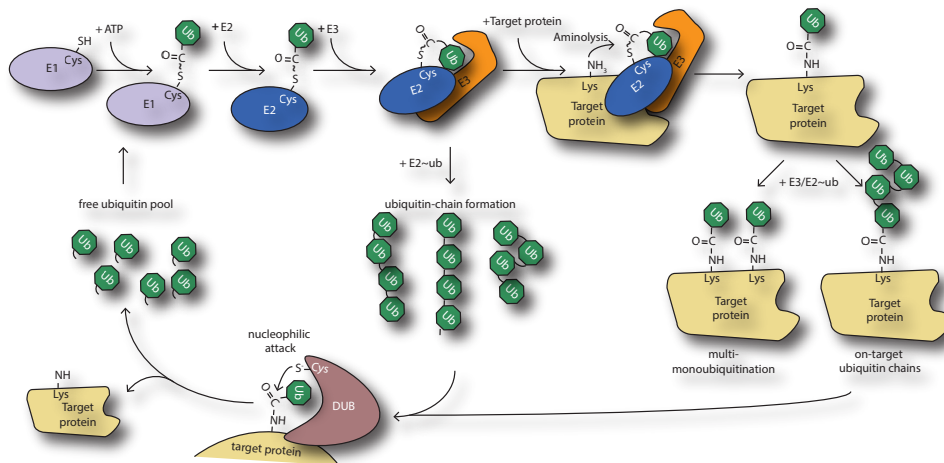


**Figure 1:** Overview of the RING E3 ligase ubiquitination system. The E1 transfers activated ubiquitin to the E2 active site. The E2 is bound by the E3 to stabilize a conformation prone to aminolysis. At the same time the E3 will specifically bind the target protein to orient the E2 towards the target lysine to allow ubiquitin conjugation to take place. Products of this reaction can be ubiquitin chains of different linkage types, monoubiquitinated target proteins or target proteins modified with ubiquitin chains. Ubiquitinated substrates can be cleaved by deubiquitinating enzymes to regenerate the free ubiquitin pool.

then transferred to the E2 active site cysteine and eventually the E3 catalyzes the isopeptide bond formation with the target protein lysine (Figure 1)<sup>12</sup>. This can lead to monoubiquitination of a target protein or the formation of ubiquitin chains by conjugating one ubiquitin to one of the 7 lysine residues, or the N-terminus, of another ubiquitin. These chains can be linkage specific (e.g. only linked via lysine 48 of ubiquitin) or they can consist of mixed linkages, they can be free or attached to a target protein<sup>13</sup>.

The diversity of possible ubiquitin based signaling entities allows for a great variety of different biological responses directed by this one signaling molecule. Different chains are involved in different cellular processes<sup>13</sup>. The most prominent example are K48-linked chains that are attached to target proteins and mark them for proteasomal degradation. K63-linked chains are involved in non-proteolytic signaling networks, for example in the DNA damage response. Monoubiquitination of specific lysine residues on different proteins is part of many different signaling cascades. The role of H2A monoubiquitination and K63-linked chains in the DNA damage response will be discussed in detail in chapter 2.

### Specificity in ubiquitin signaling

Given the complexity of the ubiquitin signaling network, ubiquitination reactions need to have a certain degree of specificity to make sure only the desired signaling output is achieved and to prevent short-circuiting the cell. Specificity in the conjugation reaction is provided by the E3 ligases.

## E3 ligases

E3 ligases exert a dual function, they select the right target and promote catalysis. There are three classes of E3 ligases, HECT, RING between RING (RBR) and RING E3 ligases. HECT and RBR E3 ligases transfer ubiquitin to the target lysine via their active site cysteine, forming a thioester intermediate with the C-terminus of ubiquitin. RING E3 ligases lack an active site. They exert their function by facilitating the ubiquitin transfer directly from the E2 to the target lysine. This is achieved by stabilizing the otherwise flexible<sup>14</sup> ubiquitin-charged E2 in a certain conformation that renders the active site thioester prone to aminolysis<sup>15–17</sup>. The RING domain of the E3 interacts with a hydrophobic patch on ubiquitin, locking its conformation perched against a central alpha helix on the E2. The C-terminal tail of ubiquitin is embedded in a channel leading to the E2 active site. This orients and immobilizes the thioester linkage in a position in which the target lysine can attack, which leads to increased catalytic rates<sup>15–18</sup>. The E3 mediated conformational selection leads to correct positioning of flanking residues with respect to the thioester and the target lysine, including residues that are crucial for activity such as aspartic acid 117 and asparagine 77 (in UBE2D3)<sup>15,16,19,20</sup>. Apart from promoting catalysis the RING E3 interacts with the target protein in order to place the E2 active site in close vicinity to the target lysine<sup>21,22</sup>.

Ubiquitin conjugation catalyzed by RING E3 ligases formally follows a bisubstrate kinetic mechanism<sup>21</sup> where the charged E2 is one substrate and the target protein the other. Structures of E3-E2 complexes have been very informative in establishing the mechanism of thioester activation and conformational selection<sup>15–17</sup>, which seems to be a shared mechanism among all RING E3 ligases<sup>23</sup>. The recognition of target proteins on the other hand is less well understood and mechanisms seem to be more diverse. Target recognition can follow very general patterns. San1, for example, is an E3 ligase that recognizes exposed hydrophobic stretches in misfolded target proteins via its own disordered domains and marks them for degradation<sup>24</sup>.

Cullin-RING ligases are more specialized. They recognize their targets through degron motifs, short sequence motifs that serve as a recognition signal for the E3 which will then ubiquitinate target proteins in a defined 'ubiquitination zone', marking them for proteasomal degradation<sup>25–29</sup>. Posttranslational modification of the degron is often necessary for recognition by the E3 ligase<sup>30–32</sup>. The propensity of some E3 ligase to form homo- and heterodimers can extend the range of substrates by employing two degrons for recognition<sup>29,33</sup>. Enzymes of the N-end rule pathway use a ubiquitin recognin- (UBR-) domain to specifically bind N-terminal arginine residues<sup>34,35</sup>.

Other E3s select specific lysine residues on defined target proteins for ubiquitination. Through protein-protein interaction with the target protein they orient the E2 active site

towards the target lysine, thus restricting ubiquitination to one, or a group of, specific lysines<sup>22,36</sup>. In chapter 4 of this thesis we show that the target protein itself can play an active role in promoting site-specific ubiquitination. The nucleosome, the target of the RING E3 ligase RNF168, contributes to the reaction by activating RNF168 catalyzed ubiquitin discharge from the E2 to the target lysine through an acidic patch on the nucleosome surface<sup>37</sup>.

Ubiquitination of nucleosomes, more specifically ubiquitination of histone H2A, is a remarkable example of lysine specificity of E3 ligases. Three distinct ubiquitination sites on H2A are ubiquitinated specifically by three different E3 ligases. Lysine 118/119 is ubiquitinated by RING1B (RNF2) in a PRC1 complex<sup>38</sup>, lysine 13/15 by RNF168<sup>39,40</sup> and lysine 125/127/129 by BRCA1/BARD1<sup>41</sup>. Ubiquitination of these sites has distinct biological outcomes and a detailed discussion on specific H2A ubiquitination follows in chapter 2.

A structure of a RING1B/BMI1-E2 fusion construct in complex with a nucleosome core particle (NCP)<sup>22</sup> explains the specificity of RING1B for lysine 119. The E2-E3 complex makes contacts with the nucleosomal acidic patch and DNA to orient the E2 active site towards K119. These specific E2-E3-target interactions are a common theme in lysine selection in the ubiquitin and ubiquitin-like systems. PCNA can be sumoylated on lysine 164. The E3 Siz1 is responsible for specificity by forcing a complex conformation that only allows K164 to be ubiquitinated<sup>36</sup>. CULLIN1 gets neddylated at lysine 720 by the E3 ligase RBX1. Again specific E2-E3-target interaction guides lysine selection. Additionally, the UBL itself contributes by interacting with residues on RBX1. These residues act as a 'pivot' and 'lever' to translate UBL-E3 interaction to a conformation of the E2-E3 complex on the target that favors specific neddylation of lysine 720<sup>42</sup>.

### **Specificity of deubiquitinating enzymes**

Ubiquitination can be reversed, or cleaved off, by deubiquitinating enzymes (DUBs). There are about 100 DUBs encoded in the human genome<sup>43</sup> and all are members of one of six families of isopeptidases. Ubiquitin specific protease (USP), Ubiquitin C-terminal hydrolase (UCH), Ovarian Tumor protease (OTU), Machado Joseph Disease protease (MJD) and the newly discovered motif interacting with Ub-containing novel DUB (MINDY)<sup>44</sup> family are all families of cysteine proteases whereas the Jab1/Mov34/Mpn protease (JAMM) family members are metalloproteases. All of these DUB families have evolved to cleave ubiquitinated substrates. The USP family is the biggest of these DUB families<sup>43</sup>.

USPs are cysteine proteases that cleave isopeptide linkages through a nucleophilic attack on the isopeptide bond catalyzed by three, sometimes two, active site residues. The active site histidine, coordinated by an aspartate or asparagine residue, lowers the pKa of the catalytic

cysteine, allowing the nucleophilic attack<sup>45</sup>.

The degree of lysine-specificity of DUBs varies between families and within the same family<sup>46</sup>. Some DUBs are specific for a certain linkage type of polyubiquitin chains. The members of the OTU family show a remarkable variety in their specificity for different linkage types, with different family members cleaving certain linkage types exclusively<sup>47</sup>. Most JAMM proteases seem to cleave K63-linked chains<sup>48–50</sup>. MINDY-1 has been shown to be specific for longer K48-linked chains<sup>44</sup>, which it recognizes via a ubiquitin binding domain<sup>51</sup>.

In contrast, USPs show very little linkage specificity<sup>48,52</sup>, with the exception of the K63 and M1 specific CYLD<sup>53–55</sup>. Rather than cleaving chains of a specific linkage type, USPs can cleave monoubiquitination and polyubiquitin chains off target proteins and disassemble polyubiquitin chains without apparent linkage specificity. Regulation of these DUBs is likely achieved through inter- and intramolecular mechanisms that regulate localization and restrict activity<sup>56</sup>. It should be stressed that studies on linkage specificity so far have only been done using di-ubiquitin substrates and these di-ubiquitins do not necessarily resemble the geometry of longer chains. It remains possible that USPs recognize features only conserved in longer chains and only retain their linkage selectivity on chains of a certain length.

USPs can be specific for defined monoubiquitination sites on their target proteins. USP1 cleaves monoubiquitinated PCNA<sup>57</sup> and FANCD2<sup>58</sup>. USP22 (Ubp8 in yeast), the DUB module of the SAGA complex, deubiquitinates lysine 120 (lysine 123 in yeast) on histone H2B<sup>59</sup>. The structure of the yeast SAGA DUB module, consisting of Ubp8 /Sgf11/Sus1 and Sgf73, in complex with the nucleosome has been solved recently<sup>60</sup>. It shows how defined interactions with the acidic patch on the nucleosome aid lysine selection by positioning the DUB towards K123.

Given the exclusive specificity of the E3 ligases acting on H2A it seemed reasonable to assume that there are equally specific DUBs removing ubiquitin from the three different H2A ubiquitination sites. USP3<sup>61</sup>, USP16<sup>62</sup>, USP44<sup>63</sup>, USP51<sup>64</sup>, USP11<sup>65</sup> and BAP1/ASXL1<sup>66,67</sup> have all been proposed to deubiquitinate H2A. However, none of these enzymes has been shown to be exclusively specific for one site. In chapter 3 we test a subset of DUBs for site specificity on ubiquitinated H2A. We identify USP48, a previously little studied DUB, to be specific for the BRCA1/BARD1 catalyzed ubiquitination of H2A.

### **Specific ubiquitination and deubiquitination in cancer**

Due to its diverse role in many different regulatory pathways the ubiquitin system is connected to a variety of malignancies. With respect to cancer it can regulate both tumor suppressors and oncogenes<sup>68</sup>. Misregulation of tumor suppressors and oncogenes can lead to sus-



tained proliferative signaling, evasion of growth suppressors, the ability to resist cell death and genomic instability, processes considered to be among the hallmarks of cancer<sup>69</sup>. The role of the ubiquitin system in cancer development and treatment has been reviewed extensively elsewhere (e.g.<sup>68,70,71</sup>). Here we focus on selected examples of oncogenic or tumor suppressive mechanisms where specific E3-substrate or DUB-substrate pairs are key to tumorigenesis and as such present possible targets for therapeutic intervention. The examples discussed are limited to DNA repair and cell cycle regulation.

The anaphase promoting complex/cyclosome (APC/C) and S-phase kinase-associated protein 1 (SKP1)–CUL1–F-box protein (SCF) complex are multi-protein complexes of the cullin-RING ligase family that utilize substrate adapters to gain specificity. The APC/C regulates ordered progression in the cell cycle through ubiquitin mediated degradation of Securin (PTTG1), Shugoshin 1 (SGO1) and G2/mitotic-specific cyclin-B1 (Cyclin B). Degradation of Securin and Shugoshin 1 triggers anaphase and degradation of cyclin B regulates the exit from mitosis<sup>72,73</sup>. A dysfunctional APC/C complex will lead to accumulation of its target proteins, a defective cell cycle progression and ultimately genomic instability<sup>74,75</sup>. On the other hand, a prematurely activated APC/C will lead to early degradation of its substrates and premature entry into mitosis, which can lead to aneuploidy<sup>76</sup>. The APC/C furthermore affects genome stability via regulation of the DNA damage response through ubiquitinating its substrates CtIP (RBBP8)<sup>77</sup>, Claspin<sup>78</sup>, USP1<sup>79</sup> and RAD17<sup>80</sup>.

SCF complexes are also implicated in various oncogenic mechanisms. The SCF complex utilizing SKP2 as a substrate adapter (SCF<sup>SKP2</sup>) ubiquitinates the tumor suppressor p27 and marks it for degradation<sup>81–83</sup>. Several other tumor suppressors have also been identified to be SKP2 targets<sup>84</sup>. By degrading a wide array of tumor suppressors, SCF<sup>SKP2</sup> can act as an oncogene and SCF<sup>SKP2</sup> overexpression promotes tumor growth in different model systems<sup>84</sup>. In combination with a different substrate adapter, FBW7 (FBXW7), the SCF complex marks targets for degradation that positively regulate cell cycle progression<sup>85</sup> and as such acts as a tumor suppressor itself, showing that one E3-ligase (-complex) can have opposing functions through altering its specificity. This once again highlights the importance for regulation to assure the right proteins are degraded at the right moment. On the other hand it opens up opportunities for targeted intervention. Unique interaction of the SCF and APC adaptor proteins with their substrates could be exploited to inhibit or enhance degradation of only selected targets.

p53 (TP53) is a tumor suppressor which carries inactivating mutations in about 50 % of human cancers<sup>86</sup>. It is ubiquitinated by the E3 ligase MDM2 with the consequence that p53 and the ligase itself are targeted for degradation by the proteasome<sup>87–91</sup>. Based on this mechanism, overexpression or amplification of MDM2 can be a means for cancer cells to

evade growth regulation<sup>92</sup>. Given the specificity of the MDM2-p53 interaction, MDM2 is an interesting drug target, following the rationale that inhibiting MDM2 driven ubiquitination would increase p53 stability and trigger apoptosis in tumor cells. The small molecule inhibitors nutlin-3a and RITA target MDM2-p53 interaction<sup>93,94</sup> and nutlin-3a has reached phase I/II clinical trials, highlighting the possible opportunities in targeting E3-target interactions.

Several E3 ligases involved in the DNA damage response are related to cancer development. FANCL is a ubiquitin ligase and part of the Fanconi Anemia (FA) core complex<sup>95</sup>. It site-specifically monoubiquitinates FANCD2 (on lysine 561) and FANCI (on lysine 523) in response to DNA damage<sup>96,97</sup>. Several mutations in FANCL have been identified as a possible causes of FA (see Fanconi Anemia Mutation Database: <http://www2.rockefeller.edu/fanconi/>), a rare disorder that causes defects in the repair of interstrand DNA crosslinks and predisposes patients to develop solid tumors and leukemia due to genomic instability<sup>95</sup>.

Germline mutations in BRCA1, an E3 ligase involved in the DNA damage response, render individuals susceptible to breast and ovarian cancer. BRCA1 dimerizes with BARD1 through its RING domain and ubiquitinates H2A to direct DNA repair pathway choice towards HR<sup>98</sup> but the importance of the E3 ligase function in tumor development is still a matter of debate<sup>11</sup>. Tumors that are impaired in BRCA1 function are, due to HR defects, exceptionally vulnerable to PARP inhibitor treatment and this synthetic lethality is exploited in cancer therapy<sup>99</sup>.

A recent study showed that a triple negative breast cancer cell line resistant to proteotoxic stress achieved this resistance through upregulation of the E3 ligase RNF168<sup>100</sup>. A consequence of proteotoxic stress is the depletion of free ubiquitin due to the overload of the ubiquitin proteasome system. Ubiquitin will be sequestered on proteins in line for degradation and will not be available for its other signaling functions, such as regulation of the DNA damage response. High levels of RNF168 can compensate, to a certain extent, by competing for the little available free ubiquitin. As a consequence DNA repair through NHEJ will proceed normally in cells with high RNF168 levels despite proteotoxic stress, conferring a survival benefit, albeit at the expense of genomic instability<sup>100</sup>. In the clinic this could be exploited in two ways. Patients treated for tumors resistant to proteasome inhibitors might benefit from additional targeting of RNF168 which could override the resistance mechanism. On the other hand tumors with high RNF168 levels effectively mimic a BRCA1 deficient phenotype, making them potentially vulnerable to PARP inhibition. This is true for at least some tumor cell lines<sup>100</sup>.

Polycomb group (PcG) proteins are important regulators of gene expression and are often involved in tumorigenesis. The PcG proteins RING1B and BMI1 form a heterodimer through their RING domains. As such they form one of the possible active E3 ligases in the polycomb

repressive complex 1 (PRC1). BMI1 was identified as an oncogene functioning together with Myc proto-oncogene<sup>101</sup> and is frequently overexpressed in cancer<sup>102</sup>. PRC1 is a transcriptional repressor that silences gene expression through ubiquitination of H2A at lysine 119. Overexpression of components of the PRC1 complex leads to misregulation of several target genes and consequently induces a variety of phenotypes promoting tumorigenesis<sup>102</sup>.

Different target specific DUBs are also involved in cancer development. BAP1 together with ASXL1 forms the PR-DUB complex that deubiquitinates H2A specifically on lysine 119<sup>66</sup>. Germline mutations in BAP1 are related to development of mesotheliomas, uveal melanomas and cutaneous melanomas<sup>103,104</sup> but to what extent deubiquitination of H2A plays a role in these malignancies is not understood<sup>105</sup>.

As mentioned before, the p53 pathway features heavily in tumorigenesis and different DUBs play a role in regulating p53 stability. USP15 deubiquitinates MDM2 and protects it from degradation. USP15 overexpression was found in a melanoma and a colorectal cancer cell line and prevents apoptosis of these cells by indirectly regulating p53 levels. By stabilizing MDM2, the E3 ligase targeting p53 for degradation, USP15 activity keeps p53 levels low, thus inhibiting apoptotic signaling<sup>106</sup>. USP7 targets both MDM2 and p53, which explains the curious observation that both, deletion and overexpression of USP7, have a stabilizing effect on p53 and promote apoptosis<sup>107–109</sup>. Overexpression would directly stabilize p53 by deubiquitinating it and deletion of USP7 would destabilize MDM2, preventing p53 ubiquitination in the first place. The physiological role of this dual function of USP7 is not fully understood. By regulating the p53 pathway both DUBs present an interesting drug target.

USP1, with its activator UAF1, targets monoubiquitination on PCNA to avoid untimely recruitment of the error-prone translesion synthesis polymerase<sup>57</sup>. It also targets FANCD2 monoubiquitination and regulates inter-strand crosslink repair<sup>58</sup>. USP1 knockout renders cells hypersensitive to cis-platin and Camptothecin<sup>110</sup>, making USP1 an interesting target in cancer therapy. A selective, high affinity inhibitor has been developed for USP1/UAF1<sup>111</sup> and has been shown to sensitize cells to cisplatin<sup>112</sup>.

While lysine specific ubiquitination has a clear role in cancer development, it opens up opportunities for targeted intervention at the same time. Drugs aimed at specific ubiquitination sites can be promising and a full understanding how particular lysines are selected for ubiquitination will benefit the development of these drugs. Target sites in ubiquitin ligation reaction are selected by the E3 ligases, in deconjugation reactions by the DUBs. As such, both classes of enzymes present an interesting drug target to interfere with the ubiquitin system in a controlled manner. To understand specificity, interrogation of unique ubiquitination sites is crucial to identify which E3 ligase will ubiquitinate that particular site and which

DUB will remove the mark. When E3-target and DUB-target pairs are identified the question becomes how site specificity is achieved on a molecular level. Solving structures of E3-target complexes and DUB-target complexes to atomic resolution is essential to understand the molecular details of specificity and to identify enzyme-target interaction sites that are possibly unique for a certain complex. Once the molecular details are deciphered, informed choices can be made on how to interfere with the particular reaction. Unique interaction sites of enzyme-substrate complexes are of particular interest because they open up the possibility of therapeutic intervention aimed exclusively at this complex, thus minimizing off-target effects.

Targeting DNA repair pathways in cancer therapy is promising, as synthetic lethality can be exploited, exemplified by the efficiency of PARP inhibitors in a BRCA1-null background. Genomic instability is a hallmark of cancer and cancer cells often downregulate or shut down certain repair pathways, making them more reliable on others to prevent cell death<sup>69</sup>. Site specific ubiquitination guides and regulates several different repair pathways and knowledge of the details determining this specificity could open up opportunities for precision targeting of a certain repair pathway in a context beneficial for therapy.

Apart from the clinical relevance this thesis will help to understand basic molecular mechanisms underlying ubiquitination and deubiquitination reactions, especially with respect to target specificity of E3 ligases and DUBs and the active involvement of the target in catalysis and lysine selection.

### Outline of this thesis

**Chapter 2** provides a detailed introduction to specific ubiquitination of histone H2A in the DNA damage response with a particular emphasis on crosstalk between different histone modifications. It highlights the dynamic nature of histone modifications and propose an integrated model of DNA damage response regulation through site specific histone ubiquitination.

In **chapter 3** a set of DUBs is probed for specific deubiquitination of the three distinct H2A ubiquitination sites. USP48 is identified to be specific for the BRCA1 site and is shown to function in the DNA damage response by regulating the extent of BRCA1 induced H2A ubiquitination and thereby the extent of DNA end resection

**Chapter 4** analyzes the substrates role in an E3 ligase reaction. It shows that RNF168-catalyzed H2A ubiquitination is activated by the substrate itself through an acidic patch on the nucleosome surface.

**Chapter 5** presents different strategies to stabilize transient E3-target complexes for structural analysis. A crosslinking strategy and fusion proteins are employed to stabilize the UB-CH5C-RNF168-NCP complex.

**Chapter 6** closes with a general discussion of the results presented in this thesis and high-

lights the direction for future research.

1. Jackson, S. P. & Bartek, J. The DNA-damage response in human biology and disease. *Nature* **461**, 1071–8 (2009).
2. Malkova, A. & Haber, J. E. Mutations arising during repair of chromosome breaks. *Annu. Rev. Genet.* **46**, 455–73 (2012).
3. Ceccaldi, R., Rondinelli, B. & D’Andrea, A. D. Repair Pathway Choices and Consequences at the Double-Strand Break. *Trends in Cell Biology* **26**, 52–64 (2016).
4. San Filippo, J., Sung, P. & Klein, H. Mechanism of Eukaryotic Homologous Recombination. *Annu. Rev. Biochem.* **77**, 229–257 (2008).
5. Chapman, J. R., Taylor, M. R. G. & Boulton, S. J. Playing the End Game: DNA Double-Strand Break Repair Pathway Choice. *Molecular Cell* **47**, 497–510 (2012).
6. Dantuma, N. P. & van Attikum, H. Spatiotemporal regulation of posttranslational modifications in the DNA damage response. *EMBO J* **35**, 6–23 (2016).
7. Zhao, Y. & Garcia, B. A. Comprehensive catalog of currently documented histone modifications. *Cold Spring Harb. Perspect. Biol.* **7**, a025064 (2015).
8. Schwertman, P., Bekker-Jensen, S. & Mailand, N. Regulation of DNA double-strand break repair by ubiquitin and ubiquitin-like modifiers. *Nat Rev Mol Cell Biol* **17**, 379–394 (2016).
9. Van Attikum, H. & Gasser, S. M. Crosstalk between histone modifications during the DNA damage response. *Trends in Cell Biology* **19**, 207–217 (2009).
10. Suganuma, T. & Workman, J. L. Crosstalk among Histone Modifications. *Cell* **135**, 604–607 (2008).
11. Uckelmann, M. & Sixma, T. K. Histone ubiquitination in the DNA damage response. *DNA Repair (Amst.)*. (2017). doi:10.1016/j.dnarep.2017.06.011
12. Hochstrasser, M. Origin and function of ubiquitin-like proteins. *Nature* **458**, 422–429 (2009).
13. Komander, D. & Rape, M. The Ubiquitin Code. *Annu. Rev. Biochem.* **81**, 203–229 (2012).
14. Pruneda, J. N., Stoll, K. E., Bolton, L. J., Brzovic, P. S. & Klevit, R. E. Ubiquitin in Motion: Structural Studies of the Ubiquitin-Conjugating Enzyme Ubiquitin Conjugate. *Biochemistry* **50**, 1624–1633 (2011).
15. Plechanovová, A., Jaffray, E. G., Tatham, M. H., Naismith, J. H. & Hay, R. T. Struc-

- ture of a RING E3 ligase and ubiquitin-loaded E2 primed for catalysis. *Nature* **489**, 115–120 (2012).
16. Dou, H., Buetow, L., Sibbet, G. J., Cameron, K. & Huang, D. T. BIRC7–E2 ubiquitin conjugate structure reveals the mechanism of ubiquitin transfer by a RING dimer. *Nat. Struct. Mol. Biol.* **19**, 876–883 (2012).
  17. Pruneda, J. N. *et al.* Structure of an E3:E2-Ub Complex Reveals an Allosteric Mechanism Shared among RING/U-box Ligases. *Mol. Cell* **47**, 933–942 (2012).
  18. Berndsen, C. E. & Wolberger, C. New insights into ubiquitin E3 ligase mechanism. *Nat. Struct. Mol. Biol.* **21**, 301–307 (2014).
  19. Wu, P.-Y. *et al.* A conserved catalytic residue in the ubiquitin-conjugating enzyme family. *EMBO J.* **22**, 5241–5250 (2003).
  20. Berndsen, C. E., Wiener, R., Yu, I. W., Ringel, A. E. & Wolberger, C. A conserved asparagine has a structural role in ubiquitin-conjugating enzymes. *Nat. Chem. Biol.* **9**, 154–156 (2013).
  21. Deshaies, R. J. & Joazeiro, C. A. P. RING Domain E3 Ubiquitin Ligases. *Annu. Rev. Biochem.* **78**, 399–434 (2009).
  22. McGinty, R. K., Henrici, R. C. & Tan, S. Crystal structure of the PRC1 ubiquitylation module bound to the nucleosome. *Nature* **514**, 591–6 (2014).
  23. Zheng, N. & Shabek, N. Ubiquitin Ligases: Structure, Function, and Regulation. *Annu. Rev. Biochem.* **86**, 129–157 (2017).
  24. Rosenbaum, J. C. *et al.* Disorder Targets Misorder in Nuclear Quality Control Degradation: A Disordered Ubiquitin Ligase Directly Recognizes Its Misfolded Substrates. *Mol. Cell* **41**, 93–106 (2011).
  25. Ravid, T. & Hochstrasser, M. Diversity of degradation signals in the ubiquitin–proteasome system. *Nat. Rev. Mol. Cell Biol.* **9**, 679–689 (2008).
  26. Petroski, M. D. & Deshaies, R. J. Function and regulation of cullin–RING ubiquitin ligases. *Nat. Rev. Mol. Cell Biol.* **6**, 9–20 (2005).
  27. Petroski, M. D. & Deshaies, R. J. Context of multiubiquitin chain attachment influences the rate of Sic1 degradation. *Mol. Cell* **11**, 1435–44 (2003).
  28. Fischer, E. S. *et al.* The Molecular Basis of CRL4DDB2/CSA Ubiquitin Ligase Architecture, Targeting, and Activation. *Cell* **147**, 1024–1039 (2011).
  29. Tang, X. *et al.* Suprafacial Orientation of the SCFCdc4 Dimer Accommodates Multiple Geometries for Substrate Ubiquitination. *Cell* **129**, 1165–1176 (2007).
  30. Hao, B., Oehlmann, S., Sowa, M. E., Harper, J. W. & Pavletich, N. P. Structure of a Fbw7–Skp1–Cyclin E Complex: Multisite-Phosphorylated Substrate Recognition by

- SCF Ubiquitin Ligases. *Mol. Cell* **26**, 131–143 (2007).
31. Hao, B. *et al.* Structural Basis of the Cks1-Dependent Recognition of p27Kip1 by the SCFSkp2 Ubiquitin Ligase. *Mol. Cell* **20**, 9–19 (2005).
  32. Wu, G. *et al.* Structure of a  $\beta$ -TrCP1-Skp1- $\beta$ -Catenin Complex. *Mol. Cell* **11**, 1445–1456 (2003).
  33. Zhuang, M. *et al.* Structures of SPOP-Substrate Complexes: Insights into Molecular Architectures of BTB-Cul3 Ubiquitin Ligases. *Mol. Cell* **36**, 39–50 (2009).
  34. Matta-Camacho, E., Kozlov, G., Li, F. F. & Gehring, K. Structural basis of substrate recognition and specificity in the N-end rule pathway. *Nat. Struct. Mol. Biol.* **17**, 1182–1187 (2010).
  35. Choi, W. S. *et al.* Structural basis for the recognition of N-end rule substrates by the UBR box of ubiquitin ligases. *Nat. Struct. Mol. Biol.* **17**, 1175–1181 (2010).
  36. Streich, F. C. & Lima, C. D. Capturing a substrate in an activated RING E3/E2-SUMO complex. *Nature* **536**, 304–8 (2016).
  37. Mattioli, F., Uckelmann, M., Sahtoe, D. D., van Dijk, W. J. & Sixma, T. K. The nucleosome acidic patch plays a critical role in RNF168-dependent ubiquitination of histone H2A. *Nat. Commun.* **5**, 3291 (2014).
  38. Wang, H. *et al.* Role of histone H2A ubiquitination in Polycomb silencing. *Nature* **431**, 873–8 (2004).
  39. Mattioli, F. *et al.* RNF168 ubiquitinates K13-15 on H2A/H2AX to drive DNA damage signaling. *Cell* **150**, 1182–1195 (2012).
  40. Gatti, M. *et al.* A novel ubiquitin mark at the N-terminal tail of histone H2As targeted by RNF168 ubiquitin ligase. *Cell Cycle* **11**, 2538–2544 (2012).
  41. Kalb, R., Mallery, D. L., Larkin, C., Huang, J. T. J. & Hiom, K. BRCA1 is a histone-H2A-specific ubiquitin ligase. *Cell Rep.* **8**, 999–1005 (2014).
  42. Scott, D. C. *et al.* Structure of a RING E3 trapped in action reveals ligation mechanism for the ubiquitin-like protein NEDD8. *Cell* **157**, 1671–84 (2014).
  43. Clague, M. J. *et al.* Deubiquitylases From Genes to Organism. *Physiol. Rev.* **93**, (2013).
  44. Abdul Rehman, S. A. *et al.* MINDY-1 Is a Member of an Evolutionarily Conserved and Structurally Distinct New Family of Deubiquitinating Enzymes. *Mol. Cell* **63**, 146–155 (2016).
  45. Komander, D., Clague, M. J. & Urbé, S. Breaking the chains: structure and function of the deubiquitinases. *Nat. Rev. Mol. Cell Biol.* **10**, 550–563 (2009).

46. Mevissen, T. E. T. & Komander, D. Mechanisms of Deubiquitinase Specificity and Regulation. *Annu. Rev. Biochem.* **86**, 159–192 (2017).
47. Mevissen, T. E. T. *et al.* OTU Deubiquitinases Reveal Mechanisms of Linkage Specificity and Enable Ubiquitin Chain Restriction Analysis. *Cell* **154**, 169–184 (2013).
48. Ritorto, M. S. *et al.* Screening of DUB activity and specificity by MALDI-TOF mass spectrometry. *Nat. Commun.* **5**, 4763 (2014).
49. Cooper, E. M. *et al.* K63-specific deubiquitination by two JAMM/MPN+ complexes: BRISC-associated Brcc36 and proteasomal Poh1. *EMBO J.* **28**, 621–631 (2009).
50. Sato, Y., Yoshikawa, A., Yamashita, M., Yamagata, A. & Fukai, S. Structural basis for specific recognition of Lys 63-linked polyubiquitin chains by NZF domains of TAB2 and TAB3. *EMBO J.* **28**, 3903–3909 (2009).
51. Kristariyanto, Y. A., Abdul Rehman, S. A., Weidlich, S., Knebel, A. & Kulathu, Y. A single MIU motif of MINDY-1 recognizes K48-linked polyubiquitin chains. *EMBO Rep.* **18**, 392–402 (2017).
52. Faesen, A. C. *et al.* The Differential Modulation of USP Activity by Internal Regulatory Domains, Interactors and Eight Ubiquitin Chain Types. *Chem. Biol.* **18**, 1550–1561 (2011).
53. Sato, Y. *et al.* Structures of CYLD USP with Met1- or Lys63-linked diubiquitin reveal mechanisms for dual specificity. *Nat. Struct. Mol. Biol.* **22**, 222–229 (2015).
54. Komander, D. *et al.* The Structure of the CYLD USP Domain Explains Its Specificity for Lys63-Linked Polyubiquitin and Reveals a B Box Module. *Mol. Cell* **29**, 451–464 (2008).
55. Komander, D. *et al.* Molecular discrimination of structurally equivalent Lys 63-linked and linear polyubiquitin chains. *EMBO Rep.* **10**, 466–73 (2009).
56. Sahtoe, D. D. & Sixma, T. K. Layers of DUB regulation. *Trends in Biochemical Sciences* **40**, 456–467 (2015).
57. Huang, T. T. *et al.* Regulation of monoubiquitinated PCNA by DUB autocleavage. *Nat. Cell Biol.* **8**, 341–347 (2006).
58. Nijman, S. M. B. *et al.* The Deubiquitinating Enzyme USP1 Regulates the Fanconi Anemia Pathway. *Mol. Cell* **17**, 331–339 (2005).
59. Henry, K. W. *et al.* Transcriptional activation via sequential histone H2B ubiquitylation and deubiquitylation, mediated by SAGA-associated Ubp8. *Genes Dev.* **17**, 2648–2663 (2003).
60. Morgan, M. T. *et al.* Structural basis for histone H2B deubiquitination by the SAGA DUB module. *Science (80-. ).* **351**, 725–728 (2016).



61. Sharma, N. *et al.* USP3 counteracts RNF168 via deubiquitinating H2A and  $\gamma$ H2AX at lysine 13 and 15. *Cell Cycle* **13**, 106–114 (2014).
62. Joo, H.-Y. *et al.* Regulation of cell cycle progression and gene expression by H2A deubiquitination. *Nature* **449**, 1068–1072 (2007).
63. Mosbech, A., Lukas, C., Bekker-Jensen, S. & Mailand, N. The deubiquitylating enzyme USP44 counteracts the DNA double-strand break response mediated by the RNF8 and RNF168 ubiquitin ligases. *J. Biol. Chem.* **288**, 16579–16587 (2013).
64. Wang, Z. *et al.* USP51 deubiquitylates H2AK13, 15ub and regulates DNA damage response. *Genes Dev.* **30**, 946–959 (2016).
65. Yu, M. *et al.* USP11 is a negative regulator to  $\gamma$ H2AX ubiquitylation by RNF8/RNF168. *J. Biol. Chem.* **291**, 959–967 (2016).
66. Scheuermann, J. C. *et al.* Histone H2A deubiquitinase activity of the Polycomb repressive complex PR-DUB. *Nature* **465**, 243–7 (2010).
67. Sahtoe, D. D., van Dijk, W. J., Ekkebus, R., Ovaa, H. & Sixma, T. K. BAP1/ASXL1 recruitment and activation for H2A deubiquitination. *Nat. Commun.* **7**, 10292 (2016).
68. Popovic, D., Vucic, D. & Dikic, I. Ubiquitination in disease pathogenesis and treatment. *Nat. Med.* **20**, 1242–1253 (2014).
69. Hanahan, D. & Weinberg, R. A. Hallmarks of Cancer: The Next Generation. *Cell* **144**, 646–674 (2011).
70. Lipkowitz, S. & Weissman, A. M. RINGs of good and evil: RING finger ubiquitin ligases at the crossroads of tumour suppression and oncogenesis. *Nat. Rev. Cancer* **11**, 629–643 (2011).
71. Kirkin, V. & Dikic, I. Ubiquitin networks in cancer. *Curr. Opin. Genet. Dev.* **21**, 21–28 (2011).
72. Acquaviva, C. & Pines, J. The anaphase-promoting complex/cyclosome: APC/C. *J. Cell Sci.* **119**, 2401–2404 (2006).
73. Skaar, J. R. & Pagano, M. Control of cell growth by the SCF and APC/C ubiquitin ligases. *Curr. Opin. Cell Biol.* **21**, 816–24 (2009).
74. Engelbert, D., Schnerch, D., Baumgarten, A. & Wäsch, R. The ubiquitin ligase APC-Cdh1 is required to maintain genome integrity in primary human cells. *Oncogene* **27**, 907–917 (2008).
75. Kim, H.-S. *et al.* SIRT2 Maintains Genome Integrity and Suppresses Tumorigenesis through Regulating APC/C Activity. *Cancer Cell* **20**, 487–499 (2011).
76. Michel, L. S. *et al.* MAD2 haplo-insufficiency causes premature anaphase and chromosome instability in mammalian cells. *Nature* **409**, 355–359 (2001).

77. Lafranchi, L. *et al.* APC/C<sup>Cdh1</sup> controls CtIP stability during the cell cycle and in response to DNA damage. *EMBO J.* **33**, 2860–2879 (2014).
78. Gao, D. *et al.* Cdh1 Regulates Cell Cycle through Modulating the Caspin/Chk1 and the Rb/E2F1 Pathways. *Mol. Biol. Cell* **20**, 3305–3316 (2009).
79. Cotto-Rios, X. M., Jones, M. J. K., Busino, L., Pagano, M. & Huang, T. T. APC/C<sup>Cdh1</sup>-dependent proteolysis of USP1 regulates the response to UV-mediated DNA damage. *J. Cell Biol.* **194**, 177–186 (2011).
80. Zhang, L. *et al.* Proteolysis of Rad17 by Cdh1/APC regulates checkpoint termination and recovery from genotoxic stress. *EMBO J.* **29**, 1726–1737 (2010).
81. Tsvetkov, L. M., Yeh, K. H., Lee, S. J., Sun, H. & Zhang, H. p27(Kip1) ubiquitination and degradation is regulated by the SCF(Skp2) complex through phosphorylated Thr187 in p27. *Curr. Biol.* **9**, 661–4 (1999).
82. Sutterlüty, H. *et al.* p45SKP2 promotes p27Kip1 degradation and induces S phase in quiescent cells. *Nat. Cell Biol.* **1**, 207–214 (1999).
83. Carrano, A. C., Eytan, E., Hershko, A. & Pagano, M. SKP2 is required for ubiquitin-mediated degradation of the CDK inhibitor p27. *Nat. Cell Biol.* **1**, 193–9 (1999).
84. Frescas, D. & Pagano, M. Deregulated proteolysis by the F-box proteins SKP2 and beta-TrCP: tipping the scales of cancer. *Nat. Rev. Cancer* **8**, 438–49 (2008).
85. Welcker, M. & Clurman, B. E. FBW7 ubiquitin ligase: a tumour suppressor at the crossroads of cell division, growth and differentiation. *Nat. Rev. Cancer* **8**, 83–93 (2008).
86. Soussi, T., Dehouche, K. & Béroud, C. p53 website and analysis of p53 gene mutations in human cancer: Forging a link between epidemiology and carcinogenesis. *Hum. Mutat.* **15**, 105–113 (2000).
87. Fang, S., Jensen, J. P., Ludwig, R. L., Vousden, K. H. & Weissman, A. M. Mdm2 is a RING finger-dependent ubiquitin protein ligase for itself and p53. *J. Biol. Chem.* **275**, 8945–51 (2000).
88. Honda, R. & Yasuda, H. Activity of MDM2, a ubiquitin ligase, toward p53 or itself is dependent on the RING finger domain of the ligase. *Oncogene* **19**, 1473–1476 (2000).
89. Honda, R., Tanaka, H. & Yasuda, H. Oncoprotein MDM2 is a ubiquitin ligase E3 for tumor suppressor p53. *FEBS Lett.* **420**, 25–7 (1997).
90. Kubbutat, M. H. G., Jones, S. N. & Vousden, K. H. Regulation of p53 stability by Mdm2. *Nature* **387**, 299–303 (1997).
91. Haupt, Y., Maya, R., Kazaz, A. & Oren, M. Mdm2 promotes the rapid degradation of

- p53. *Nature* **387**, 296–299 (1997).
92. Brooks, C. L. & Gu, W. p53 ubiquitination: Mdm2 and beyond. *Mol. Cell* **21**, 307–15 (2006).
93. Issaeva, N. *et al.* Small molecule RITA binds to p53, blocks p53–HDM-2 interaction and activates p53 function in tumors. *Nat. Med.* **10**, 1321–1328 (2004).
94. Vassilev, L. T. *et al.* In Vivo Activation of the p53 Pathway by Small-Molecule Antagonists of MDM2. *Science (80-. )*. **303**, 844–848 (2004).
95. Walden, H. & Deans, A. J. The Fanconi Anemia DNA Repair Pathway: Structural and Functional Insights into a Complex Disorder. *Annu. Rev. Biophys.* **43**, 257–278 (2014).
96. Sims, A. E. *et al.* FANCI is a second monoubiquitinated member of the Fanconi anemia pathway. *Nat. Struct. Mol. Biol.* **14**, 564–567 (2007).
97. Smogorzewska, A. *et al.* Identification of the FANCI Protein, a Monoubiquitinated FANCD2 Paralog Required for DNA Repair. *Cell* **129**, 289–301 (2007).
98. Densham, R. M. *et al.* Human BRCA1-BARD1 ubiquitin ligase activity counteracts chromatin barriers to DNA resection. *Nat. Struct. Mol. Biol.* **23**, 647–55 (2016).
99. Farmer, H. *et al.* Targeting the DNA repair defect in BRCA mutant cells as a therapeutic strategy. *Nature* **434**, 917–921 (2005).
100. Chroma, K. *et al.* Tumors overexpressing RNF168 show altered DNA repair and responses to genotoxic treatments, genomic instability and resistance to proteotoxic stress. *Oncogene* **36**, 2405–2422 (2017).
101. Van Lohuizen, M. *et al.* Identification of cooperating oncogenes in E mu-myc transgenic mice by provirus tagging. *Cell* **65**, 737–52 (1991).
102. Valk-Lingbeek, M. E., Bruggeman, S. W. M. & van Lohuizen, M. Stem Cells and Cancer. *Cell* **118**, 409–418 (2004).
103. Wiesner, T. *et al.* Germline mutations in BAP1 predispose to melanocytic tumors. *Nat. Genet.* **43**, 1018–21 (2011).
104. Testa, J. R. *et al.* Germline BAP1 mutations predispose to malignant mesothelioma. *Nat. Genet.* **43**, 1022–1025 (2011).
105. Carbone, M. *et al.* BAP1 and cancer. *Nat. Rev. Cancer* **13**, 153–9 (2013).
106. Zou, Q. *et al.* USP15 stabilizes MDM2 to mediate cancer-cell survival and inhibit antitumor T cell responses. *Nat. Immunol.* **15**, 562–570 (2014).
107. Cummins, J. M. & Vogelstein, B. HAUSP is required for p53 destabilization. *Cell Cycle* **3**, 689–92 (2004).

108. Li, M., Brooks, C. L., Kon, N. & Gu, W. A Dynamic Role of HAUSP in the p53-Mdm2 Pathway. *Mol. Cell* **13**, 879–886 (2004).
109. Li, M. *et al.* Deubiquitination of p53 by HAUSP is an important pathway for p53 stabilization. *Nature* **416**, 648–653 (2002).
110. Murai, J. *et al.* The USP1/UAF1 complex promotes double-strand break repair through homologous recombination. *Mol. Cell. Biol.* **31**, 2462–9 (2011).
111. Dexheimer, T. S. *et al.* Synthesis and Structure–Activity Relationship Studies of *N*-Benzyl-2-phenylpyrimidin-4-amine Derivatives as Potent USP1/UAF1 Deubiquitinase Inhibitors with Anticancer Activity against Nonsmall Cell Lung Cancer. *J. Med. Chem.* **57**, 8099–8110 (2014).
112. Liang, Q. *et al.* A selective USP1–UAF1 inhibitor links deubiquitination to DNA damage responses. *Nat. Chem. Biol.* **10**, 298–304 (2014).





# Chapter 2

## **Histone ubiquitination in the DNA damage response**

Michael Uckelmann and Titia K. Sixma

*Division of Biochemistry and Cancer Genomics Centre  
Netherlands Cancer Institute, Plesmanlaan 121, 1066CX Amsterdam*

DNA Repair (Amst). 2017 Aug;56:92-101

**Abstract**

DNA double strand breaks need to be repaired in an organized fashion to preserve genomic integrity. In the organization of faithful repair, histone ubiquitination plays a crucial role. Recent findings suggest an integrated model for DNA repair regulation through site-specific histone ubiquitination and crosstalk to other posttranslational modifications. Here we discuss how site-specific histone ubiquitination is achieved on a molecular level and how different multi-protein complexes work together to integrate different histone ubiquitination states. We propose a model where site-specific H2A ubiquitination organizes the spatio-temporal recruitment of DNA repair factors which will ultimately contribute to DNA repair pathway choice between homologous recombination and non-homologous end joining.

**Introduction**

To ensure genomic integrity and prevent diseases such as cancer, DNA double strand breaks (DSB) need to be faithfully repaired<sup>1</sup>. The two major pathways responsible for this repair are non-homologous end joining (NHEJ) and homologous recombination (HR). The choice between these two depends on the cell cycle phase with pathway choice carefully regulated by integrated signaling networks<sup>2</sup>.

Histone modifications play an important part in these signaling networks. In response to DNA damage, different posttranslational modifications (e.g. methylation, ubiquitination, acetylation) form recruitment platforms for downstream effectors, guide the activity of chromatin remodelers and modulate enzymatic signaling cascades<sup>3</sup>. In this way the histone modifications act as conductors, orchestrating the appropriate damage response (Figure 1).

This histone signaling network is organized by multi-protein complexes, containing different functional modules able to “read”, “write” and “erase” chromatin marks. The modularity of these complexes allows for integration of different histone modifications. For instance a chromatin modifying complex might read methylated histones through one module and erase ubiquitination with another. These modular assemblies allow a great complexity of possible signaling events.

Ubiquitination of histone H2A and H2B is one important posttranslational modification in the DNA damage response<sup>4</sup>. H2A and H2B ubiquitination is unusually site-selective. Three enzymes or enzyme complexes, RNF168, RING1B(RNF2) in polycomb repressive complex 1 (PRC1) and BRCA1/BARD1, modify H2A on three distinct sites (K13/K15, K119 and K127/129 respectively). RNF20/RNF40 specifically modifies K120 on H2B<sup>5-9</sup>. All four ligases, with the possible exception of RNF168, exert their function as parts of bigger multiprotein complexes allowing for functional integration through the above mentioned modularity of readers, wri-



ters and erasers. Several different PRC1 complexes have in fact been identified and subunit composition has been shown to have functional importance<sup>10</sup>.

Ubiquitination of different sites on H2A has distinct physiological consequences. In the DNA damage response ubiquitination of H2A by BRCA1/BARD1 is believed to promote HR<sup>11</sup> and ubiquitination by RNF168 seems to promote NHEJ<sup>2,12</sup>. Ubiquitination of H2A by PRC1 complexes has a global function in transcriptional silencing<sup>13</sup> and it may fulfil the same role locally around the damage site. H2B ubiquitination in the context of DNA damage is crucial for damage checkpoint activation and timely initiation of repair<sup>4,12</sup>.

Specific histone ubiquitination forms an integral part of the regulatory network guiding the DNA damage response and recent advances help to explain the molecular basis of specificity and its consequences with respect to repair pathway choice. Those advances also support the notion of a form of crosstalk, where specific ubiquitination states at different sites affect each other and are affected themselves by different PTMs. In such a model, integration over several signaling entities will ultimately decide repair pathway choice.

### **H2A13/15ub – RNF168 driven decision making**

The E3 ligase RNF168 catalyzes the formation of two different signaling entities in response to double strand breaks, H2A K15 monoubiquitination and K63-linked ubiquitin chains (Figure 2A). Both are strictly dependent on another E3 ligase, RNF8, which is recruited first to the damage site, in response to a phosphorylation cascade initiated by ATM. Initially it was proposed that RNF8 acts first as a priming E3 ligase, initiating H2A ubiquitination, which would then recruit RNF168 to extend K63-linked chains to recruit other downstream effectors<sup>14–16</sup>. Later it became clear that in fact RNF168 is responsible for the priming event by monoubiquitinating H2A and RNF8 can extend a monoubiquitination on H2A to form K63-linked ubiquitin chains<sup>6</sup>. Furthermore RNF168 was shown to be exclusively specific for K13/15 on H2A and not 119<sup>6,17</sup>, identifying the first non-canonical H2A ubiquitination site. Recently the question how RNF8 manages to recruit RNF168 was solved with the identification of the linker histone H1 as its main target<sup>18</sup>. In our current understanding RNF8 will first ubiquitinate H1, leading to the recruitment of RNF168 which in turn monoubiquitinates H2A at lysine 13/15. RNF168 can bind its own product which will lead to increasing concentrations of RNF168 at the break site and amplification of H2A monoubiquitination<sup>19,20</sup>. The priming ubiquitination may then get extended by RNF8 to form K63-linked ubiquitin chains which are important to recruit downstream effectors, although this step is uncertain as it is only seen with RNF168 overexpression<sup>6</sup>. Under physiological conditions RNF168 concentrations are kept at low levels to prevent excessive amplification of its signaling function. TRIP12 and UBR5 have been shown to be responsible for this regulation<sup>21</sup>.

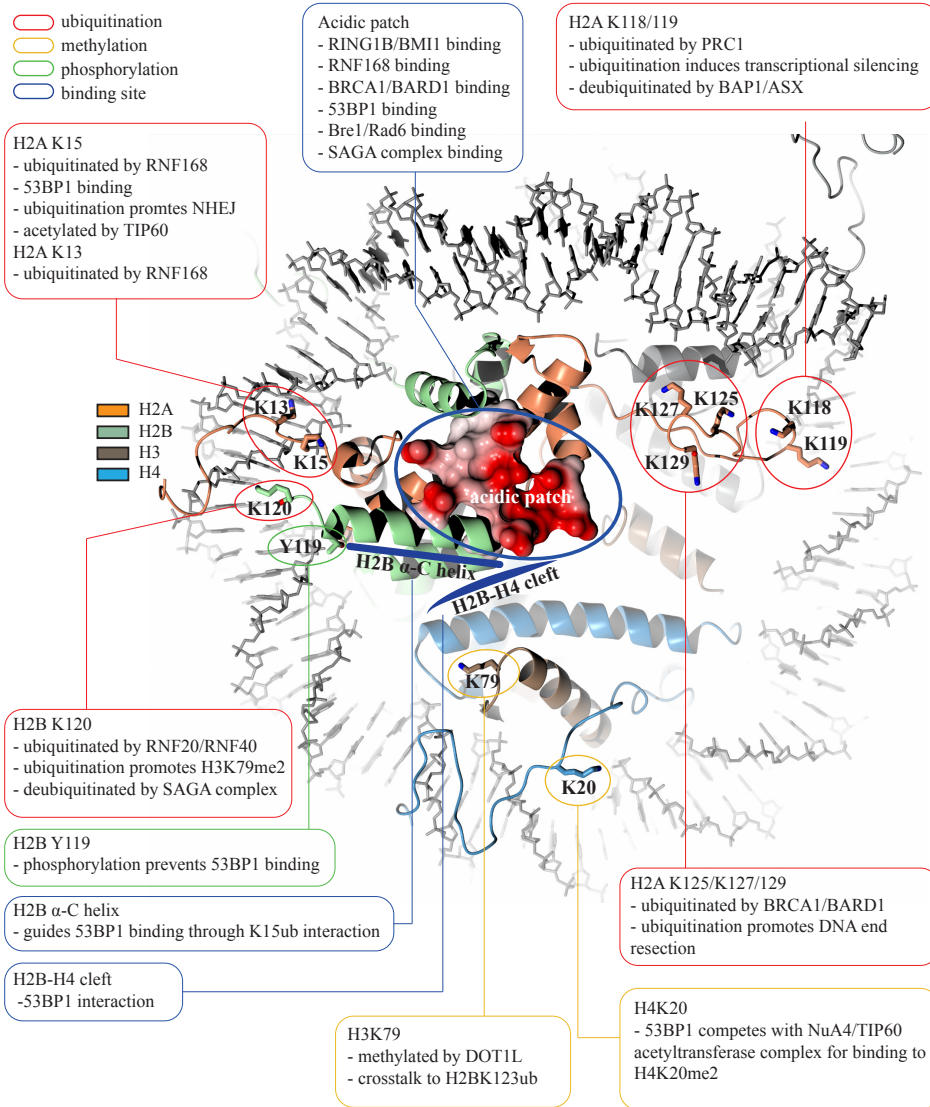


**Figure 1:** Structure of the nucleosome core particle, indicating discussed modifications and interaction sites highlighted. Four different E3 ligases play a role in DNA damage response, each modifying a specific site on the nucleosome. In vivo RNF168 ubiquitinates both K13 and K15, but only K15 has so far been shown to have functional relevance. The PRC1 E3 ligases modify only K119 in vivo, unless this residue is deleted, when K118 can substitute. Proteomics analysis showed that BRCA1/BARD1 can modify K127 and K129, but in vitro K125 is also modified. Residue numbers of human histones are mapped to the location on a *Xenopus laevis* crystal structure that contains the tails (PDB code: 1KX5<sup>123</sup>).

One downstream factor that is recruited by K63-linked chains is the BRCA1-A complex<sup>22</sup>. The complex consists of RAP80 (UIMC1), Abraxas (FAM175A), MERIT40 (BABAM1), BRCC36 (BRCC3), BRCC45 (BRE) and BRCA1/BARD1. RAP80 is responsible for recruitment of the complex to break sites by interaction with K63-linked ubiquitin chains through its ubiquitin

interacting motif (UIM) motifs. Once recruited the complex is understood to limit DNA end resection and protect from hyper-active HR<sup>23,24</sup>. BRCC36 is a DUB believed to cleave K63-linked chains and its catalytic activity has been shown to be crucial for limiting end resection<sup>25</sup>. The role of BRCA1 and its catalytic activity in this complex is poorly understood. However, the mechanism RNF168 works together with RNF8 to initiate the recruitment of BRCA1 highlights the possibility of a crosstalk between both pathways.

RNF168-catalyzed H2A monoubiquitination is understood to affect repair pathway choice through recruitment of 53BP1 (TP53BP1) to sites of damage. 53BP1 binds directly and selectively to H2AK15ub, but not H2AK13ub, making 53BP1 one of the first site-specific readers of histone monoubiquitination<sup>26</sup> (Figure 1). H2AK13ub occurs in cells as well, but has not been assigned a specific role yet<sup>26,27</sup>. The recruitment of 53BP1 is suggested to tip the balance in favor of NHEJ by inhibiting DNA end resection, the critical first step in HR<sup>2,28</sup>. This binary model is challenged by recent findings that suggest a more dynamic regulation where 53BP1 is not merely blocking but rather fine-tuning resection length through relative abundance at the break site and competition with end resecting enzymes<sup>29</sup>. 53BP1, once recruited to the break site, acts as a scaffold to assemble other proteins that restrict and guide DNA end resection<sup>30</sup>. Recruitment relies on integration of two histone modifications, H2AK15ub and lysine 20 dimethylation on histone H4 (H4K20me2). 53BP1 engages with H4K20me2 through a tandem TUDOR domain<sup>31</sup> and with H2AK15ub via a ubiquitin dependent recruitment (UDR) domain C-terminal of the TUDOR domain<sup>26</sup>. The presence of both domains is necessary for formation of ionizing radiation induced foci (IRIF)<sup>26</sup>.

A recent cryo-EM structure of a 53BP1 dimer bound to a nucleosome modified with a dimethyl-lysine mimic at H4K20 and a ubiquitin at K15 of H2A shed light on the molecular details of this interaction<sup>27</sup>. It shows how 53BP1 establishes its binding specificity through interaction with both PTMs, the H2B-H4 cleft on the nucleosome and the nucleosomal acidic patch, a known binding hotspot for chromatin interacting proteins<sup>32-41</sup>, making it a prime example for multivalent recognition of epigenetically modified chromatin. The structure explains the strict binding specificity of 53BP1 for H2AK15ub over H2AK13ub, which is governed by interaction of nucleosomal DNA with the N-terminal tail of H2A, and illustrates the importance of ubiquitin making specific interaction with the H2B alpha-C Helix for 53BP1 binding<sup>27</sup>.

The specifics of these interactions emphasize the possibility of crosstalk with other signaling pathways. The nucleosomal acidic patch is a known interaction surface for a number of chromatin interacting proteins in addition to 53BP1<sup>32-41</sup>. Use of the same binding platform by many chromatin interactors creates a strong competition for access to the acidic patch. Relative protein levels, local concentrations and relative affinities will likely play an important regulatory function in chromatin biology to decide which protein engages in productive

interaction with the nucleosome. The importance of ubiquitin interaction with the alpha-C helix of H2B suggests the possibility of crosstalk to other histone PTMs. In close proximity to the alpha-C helix tyrosine 119 can get phosphorylated<sup>42</sup>, and lysine 120 on H2B can get ubiquitinated<sup>8,9</sup>. In principle either of these modifications could interfere with 53BP1 recruitment but only phosphorylation of T119 has been shown to reduce 53BP1 binding, making a regulatory histone PTM crosstalk plausible<sup>27</sup>. Ubiquitination at K120 does not seem to have an effect on 53BP1 recruitment<sup>27</sup>.

Intriguingly, H4K20me2 has recently been identified as a binding platform for the NuA4/TIP60 acetyltransferase complex<sup>43</sup>. TIP60 (histone acetyltransferase KAT5) acetylates the histone H4 tail<sup>44</sup> and has been proposed to disrupt 53BP1 interaction with the nucleosome, thus inhibiting NHEJ and promoting HR<sup>45</sup>. Now it has been shown that the Nu4A/TIP60 complex directly competes for H4K20me2 binding with 53BP1<sup>43</sup>. Interestingly, TIP60 is able to acetylate K15 on H2A<sup>43</sup>. Acetylation of K15 is mutually exclusive with K15 ubiquitination responsible for 53BP1 recruitment, further establishing regulation of 53BP1 biology through the Nu4A/TIP60 complex and illustrating a complex regulatory network revolving around three different H2A PTMs (acetylation, ubiquitination and methylation), and the proteins that read and write these PTMs.

As every on-switch is usually opposed by an off-switch it is to be expected that RNF168 dependent histone ubiquitination will be counteracted by equally specific deubiquitinating enzymes (DUBs). Among the DUBs reported to potentially deubiquitinate H2A USP51, USP44, USP11 and USP3 stand out as likely regulators of the H2AK15ub-centered pathway<sup>46-50</sup>.

USP3 deubiquitinates H2AK13/15ub as well as H2A119ub in response to DNA damage and affects recruitment of 53BP1 in cells<sup>19,46</sup>. USP3 knockout mice show elevated levels of histone ubiquitination, reduced hematopoietic stem cell reserves over time, defective double strand break response and spontaneous tumor development, all phenotypes with possible links to RNF168 induced damage response<sup>48</sup>. However, direct evidence for USP3 counteracting the RNF168 catalyzed DSB response is lacking.

USP44 was identified in an USP overexpression screen to counteract RNF8/RNF168 dependent 53BP1 recruitment<sup>50</sup>. Recruitment of USP44 to DNA damage sites was shown to be dependent on RNF168 and it was suggested that USP44 binds to and deubiquitinates RNF8/RNF168 dependent ubiquitination at DSB breaks, though it is not clear if H2A is a direct target of USP44<sup>50</sup>.

USP51 deubiquitinates H2A specifically at K13/15 in vitro. In cells depletion of USP51 leads to a higher sensitivity to ionizing radiation, increased 53BP1 foci formation and slower clea-

rance of these foci<sup>47</sup>. USP11 was shown to specifically deubiquitinate H2AX phosphorylated at serine 139 ( $\gamma$ H2AX)<sup>51</sup>. Even though site-specificity of the deubiquitination activity was not established it was shown that USP11 knockdown affects residence time of 53BP1 at IRIF, suggesting a link to the DSB response. The unique specificity for  $\gamma$ H2AX is another example of PTM crosstalk and it will be interesting to clarify the molecular details underlying this specificity.

Two DUBs, USP26 and USP37, have recently been reported to affect BRCA1 signaling, likely by affecting RNF168/RNF8 dependent ubiquitination<sup>52</sup>. Both are recruited to DSBs and their knockdown induces HR defects. The authors propose a mechanism where USP26 and USP37 counterbalance RNF168/RNF8 ubiquitination-dependent sequestering of BRCA1 in the unproductive RAP80 complex<sup>52</sup>. The substrate specificity of USP26 and USP37 still needs to be addressed to substantiate such a model. It nevertheless highlights the interconnection of the BRCA1 and RNF168 pathways.

The recent advances in our understanding of the RNF168 dependent DNA damage response paint an intricate picture of regulatory switches centered around H2A monoubiquitination at lysine 15 and formation of K63-linked chains. It suggests a dual role of RNF168 in repair pathway choice: 1. Fine tuning of HR through K63-linked ubiquitin chains and 2. Promotion of NHEJ by H2A monoubiquitination. Both modifications should be viewed as part of a bigger signaling network relying on crosstalk between different histone modifications and their readers, writers and erasers. Integration over several signals will eventually guide the appropriate repair pathway choice and there seems to be substantial crosstalk with the BRCA1 pathway.

### **H2AK127/129ub – BRCA1 initiated end resection**

The tumor suppressor network centered around BRCA1 and its cognate protein complexes has long been acknowledged for its importance in cancer development and cancer predisposition and this has been reviewed extensively elsewhere (e.g.<sup>53,54</sup>). Here we focus on recent findings that advance our understanding of BRCA1 enzymatic function as ubiquitin E3 ligase and its role in HR (Figure 2B).

BRCA1 forms a heterodimer with BARD1 through its N-terminal RING domain<sup>55</sup> and the BRCA1/BARD1 dimer possesses E3 ligase activity<sup>56</sup>. The target of BRCA1/BARD1 E3 ligase activity has recently been identified as lysine 127 and 129 on H2A<sup>5</sup> (Figure 1). Specificity for this site is already present within the minimal RING/RING dimer<sup>5</sup>. Ubiquitination at K127/129 was shown to promote end resection and HR in a SMARCAD1 dependent manner<sup>11</sup>. This established a third distinct ubiquitination site on H2A that is independent of K13/15 (modified

by RNF168) and K119 (modified by RING1B/BMI1 or its PRC1 paralogs) and is suggested to be involved in DNA damage response. The exclusive specificity of BRCA1/BARD1 for a site just eight residues away from the polycomb site is remarkable and so far mechanistic and structural explanations are missing. It has been proposed that the BRCA1/BARD1 dimer engages with the nucleosome in a similar manner to RING1B/BMI1<sup>37</sup>, where the orientation towards the target lysine is guided by interaction with the nucleosomal acidic patch and flanking residues. The molecular differences that determine the unique specificity of the two ligases will need to be worked out.

In the DNA damage response BRCA1/BARD1 can participate in the formation of several multi-protein complexes that differ in subunit composition and localization with respect to the break site<sup>24</sup>. These BRCA1 complexes can integrate signals from different histone modifications to orchestrate HR and tip the balance of pathway choice towards HR by fine-tuning resection-length and RAD51 recruitment<sup>57</sup>. It is still unclear to which extent the E3 ligase activity of BRCA1/BARD1 itself is involved in this, but the molecular details defining this signal integration are starting to become known.

BRCA1 protein levels peak in close vicinity to the break site and spread up to 10 kilobases around it. The already mentioned BRCA1-A complex is formed several kilobases away from the break site and complex formation is governed by RAP80 interaction with RNF168/RNF8 catalyzed K63-linked ubiquitin chains<sup>58,59</sup>. RAP80 has been shown to also bind to ubiquitinated H2B but the importance of this interaction in the DNA damage response is uncertain<sup>60</sup>. The RAP80 sequestered BRCA1-A complex was shown to restrict rather than promote DNA end resection<sup>23,58</sup>. In direct vicinity to the DSB BRCA1 is recruited through BARD1 interaction with K9-dimethylated histone H3 (H3K9me2) mediated by heterochromatin protein 1 (HP1) and seems to promote HR through CtIP (RBBP8) interaction in an MRN (RAD50/NBS1/MRE11)-dependent manner<sup>24,61</sup>. Recruitment of the BRCA1/CtIP/MRN complex (sometimes referred to as BRCA1-C) is dependent on ATM and poly ADP-ribosylation (PARylation) but not on RNF168/RNF8<sup>61</sup>. The interaction with K9me2 opens up the possibility of integrating methylation signaling and H2A ubiquitination through BRCA1 catalytic activity, though a role for BRCA1-dependent ubiquitination activity in this signaling cascade has not yet been established.

BRCA1 forms another complex with PALB2, RAD51 and BRCA2 which is understood to facilitate RPA displacement by RAD51. This function depends on direct interaction of BRCA1 with PALB2<sup>62-64</sup>. BRCA1-PALB2 interaction is modulated by site-specific ubiquitination of the N-terminus of PALB2 by the KEAP1-CUL3-RBX1 E3 ligase complex<sup>65</sup>. Ubiquitination of PALB2 is cell cycle dependent and will prevent HR in G1 phase by disrupting BRCA1 interaction with ubiquitinated PALB2. This provides an explanation for HR inhibition in G1<sup>65</sup>. Also for this

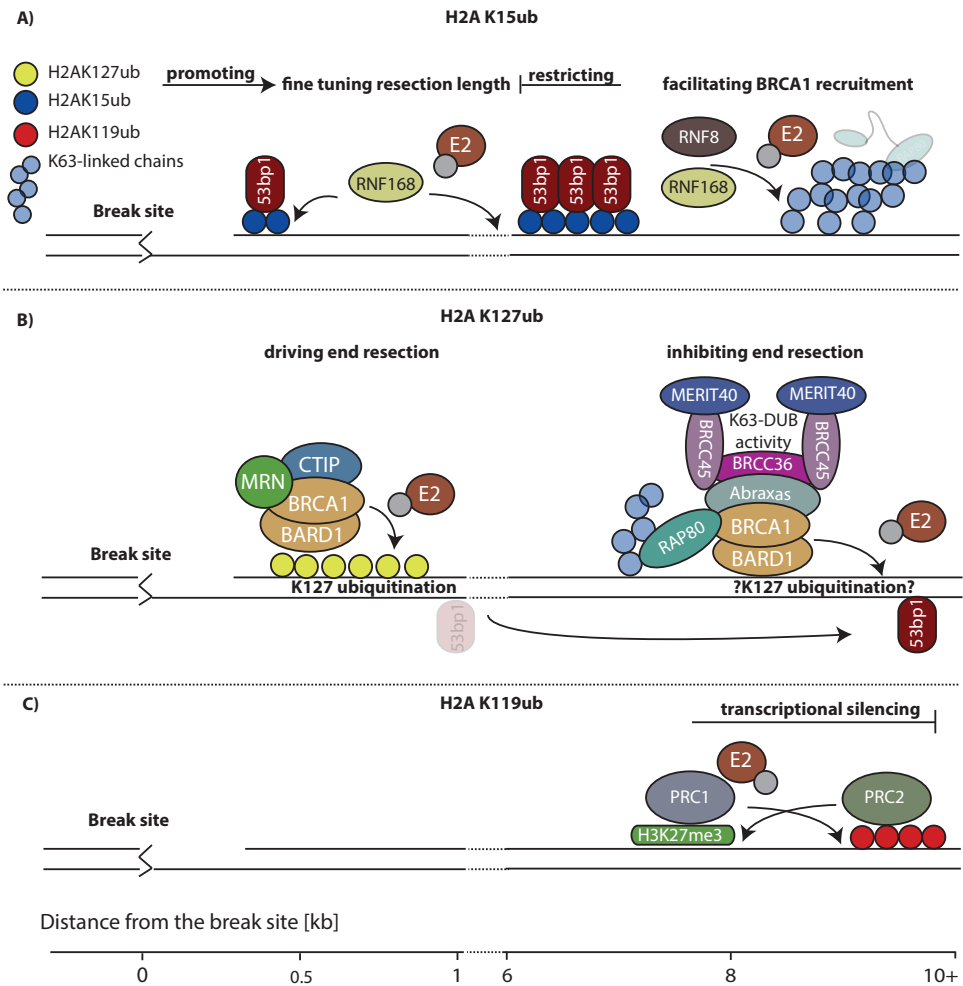


**Figure 2:** Model of site-specific ubiquitination in the DNA damage response. (A) RNF168 induced H2AK15ub regulates end resection through regulation of relative abundance of 53BP1. Low levels of 53BP1 promote end resection and high levels of 53BP1 inhibit end resection. K63-linked chains recruit the BRCA1-A complex distant from the break site (B) BRCA1 induced H2AK127ub (and/or H2AK129ub) drives end resection close to the break site, the BRCA1-A complex distant from the break inhibits resection. (C) PRC1 and PRC2 establish a H2AK119ub dependent transcription barrier distant from the break site.

process the role of BRCA1/BARD1 E3 ligase activity is unclear.

The presence of three functionally distinct BRCA1 complexes involved in DSB response with different effects on end resection stresses the need for mechanistic explanations. Most microscopy studies do not distinguish between the different BRCA1 complexes and it will be interesting to address where, with respect to the break site, BRCA1 engages in which complexes. Of particular interest is what role the E3 ligase activity of BRCA1 might play in the context of different complexes.



Overall the role of H2A ubiquitination by BRCA1/BARD1 in the DNA damage response is poorly understood and literature is at times contradicting. Studies on a catalytically inactive BRCA1 mutant (I26A) found no effect on tumor formation in mice<sup>66</sup> and in ES cells the same mutant had no effect on DNA repair through homologous recombination<sup>67</sup>. Knock-down of BRCA1 has been shown to reduce ubiquitination at alpha satellite repeats and induce transcriptional de-repression. The phenotype can be rescued by ectopic expression of a H2A-ubiquitin fusion protein, indicating that catalytic activity is important in this context<sup>68</sup>.

In mice loss of BRCA1 is embryonically lethal and lethality can be rescued by loss of 53BP1<sup>69,70</sup>. Mice expressing an E3 ligase deficient BRCA1 mutant (C61G)<sup>71</sup> or a RING-less variant<sup>72,73</sup> also show embryonic lethality, stressing the importance of the RING domain. Conditional tumor models of these variants show that they develop sporadic mammary tumors with a similar frequency compared to tumor models for BRCA1 loss and tumors show high genomic instability<sup>71,73,74</sup>. In cell lines C61G mutant and RING-less BRCA1 variants show partial HR defects but still form RAD51 foci<sup>71-73,75</sup>.

A recent study suggests a subtle role of BRCA1 catalytic activity in fine tuning DNA end resection<sup>11</sup>. The authors identified a point mutation in BARD1 (R99E) that abrogates BRCA1 catalytic activity without destabilizing the BRCA1/BARD1 dimer. Using this mutant it was possible to show that BRCA1/BARD1 catalytic activity promotes long range DNA end resection by facilitating SMARCAD1 dependent displacement of 53BP1 from the center of IRIF to the flanking regions. This is in agreement with high resolution microscopy studies that placed BRCA1 in the center of IRIF and 53BP1 at the periphery<sup>76,77</sup>. Initial limited resection was shown to be independent of BRCA1 catalytic activity and relying on CtIP and MRE11 activity<sup>11</sup>. These findings underline the importance of BRCA1 activity in regulating DNA end resection and thereby pathway choice, in line with previous suggestions<sup>70,78</sup>.

Many mechanistic details of the BRCA1 dependent DNA damage response are still unclear but regulation of DNA end resection seems to be one important regulatory function of BRCA1. Its catalytic activity, monoubiquitination of H2A, could be one of the factors guiding resection length.

### **K119ub – Polycomb repression, transcriptional regulation and repair**

H2A ubiquitination at K119 was the first histone mark to be identified<sup>79</sup>. It is deposited by the catalytic subunit of some polycomb repressive complexes 1 (PRC1)<sup>7</sup>. The polycomb repressive complexes 1 and 2 (PRC1/PRC2) are well known regulators of development and transcriptional silencing. Both are multi-protein complexes that can be composed of several different subunits<sup>10</sup> and they exhibit distinct enzymatic activity. PRC1 ubiquitinates H2A at



lysine 119<sup>7</sup> and PRC2 catalyzes the methylation of lysine 27 on H3 (H3K27me3)<sup>80</sup>. Polycomb complexes and their biology have been reviewed extensively elsewhere (e.g.<sup>13</sup>) and it has been shown that subunit composition will affect their function<sup>10</sup>. Here we will focus on the recent advances in our understanding of the functional interdependence of PRC1 and PRC2 as an example for histone PTM crosstalk, the mechanistic details underlying the PRC1 ubiquitin ligase activity and emerging roles of PRC1 in the DNA damage response (Figure 2C).

Recruitment of PRC1 and PRC2 has long been thought of as a hierarchical process. Based on the observation that some PRC1 complexes recognize H3K27me3 through their CBX proteins, it was proposed that PRC2 first methylates target chromatin which allows PRC1 to engage and catalyze H2AK119ub, thus establishing genetic silencing<sup>81–83</sup>. However, this seemingly solid model was basically turned upside down by recent findings that PRC2 recruitment can depend on PRC1 activity<sup>84,85</sup>. The authors provide evidence that ubiquitination of H2A at lysine 119 can be important for recruitment of PRC2 and show that PRC1 will bind to unmethylated CpG islands via its KDM2B subunit, switching the hierarchy of recruitment.

Mechanistic insight into the nature of PRC2 recruitment has been gained by the finding that its JARID2 subunit is required for recruitment to H2AK119ub via direct interaction with ubiquitinated H2A through its ubiquitin interacting motif (UIM)<sup>86</sup>. This establishes PRC1 and PRC2 as multiprotein chromatin modifying complexes with bivalent function as readers and writers of chromatin marks. PRC1 reads H3K27me3 and writes H2AK119ub, PRC2 reads H2AK119ub and writes H3K27me3, supporting the notion that multi protein complexes can act as one entity providing reader and writer functions to integrate diverse epigenetic signals. The mechanistic and biological details of this integrative signaling network have yet to be worked out. Some progress has been made in our understanding of the basic biochemistry underlying PRC1 catalytic activity and of its biological significance in transcriptional regulation and DNA damage response which we will discuss in the following.

RING1B with a PCGF subunit, such as BMI1 or MEL18 forms the catalytic core of the PRC1 complex<sup>7,87,88</sup>, which specifically ubiquitinates K119 on H2A (not K13/15 or K127/129<sup>5,6</sup>). The basis for this specificity has been explained by a crystal structure of the nucleosome core particle bound by RING1B/BMI1 fused to its cognate E2, UBCH5C (UBE2D3)<sup>37</sup>. The binding is primarily governed by RING1B interaction with the nucleosomal acidic patch. Most prominently, R98 of RING1B serves as an anchor and inserts into an acidic pocket provided by the H2A-H2B dimer, analogous to other published structures of chromatin binding modules<sup>34–36,40</sup>. Further interaction of RING1B and BMI1 with all four histone proteins, and importantly of UBCH5C with the nucleosomal DNA, arrange the complex in the appropriate orientation, placing the active site in a catalytically competent position towards the target lysine and restricting its movement to avoid unspecific reaction with other lysines<sup>37</sup>. Mutational

studies suggest a similar mode of interaction for BRCA1/BARD1 even though mechanistic details explaining the different specificity are missing<sup>37</sup>.

A link between PRC1 catalyzed H2A ubiquitination and the DNA damage response has long been suggested<sup>89–92</sup> but the underlying mechanisms are not clear. Furthermore, another report suggest no recruitment of PRC1 complexes to double strand break sites induced by the restriction enzyme ASiS1<sup>93</sup> and there is no clear consensus in the field.

The established function of polycomb group proteins in gene repression and the observation of H2A ubiquitination at sites of double strand breaks has prompted the idea that PRC1 and PRC2 could be involved in transcriptional silencing in response to DNA damage<sup>94</sup>. Transcription was found to be silenced up to several kilobases away from the DSB site in an ATM and H2AK119ub dependent manner<sup>94,95</sup>. H2A ubiquitination at double strand breaks depends on the PBAF chromatin remodeling complex and is important for rapid repair of DNA damage occurring in close proximity to the transcription machinery, likely through promoting NHEJ<sup>95</sup>. Intriguingly, it was found that both, BMI1 and EZH2 (the catalytic subunit of PRC2), are required for DSB-induced transcriptional silencing<sup>95</sup>, hinting at crosstalk of both enzyme complexes in response to DNA damage. Further functional insight came through a recent study<sup>96</sup> which showed that in response to double strand breaks transcriptional elongation factor ENL is phosphorylated by ATM. This enables direct interaction with BMI1, leading to enhanced ubiquitination of H2A on K119 and resulting in transcriptional silencing, providing a functional rationale for ATM dependence of H2A K119 ubiquitination<sup>96</sup>. The physiological role of H2AK119ub in the DNA damage response is not very well understood but one possibility is that it shields the break site from intrusion of the transcription machinery by establishing a H2AK119ub-dependent barrier of silenced transcription at a defined distance from the break site. The involvement of chromatin remodelers like PBAF adds another layer of complexity to the regulation of the damage response and it will be interesting to study if histone ubiquitination might affect histone eviction and chromatin remodeling.

The best characterized deubiquitinating enzyme specific for H2AK119ub is the UCH-class DUB BAP1 with its activator ASXL1. BAP1/ASXL1 form the PR-DUB complex which has been shown deubiquitinate H2A<sup>97</sup>. In vitro studies showed that the enzyme complex exclusively deubiquitinates H2AK119ub, not H2AK13/15ub<sup>98</sup>. BAP1/ASXL1 has two closely related paralogues, UCHL5/RPN13 and UCHL5/INO80G, for which the molecular mechanisms of activation have been worked out by detailed structure-function studies<sup>99,100</sup>. BAP1 is activated by ASXL1 in a similar manner where the DEUBAD domain of ASXL1 increases affinity of BAP1 for the ubiquitinated substrate<sup>98</sup>. Additionally, the C-terminal tail of BAP1 is crucial for nucleosome binding. This suggests a two-way model to explain activation and specificity where BAP1 is tethered to the nucleosome via its C-terminal tail but only engages in produc-

tive deubiquitination of H2AK119ub after activation by ASXL1<sup>98</sup>. While in vitro specificity of BAP1/ASXL1 is well established, the physiological role it plays in DSB response is not as clear and deserves further attention. First studies into this subject have shown that BAP1 is recruited to DSB sites in an ATM dependent manner and counteracts H2AK119ub in the vicinity of DNA break sites. Depletion of BAP1 results in a small reduction in HR efficiency<sup>101,102</sup>. This suggests that deubiquitination of H2A by BAP1 promotes HR which is complementary to the finding that ubiquitination of K119 in response to DNA damage favors NHEJ<sup>95</sup>.

Another DUB suggested to deubiquitinate H2AK119ub is USP16. Biological evidence suggests that USP16 restarts transcription upon H2AK119ub induced silencing by reducing ubiquitination levels<sup>94</sup>, though biochemical confirmation of USP16 target specificity is missing.

### **H2B K120 ubiquitination and damage response**

Ubiquitination of histone H2B has been implicated in transcriptional elongation<sup>103</sup>, replication<sup>104</sup> and DNA damage response<sup>105–109</sup>. We will discuss recent advances in our understanding of the molecular mechanisms that guide site-specificity and the involvement of H2BK120ub in the damage response.

H2Bub-dependent signaling in the DNA damage response centers around specific ubiquitination of lysine 120 (123 in yeast) on H2B by RNF20/RNF40 (Bre1 in yeast) working in concert with the E2 UBE2B (Rad6 in yeast)<sup>8,9</sup>. A recent mass spectrometry study highlights some details governing specificity, showing that binding of the Bre1/Rad6 complex to the nucleosome depends on the nucleosomal acidic patch<sup>41</sup>. The importance of the acidic patch for the ubiquitination reaction was confirmed by mutagenesis and several residues crucial for Bre1/Rad6 interaction have been identified.

Almost simultaneously the crystal structure of the nucleosome complex of the yeast SAGA DUB module, the protein complex responsible for removal of H2BK123ub<sup>110</sup>, was solved<sup>38</sup>. The yeast SAGA DUB module is a multi-protein complex consisting of Ubp8/Sgf11/Sus1/Sgf73, where the deubiquitination activity is provided by Ubp8 (USP22 in human)<sup>38</sup>. The structure revealed that the SAGA DUB module contacts the nucleosome almost exclusively through the H2A/H2B dimer via interaction of the Sgf11 zinc finger with the nucleosomal acidic patch. Further contacts are made between Ubp8, H2A and ubiquitin. The fact that both writer and eraser complexes engage the nucleosome through the acidic patch opens up interesting regulatory possibilities through competition for access amongst each other<sup>38,41</sup> and with other chromatin binders.

The physiological role of H2B ubiquitination in the response to DNA damage is not very well understood. It has been shown that H2B ubiquitination is important for DNA damage

checkpoint activation and timely initiation of repair<sup>107,109</sup>. RNF20/RNF40 dependent H2B monoubiquitination is needed for recruitment of repair factors in an ATM dependent manner and is necessary for faithful repair through both pathways, HR and NHEJ<sup>107</sup>. Knockdown of RNF20/40 was shown to not affect formation of  $\gamma$ H2AX foci but rather their persistence<sup>107</sup>. A recent study showed that H2B deubiquitination by the SAGA complex is crucial for proper DNA repair function, reminiscent of PR-DUB which is important for PRC1 function<sup>97</sup>. Deubiquitination was shown to act downstream of ATM and to facilitate formation of  $\gamma$ H2AX foci<sup>111</sup>. More work in this direction will be needed to work out mechanistic details and explain why ubiquitination and deubiquitination seem to have a similar role.

In yeast, knockout of Bre1 leaves cells unable to activate the DNA damage checkpoint as measured by Rad53 phosphorylation<sup>112</sup>. This checkpoint defect can be rescued by expression of a H2A construct with a ubiquitin tethered to Serine 1 or 19, a position resembling H2BK123ub, suggesting a global function of H2B ubiquitination in the damage response<sup>112</sup>. Another study links H2B ubiquitination to transcription coupled nucleotide excision repair, showing rapid deubiquitination of H2B by yeast Ubp8 and Ubp10 upon UV damage and transcriptional stalling<sup>113</sup>. Furthermore, yeast Ubp8/Ubp10 knockout strains show much slower transcription coupled repair kinetics<sup>113</sup>.

H2BK120ub exhibits interesting functional crosstalk with DOT1L catalyzed methylation of histone H3 on lysine 79<sup>114,115</sup> where histone ubiquitination is crucial for efficient methylation of H3. Biochemical analysis has shown that ubiquitinated H2B directly stimulates DOT1L catalytic activity<sup>116–118</sup> and a recent study has elucidated molecular details of this activation<sup>119</sup>. Based on crosslinking experiments and biochemical validation the authors show specific interaction of ubiquitin with the N-terminal tail of H2A but not with DOT1L. The authors propose a “corralling” mechanism where DOT1L binds to unmodified nucleosomes aspecifically and thus will mostly be in a catalytically incompetent position. In presence of H2BK120ub DOT1L binding is restricted to the catalytically competent mode, leading to more efficient methylation of H3K79<sup>119</sup>. This model is in agreement with *in vivo* studies in yeast where the exact position of ubiquitin on the nucleosome was not found to be crucial for Dot1 activation, establishing a certain plasticity in the H2BK120ub-Dot1 crosstalk<sup>112</sup>. Plasticity of Dot1 activation was also observed *in vitro*<sup>116</sup>. DOT1L has been implicated in the 53BP1 dependent DNA damage response in human<sup>120</sup> and chicken DT40 cells<sup>121</sup> an knockdown of DOT1L in mouse embryonic fibroblasts leads to hypersensitivity to UV damage and affects transcriptional restart<sup>122</sup>.

Future research needs to establish a clear correlation of repair phenotypes with H2B ubiquitination and elaborate on the mechanistic details that define specificity to clarify the role of H2B ubiquitination in the damage response.

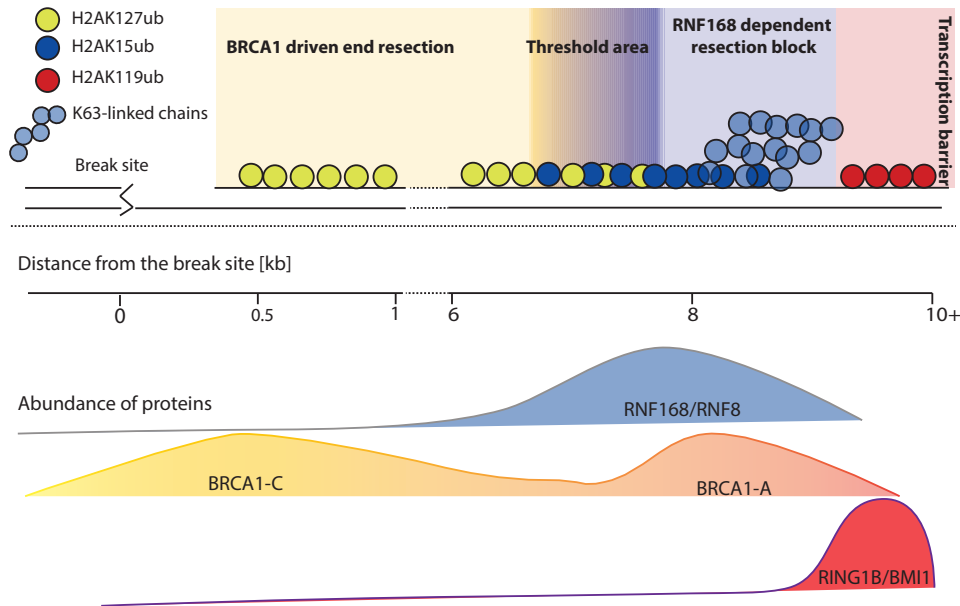


**Figure 3:** Site-specific H2A ubiquitination defines regulatory zones in the DNA damage response dependent on relative abundance of E3 ligases and localization with respect to the DNA break site

### Closing thoughts – an integrated model for DNA damage signaling through H2A ubiquitination

Recent advances in our understanding of the mechanisms guiding the DNA damage response put forward the notion of an integrated signaling network where specific ubiquitination of histones at four different sites will contribute to faithful repair by promoting appropriate repair pathway choice. This choice is heavily influenced by crosstalk between the four sites and to other PTMs.

Here we reviewed how RNF168 catalyzes H2AK13/15ub, limits resection and tips the balance in favor of NHEJ via 53BP1 recruitment<sup>2,6,14,15,17,29,78</sup> and how BRCA1/BARD1 pulls into the opposite direction, ubiquitinating H2AK127/129<sup>5</sup> and thus promoting end resection and HR<sup>57</sup>. However, not all BRCA1 complexes act in the same way, as they come in different flavors with seemingly opposing function, one promoting resection near the break site<sup>24,61</sup> and one inhibiting it together with RAP80 distant from the break<sup>23,58,59</sup>. At the fringes of the double strand break PRC1 and PRC2 play a game of mutual recruitment<sup>81–86</sup> to inhibit transcription and guard faithful repair from the distance<sup>94–96</sup>.

Since all these enzyme complexes will likely be recruited to the same break site, the outcome will be determined by how, when, where and to what extent they influence each other in response to a defined physiological challenge, during a defined moment in the cell cycle and

in a particular cell type. The outcome is expected to be different in different situations but their enzymatic activity, ubiquitination of the nucleosome, and crosstalk to other histone modifications will likely play an important role.

Repair pathway choice seems to be one process that is guided by specific histone ubiquitination and the first crucial step is the tight regulation of resection length. Over-resection is detrimental and inhibition of resection prevents error-free HR<sup>2</sup>. We have discussed how 53BP1 limits DNA end resection in a H2AK15ub dependent manner<sup>26,29</sup> and how BRCA1 counteracts this by promoting resection through H2A K127 ubiquitination and displacement of 53BP1<sup>11</sup>. In the most simple straight forward model (Figure 3) one could assume that the extent of either one of these epigenetic marks defines the extent of DNA end resection by defining molecular reaction chambers at a defined position with respect to the break, through specific recruitment of some factors and selective exclusion of others. BRCA1 catalyzed ubiquitination near the break would initially drive resection until it reaches a threshold area where it is overwhelmed by RNF168-driven K15 ubiquitination. This threshold area would be enforced by the presence of K63-linked chains that sequester BRCA1 into the RAP80-BRCA1 complex with possible effects on its catalytic activity. The PRC1 complex would establish a H2AK119ub dependent boundary at a certain distance from the break site to guard against intrusion of the transcription machinery. In this model RNF168 and BRCA1 would be in constant catalytic competition and tight regulation is expected to fine-tune resection length and pathway choice in response to distinct challenges. Regulation can be as simple as changes in protein abundance throughout the cell cycle or more elaborate such as PTMs that affect catalytic activity and protein stability and the crosstalk with other histone modifications. As we have seen, active remodeling of chromatin around the break site by chromatin remodelers such as PBAF is crucial for efficient DNA repair and will add another layer of complexity<sup>95</sup>.

The proposed model should be viewed as a working hypothesis rather than a scientifically sound model as experimental evidence for such a regulatory mechanism is still scarce. Support for a more dynamic view of the players involved in the damage response comes from a recent study that emphasizes the importance of RNF168 dynamic range in regulating DNA end resection and proposes that relative protein levels rather than simply the presence or absence of major regulators such as 53BP1 are the deciding factor in pathway choice<sup>29</sup>. In the future it will be crucial to look at the precise molecular architecture of a single double strand break site. Which protein complexes and PTMs are present at what levels and in what distance to the break site? Answering these questions will be imperative in understanding the biology of the DNA damage response. Super-resolution fluorescent microscopy and single molecule biophysics will help to address these questions.

**Acknowledgements:**

We thank Jiri Lukas, Jo Morris, Fred van Leeuwen, Ruth Densham, Peter Bouwman and Elisabetta Citterio for helpful discussions on the manuscript. Funding was provided by NWO-CW TOP 714.012.001

**References**

1. Jackson, S. P. & Bartek, J. The DNA-damage response in human biology and disease. *Nature* **461**, 1071–8 (2009).
2. Chapman, J. R., Taylor, M. R. G. & Boulton, S. J. Playing the End Game: DNA Double-Strand Break Repair Pathway Choice. *Molecular Cell* **47**, 497–510 (2012).
3. Dantuma, N. P. & van Attikum, H. Spatiotemporal regulation of posttranslational modifications in the DNA damage response. *EMBO J* **35**, 6–23 (2016).
4. Jackson, S. P. & Durocher, D. Regulation of DNA Damage Responses by Ubiquitin and SUMO. *Mol. Cell* **49**, 795–807 (2013).
5. Kalb, R., Mallery, D. L., Larkin, C., Huang, J. T. J. & Hiom, K. BRCA1 is a histone-H2A-specific ubiquitin ligase. *Cell Rep.* **8**, 999–1005 (2014).
6. Mattioli, F. *et al.* RNF168 ubiquitinates K13-15 on H2A/H2AX to drive DNA damage signaling. *Cell* **150**, 1182–1195 (2012).
7. Wang, H. *et al.* Role of histone H2A ubiquitination in Polycomb silencing. *Nature* **431**, 873–8 (2004).
8. Wood, A. *et al.* Bre1, an E3 ubiquitin ligase required for recruitment and substrate selection of Rad6 at a promoter. *Mol. Cell* **11**, 267–274 (2003).
9. Robzyk, K., Recht, J. & Osley, M. A. Rad6-Dependent Ubiquitination of Histone H2B in Yeast. *Science (80-. )*. **287**, (2000).
10. Gao, Z. *et al.* PCGF Homologs, CBX Proteins, and RYBP Define Functionally Distinct PRC1 Family Complexes. *Mol. Cell* **45**, 344–356 (2012).
11. Densham, R. M. *et al.* Human BRCA1-BARD1 ubiquitin ligase activity counteracts chromatin barriers to DNA resection. *Nat. Struct. Mol. Biol.* **23**, 647–55 (2016).
12. Schwertman, P., Bekker-Jensen, S. & Mailand, N. Regulation of DNA double-strand break repair by ubiquitin and ubiquitin-like modifiers. *Nat Rev Mol Cell Biol* **17**, 379–394 (2016).
13. Simon, J. A. & Kingston, R. E. Occupying Chromatin: Polycomb Mechanisms for

- Getting to Genomic Targets, Stopping Transcriptional Traffic, and Staying Put. *Molecular Cell* **49**, 808–824 (2013).
14. Mailand, N. *et al.* RNF8 Ubiquitylates Histones at DNA Double-Strand Breaks and Promotes Assembly of Repair Proteins. *Cell* **131**, 887–900 (2007).
  15. Kolas, N. K. *et al.* Orchestration of the DNA-damage response by the RNF8 ubiquitin ligase. *Science (80-. )*. **318**, 1637–1640 (2007).
  16. Huen, M. S. Y. *et al.* RNF8 Transduces the DNA-Damage Signal via Histone Ubiquitylation and Checkpoint Protein Assembly. *Cell* **131**, 901–914 (2007).
  17. Gatti, M. *et al.* A novel ubiquitin mark at the N-terminal tail of histone H2As targeted by RNF168 ubiquitin ligase. *Cell Cycle* **11**, 2538–2544 (2012).
  18. Thorslund, T. *et al.* Histone H1 couples initiation and amplification of ubiquitin signalling after DNA damage. *Nature* **527**, 389–93 (2015).
  19. Doil, C. *et al.* RNF168 Binds and Amplifies Ubiquitin Conjugates on Damaged Chromosomes to Allow Accumulation of Repair Proteins. *Cell* **136**, 435–446 (2009).
  20. Stewart, G. S. *et al.* The RIDDLE Syndrome Protein Mediates a Ubiquitin-Dependent Signaling Cascade at Sites of DNA Damage. *Cell* **136**, 420–434 (2009).
  21. Gudjonsson, T. *et al.* TRIP12 and UBR5 Suppress Spreading of Chromatin Ubiquitylation at Damaged Chromosomes. *Cell* **150**, 697–709 (2012).
  22. Sobhian, B. *et al.* RAP80 targets BRCA1 to specific ubiquitin structures at DNA damage sites. *Science* **316**, 1198–202 (2007).
  23. Hu, Y. *et al.* RAP80-directed tuning of BRCA1 homologous recombination function at ionizing radiation-induced nuclear foci. *Genes Dev.* **25**, 685–700 (2011).
  24. Savage, K. I. & Harkin, D. P. BRCA1, a ‘complex’ protein involved in the maintenance of genomic stability. *FEBS Journal* **282**, 630–646 (2015).
  25. Ng, H. M., Wei, L., Lan, L. & Huen, M. S. Y. The Lys63-deubiquitylating enzyme BRCC36 limits DNA break processing and repair. *J. Biol. Chem.* **291**, 16197–16207 (2016).
  26. Fradet-Turcotte, A. *et al.* 53BP1 is a reader of the DNA-damage-induced H2A Lys 15 ubiquitin mark. *Nature* **499**, 50–54 (2013).
  27. Wilson, M. D. *et al.* The structural basis of modified nucleosome recognition by 53BP1. *Nature* **536**, 100–103 (2016).
  28. Nakamura, K. *et al.* Genetic dissection of vertebrate 53BP1: A major role in non-homologous end joining of DNA double strand breaks. *DNA Repair (Amst)*. **5**, 741–749 (2006).



29. Ochs, F. *et al.* 53BP1 fosters fidelity of homology-directed DNA repair. *Nat. Struct. Mol. Biol.* **23**, 714–21 (2016).
30. Panier, S. & Boulton, S. J. Double-strand break repair: 53BP1 comes into focus. *Nat. Rev. Mol. Cell Biol.* **15**, 7–18 (2014).
31. Botuyan, M. V. *et al.* Structural Basis for the Methylation State-Specific Recognition of Histone H4-K20 by 53BP1 and Crb2 in DNA Repair. *Cell* **127**, 1361–1373 (2006).
32. Mattioli, F., Uckelmann, M., Sahtoe, D. D., van Dijk, W. J. & Sixma, T. K. The nucleosome acidic patch plays a critical role in RNF168-dependent ubiquitination of histone H2A. *Nat. Commun.* **5**, 3291 (2014).
33. Leung, J. W. *et al.* Nucleosome Acidic Patch Promotes RNF168- and RING1B/BMI1-Dependent H2AX and H2A Ubiquitination and DNA Damage Signaling. *PLoS Genet.* **10**, e1004178 (2014).
34. Barbera, A. *et al.* The Nucleosomal Surface as a Docking Station for Kaposi's Sarcoma Herpesvirus LANA. *Science* **311**, 856–862 (2006).
35. Armache, K.-J., Garlick, J. D., Canzio, D., Narlikar, G. J. & Kingston, R. E. Structural Basis of Silencing: Sir3 BAH Domain in Complex with a Nucleosome at 3.0 Å Resolution. *Science (80-. )*. **334**, 977–982 (2011).
36. Makde, R. D., England, J. R., Yennawar, H. P. & Tan, S. Structure of RCC1 chromatin factor bound to the nucleosome core particle. *Nature* **467**, 562–566 (2010).
37. McGinty, R. K., Henrici, R. C. & Tan, S. Crystal structure of the PRC1 ubiquitylation module bound to the nucleosome. *Nature* **514**, 591–6 (2014).
38. Morgan, M. T. *et al.* Structural basis for histone H2B deubiquitination by the SAGA DUB module. *Science (80-. )*. **351**, 725–728 (2016).
39. Cucinotta, C. E., Young, A. N., Klucsevsek, K. M. & Arndt, K. M. The Nucleosome Acidic Patch Regulates the H2B K123 Monoubiquitylation Cascade and Transcription Elongation in *Saccharomyces cerevisiae*. *PLoS Genet.* **11**, 1–25 (2015).
40. Kato, H. *et al.* A conserved mechanism for centromeric nucleosome recognition by centromere protein CENP-C. *Science* **340**, 1110–3 (2013).
41. Gallego, L. D. *et al.* Structural mechanism for the recognition and ubiquitination of a single nucleosome residue by Rad6-Bre1. *Proc. Natl. Acad. Sci. U. S. A.* **113**, 10553–8 (2016).
42. Baarends, W. M. *et al.* Increased phosphorylation and dimethylation of XY body histones in the Hr6b-knockout mouse is associated with derepression of the X chromosome. *J. Cell Sci.* **120**, 1841–51 (2007).
43. Jacquet, K. *et al.* The TIP60 Complex Regulates Bivalent Chromatin Recognition

- by 53BP1 through Direct H4K20me Binding and H2AK15 Acetylation. *Mol. Cell* **62**, 409–421 (2016).
44. Steunou, A. L., Rossetto, D. & Côté, J. in *Fundamentals of Chromatin* 147–212 (Springer New York, 2014). doi:10.1007/978-1-4614-8624-4\_4
  45. Tang, J. *et al.* Acetylation limits 53BP1 association with damaged chromatin to promote homologous recombination. *Nat. Struct. Mol. Biol.* **20**, 317–25 (2013).
  46. Sharma, N. *et al.* USP3 counteracts RNF168 via deubiquitinating H2A and  $\gamma$ H2AX at lysine 13 and 15. *Cell Cycle* **13**, 106–114 (2014).
  47. Wang, Z. *et al.* USP51 deubiquitylates H2AK13, 15ub and regulates DNA damage response. *Genes Dev.* **30**, 946–959 (2016).
  48. Lancini, C. *et al.* Tight regulation of ubiquitin-mediated DNA damage response by USP3 preserves the functional integrity of hematopoietic stem cells. *J. Exp. Med.* **211**, 1759–77 (2014).
  49. Nicassio, F. *et al.* Human USP3 Is a Chromatin Modifier Required for S Phase Progression and Genome Stability. *Curr. Biol.* **17**, 1972–1977 (2007).
  50. Mosbech, A., Lukas, C., Bekker-Jensen, S. & Mailand, N. The deubiquitylating enzyme USP44 counteracts the DNA double-strand break response mediated by the RNF8 and RNF168 ubiquitin ligases. *J. Biol. Chem.* **288**, 16579–16587 (2013).
  51. Yu, M. *et al.* USP11 is a negative regulator to  $\gamma$ H2AX ubiquitylation by RNF8/RNF168. *J. Biol. Chem.* **291**, 959–967 (2016).
  52. Typas, D. *et al.* The de-ubiquitylating enzymes USP26 and USP37 regulate homologous recombination by counteracting RAP80. *Nucleic Acids Res.* **43**, 6919–6933 (2015).
  53. Jiang, Q. & Greenberg, R. A. Deciphering the BRCA1 tumor suppressor network. *Journal of Biological Chemistry* **290**, 17724–17732 (2015).
  54. Jasin, M. Homologous repair of DNA damage and tumorigenesis: the BRCA connection. *Oncogene* **21**, 8981–8993 (2002).
  55. Wu, L. *et al.* Identification of a RING protein that can interact in vivo with the BRCA1 gene product. *Nat. Genet.* **14**, 430–40 (1996).
  56. Lorick, K. L. *et al.* RING fingers mediate ubiquitin-conjugating enzyme (E2)-dependent ubiquitination. *Proc. Natl. Acad. Sci. U. S. A.* **96**, 11364–11369 (1999).
  57. Huen, M. S. Y., Sy, S. M. H. & Chen, J. BRCA1 and its toolbox for the maintenance of genome integrity. *Nat. Rev. Mol. Cell Biol.* **11**, 138–148 (2010).
  58. Coleman, K. A. & Greenberg, R. A. The BRCA1-RAP80 complex regulates DNA repair mechanism utilization by restricting end resection. *J. Biol. Chem.* **286**, 13669–

- 13680 (2011).
59. Goldstein, M. & Kastan, M. B. Repair versus checkpoint functions of BRCA1 are differentially regulated by site of chromatin binding. *Cancer Res.* **75**, 2699–2707 (2015).
  60. Wu, J. *et al.* Histone ubiquitination associates with BRCA1-dependent DNA damage response. *Mol. Cell. Biol.* **29**, 849–860 (2009).
  61. Wu, W. *et al.* Interaction of BARD1 and HP1 is required for BRCA1 retention at sites of DNA damage. *Cancer Res.* **75**, 1311–1321 (2015).
  62. Zhang, F., Bick, G., Park, J.-Y. & Andreassen, P. R. MDC1 and RNF8 function in a pathway that directs BRCA1-dependent localization of PALB2 required for homologous recombination. *J. Cell Sci.* **125**, 6049–57 (2012).
  63. Zhang, F. *et al.* PALB2 Links BRCA1 and BRCA2 in the DNA-Damage Response. *Curr. Biol.* **19**, 524–529 (2009).
  64. Sy, S. M. H., Huen, M. S. Y. & Chen, J. PALB2 is an integral component of the BRCA complex required for homologous recombination repair. *Proc. Natl. Acad. Sci. U. S. A.* **106**, 7155–60 (2009).
  65. Orthwein, A. *et al.* A mechanism for the suppression of homologous recombination in G1 cells. *Nature* **528**, 422–426 (2015).
  66. Shakya, R. *et al.* BRCA1 Tumor Suppression Depends on BRCT Phosphoprotein Binding, But Not Its E3 Ligase Activity. *Science (80-. )*. **334**, 525–528 (2011).
  67. Reid, L. J. *et al.* E3 ligase activity of BRCA1 is not essential for mammalian cell viability or homology-directed repair of double-strand DNA breaks. *Proc. Natl. Acad. Sci. U. S. A.* **105**, 20876–20881 (2008).
  68. Zhu, Q. *et al.* BRCA1 tumour suppression occurs via heterochromatin-mediated silencing. *Nature* **477**, 179–184 (2011).
  69. Cao, L. *et al.* A Selective Requirement for 53BP1 in the Biological Response to Genomic Instability Induced by Brca1 Deficiency. *Molecular Cell* **35**, 534–541 (2009).
  70. Bouwman, P. *et al.* 53BP1 loss rescues BRCA1 deficiency and is associated with triple-negative and BRCA-mutated breast cancers. *Nat. Struct. Mol. Biol.* **17**, 688–695 (2010).
  71. Drost, R. *et al.* BRCA1 RING function is essential for tumor suppression but dispensable for therapy resistance. *Cancer Cell* **20**, 797–809 (2011).
  72. Li, M. *et al.* 53 BP 1 ablation rescues genomic instability in mice expressing ‘RING-less’ BRCA 1. *EMBO Rep.* **17**, 1–10 (2016).
  73. Drost, R. *et al.* BRCA1185delAG tumors may acquire therapy resistance through

- expression of RING-less BRCA1. *J. Clin. Invest.* **126**, 2903–2918 (2016).
74. Liu, X. *et al.* Somatic loss of BRCA1 and p53 in mice induces mammary tumors with features of human BRCA1-mutated basal-like breast cancer. *Proc. Natl. Acad. Sci. U. S. A.* **104**, 12111–12116 (2007).
  75. Wang, Y. *et al.* RING domain-deficient BRCA1 promotes PARP inhibitor and platinum resistance. *J. Clin. Invest.* **126**, 3145–3157 (2016).
  76. Kakarougkas, A. *et al.* Co-operation of BRCA1 and POH1 relieves the barriers posed by 53BP1 and RAP80 to resection. *Nucleic Acids Res.* **41**, 10298–10311 (2013).
  77. Chapman, J. R., Sossick, A. J., Boulton, S. J. & Jackson, S. P. BRCA1-associated exclusion of 53BP1 from DNA damage sites underlies temporal control of DNA repair. *J. Cell Sci.* **125**, 3529–34 (2012).
  78. Bunting, S. F. *et al.* 53BP1 inhibits homologous recombination in *brca1*-deficient cells by blocking resection of DNA breaks. *Cell* **141**, 243–254 (2010).
  79. Goldknopf, I. L. & Busch, H. Isopeptide linkage between nonhistone and histone 2A polypeptides of chromosomal conjugate-protein A24. *Proc. Natl. Acad. Sci. U. S. A.* **74**, 864–8 (1977).
  80. Schwartz, Y. B. & Pirrotta, V. A new world of Polycombs: unexpected partnerships and emerging functions. *Nat. Rev. Genet.* **14**, 853–64 (2013).
  81. Wang, L. *et al.* Hierarchical recruitment of polycomb group silencing complexes. *Mol. Cell* **14**, 637–646 (2004).
  82. Min, J., Zhang, Y. & Xu, R. M. Structural basis for specific binding of polycomb chromodomain to histone H3 methylated at Lys 27. *Genes Dev.* **17**, 1823–1828 (2003).
  83. Cao, R. *et al.* Role of histone H3 lysine 27 methylation in Polycomb-group silencing. *Science* **298**, 1039–43 (2002).
  84. Cooper, S. *et al.* Targeting Polycomb to Pericentric Heterochromatin in Embryonic Stem Cells Reveals a Role for H2AK119u1 in PRC2 Recruitment. *Cell Rep.* **7**, 1456–1470 (2014).
  85. Blackledge, N. P. *et al.* Variant PRC1 complex-dependent H2A ubiquitylation drives PRC2 recruitment and polycomb domain formation. *Cell* **157**, 1445–1459 (2014).
  86. Cooper, S. *et al.* Jarid2 binds mono-ubiquitylated H2A lysine 119 to mediate cross-talk between Polycomb complexes PRC1 and PRC2. *Nat. Commun.* **7**, 13661 (2016).
  87. Li, Z. *et al.* Structure of a Bmi-1-Ring1B polycomb group ubiquitin ligase complex. *J. Biol. Chem.* **281**, 20643–20649 (2006).
  88. Buchwald, G. *et al.* Structure and E3-ligase activity of the Ring-Ring complex of polycomb proteins Bmi1 and Ring1b. *EMBO J.* **25**, 2465–74 (2006).

89. Ismail, H., Andrin, C., McDonald, D. & Hendzel, M. J. BMI1-mediated histone ubiquitylation promotes DNA double-strand break repair. *J. Cell Biol.* **191**, 45–60 (2010).
90. Ginjala, V. *et al.* BMI1 is recruited to DNA breaks and contributes to DNA damage-induced H2A ubiquitination and repair. *Mol. Cell Biol.* **31**, 1972–82 (2011).
91. Pan, M.-R., Peng, G., Hung, W.-C. & Lin, S.-Y. Monoubiquitination of H2AX protein regulates DNA damage response signaling. *J. Biol. Chem.* **286**, 28599–607 (2011).
92. Liu, J. *et al.* Bmi1 regulates mitochondrial function and the DNA damage response pathway. *Nature* **459**, 387–392 (2009).
93. Chandler, H. *et al.* Role of polycomb group proteins in the DNA damage response—a reassessment. *PLoS One* **9**, e102968 (2014).
94. Shanbhag, N. M., Rafalska-Metcalf, I. U., Balane-Bolivar, C., Janicki, S. M. & Greenberg, R. A. ATM-Dependent chromatin changes silence transcription in cis to dna double-strand breaks. *Cell* **141**, 970–981 (2010).
95. Kakarougkas, A. *et al.* Requirement for PBAF in Transcriptional Repression and Repair at DNA Breaks in Actively Transcribed Regions of Chromatin. *Mol. Cell* **55**, 723–732 (2014).
96. Ui, A., Nagaura, Y. & Yasui, A. Transcriptional elongation factor ENL phosphorylated by ATM recruits polycomb and switches off transcription for DSB repair. *Mol. Cell* **58**, 468–482 (2015).
97. Scheuermann, J. C. *et al.* Histone H2A deubiquitinase activity of the Polycomb repressive complex PR-DUB. *Nature* **465**, 243–7 (2010).
98. Sahtoe, D. D., van Dijk, W. J., Ekkebus, R., Ovaa, H. & Sixma, T. K. BAP1/ASXL1 recruitment and activation for H2A deubiquitination. *Nat. Commun.* **7**, 10292 (2016).
99. Sahtoe, D. D. *et al.* Mechanism of UCH-L5 Activation and Inhibition by DEUBAD Domains in RPN13 and INO80G. *Mol. Cell* **57**, 887–900 (2015).
100. VanderLinden, R. T. *et al.* Structural Basis for the Activation and Inhibition of the UCH37 Deubiquitylase. *Mol. Cell* **57**, 901–911 (2015).
101. Yu, H. *et al.* Tumor suppressor and deubiquitinase BAP1 promotes DNA double-strand break repair. *Proc. Natl. Acad. Sci. U. S. A.* **111**, 285–90 (2014).
102. Ismail, I. H. *et al.* Germline mutations in BAP1 impair its function in DNA double-strand break repair. *Cancer Res.* **74**, 4282–4294 (2014).
103. Weake, V. M. & Workman, J. L. Histone Ubiquitination: Triggering Gene Activity. *Molecular Cell* **29**, 653–663 (2008).
104. Trujillo, K. M. & Osley, M. A. A Role for H2B Ubiquitylation in DNA Replication. *Mol. Cell* **48**, 734–746 (2012).

105. Northam, M. R. & Trujillo, K. M. Histone H2B mono-ubiquitylation maintains genomic integrity at stalled replication forks. *Nucleic Acids Res.* **44**, 9245–9255 (2016).
106. Shiloh, Y., Shema, E., Moyal, L. & Oren, M. RNF20-RNF40: A ubiquitin-driven link between gene expression and the DNA damage response. *FEBS Letters* **585**, 2795–2802 (2011).
107. Moyal, L. *et al.* Requirement of ATM-Dependent Monoubiquitylation of Histone H2B for Timely Repair of DNA Double-Strand Breaks. *Mol. Cell* **41**, 529–542 (2011).
108. Nakamura, K. *et al.* Regulation of Homologous Recombination by RNF20-Dependent H2B Ubiquitination. *Mol. Cell* **41**, 515–528 (2011).
109. Giannattasio, M., Lazzaro, F., Plevani, P. & Muzi-Falconi, M. The DNA damage checkpoint response requires histone H2B ubiquitination by Rad6-Bre1 and H3 methylation by Dot1. *J. Biol. Chem.* **280**, 9879–86 (2005).
110. Henry, K. W. *et al.* Transcriptional activation via sequential histone H2B ubiquitylation and deubiquitylation, mediated by SAGA-associated Ubp8. *Genes Dev.* **17**, 2648–2663 (2003).
111. Ramachandran, S. *et al.* The SAGA Deubiquitination Module Promotes DNA Repair and Class Switch Recombination through ATM and DNAPK-Mediated  $\gamma$ H2AX Formation. *Cell Rep.* **15**, 1554–65 (2016).
112. Vlaming, H. *et al.* Flexibility in crosstalk between H2B ubiquitination and H3 methylation in vivo. *EMBO Rep.* **15**, 1077–1084 (2014).
113. Mao, P., Meas, R., Dorgan, K. M. & Smerdon, M. J. UV damage-induced RNA polymerase II stalling stimulates H2B deubiquitylation. *Proc. Natl. Acad. Sci. U. S. A.* **111**, 12811–6 (2014).
114. Ng, H. H., Xu, R. M., Zhang, Y. & Struhl, K. Ubiquitination of histone H2B by Rad6 is required for efficient Dot1-mediated methylation of histone H3 lysine 79. *J. Biol. Chem.* **277**, 34655–34657 (2002).
115. Suganuma, T. & Workman, J. L. Crosstalk among Histone Modifications. *Cell* **135**, 604–607 (2008).
116. Chatterjee, C., McGinty, R. K., Fierz, B. & Muir, T. W. Disulfide-directed histone ubiquitylation reveals plasticity in hDot1L activation. *Nat. Chem. Biol.* **6**, 267–269 (2010).
117. McGinty, R. K. *et al.* Structure-activity analysis of semisynthetic nucleosomes: Mechanistic insights into the stimulation of Dot1L by ubiquitylated histone H2B. *ACS Chem. Biol.* **4**, 958–968 (2009).
118. McGinty, R. K., Kim, J., Chatterjee, C., Roeder, R. G. & Muir, T. W. Chemically ubiq-

- ubitylated histone H2B stimulates hDot1L-mediated intranucleosomal methylation. *Nature* **453**, 812–816 (2008).
119. Zhou, L. *et al.* Evidence that ubiquitylated H2B corrals hDot1L on the nucleosomal surface to induce H3K79 methylation. *Nat. Commun.* **7**, 10589 (2016).
  120. Wakeman, T. P., Wang, Q., Feng, J. & Wang, X.-F. Bat3 facilitates H3K79 dimethylation by DOT1L and promotes DNA damage-induced 53BP1 foci at G1/G2 cell-cycle phases. *EMBO J.* **31**, 2169–81 (2012).
  121. FitzGerald, J. *et al.* Regulation of the DNA damage response and gene expression by the Dot1L histone methyltransferase and the 53Bp1 tumour suppressor. *PLoS One* **6**, e14714 (2011).
  122. Oksenyich, V. *et al.* Histone Methyltransferase DOT1L Drives Recovery of Gene Expression after a Genotoxic Attack. *PLoS Genet.* **9**, e1003611 (2013).
  123. Davey, C. A., Sargent, D. F., Luger, K., Maeder, A. W. & Richmond, T. J. Solvent mediated interactions in the structure of the nucleosome core particle at 1.9 Å resolution. *J. Mol. Biol.* **319**, 1097–1113 (2002).





# Chapter 3

## **USP48 restrains resection by site specific cleavage of the BRCA1 ubiquitin mark from H2A.**

Michael Uckelmann<sup>\*1</sup>, Ruth M. Densham<sup>\*2</sup>, Herrie H. K. Winterwerp<sup>1</sup>, Alexander Fish<sup>1</sup>, Titia K. Sixma<sup>#1</sup>, Joanna R. Morris<sup>#2</sup>

<sup>1</sup>Division of Biochemistry and Cancer Genomics Centre, Netherlands Cancer Institute, Plesmanlaan 121, 1066 CX Amsterdam, the Netherlands

<sup>2</sup>Birmingham Centre for Genome Biology and Institute of Cancer and Genomic Sciences, Medical and Dental Schools, University of Birmingham, Birmingham, B15 2TT United Kingdom.

\* These authors contributed equally

# corresponding authors

### Abstract

BRCA1/BARD1-catalyzed ubiquitination of histone H2A is an important regulator of the DNA damage response, priming for repair by homologous recombination. However no specific deubiquitinating enzymes (DUBs) are known to antagonize this function. Here we identify USP48 as a H2A DUB, specific for the BRCA1 ubiquitination site. Detailed biochemical analysis shows that an auxiliary ubiquitin modulates USP48 activity, which has possible implications for its regulation in vivo. We show that USP48 antagonizes BRCA1 E3 ligase function in cells. Consequently, in BRCA1-proficient cells, loss of USP48 results in extended resection lengths and extended 53BP1 positioning. Moreover USP48 acts to restrain gene conversion and single strand annealing and USP48 repression confers a survival benefit to cells treated with camptothecin. We propose that USP48 promotes genome stability by antagonizing BRCA1 E3 ligase function.

### Introduction

To assure genomic integrity and protect against disease such as cancer, DNA double strand breaks (DSB) need to be faithfully repaired. The cell can employ two major pathways to repair DSB, homologous recombination (HR), commonly thought of as error free, and the more error-prone non-homologous end joining (NHEJ). The choice between these two pathways is made at the point of DNA end resection<sup>1</sup>. Long-range resection is crucial for repair through HR and short resection will initiate NHEJ repair. Specific ubiquitination of H2A by BRCA1/BARD1 can act to increase DNA resection lengths<sup>2</sup>.

Minimal processing directs repair to non-homologous end-joining (NHEJ), and 5' end resection in late S-phase and G2 directs repair to homologous recombination (HR) mechanisms including gene conversion (GC), the most accurate, and thus least mutagenic form of DSB repair (reviewed in<sup>3,4</sup>). However extensive resection can result in the use of a sub-pathway of HR-repair known as single-strand annealing (SSA). In this process extended resection reveals direct repeat sequences around the DNA breaks that can be annealed, followed by flap processing to delete the material between the repeats (reviewed in<sup>4-6</sup>). SSA and GC compete for the repair of DSBs in budding yeast<sup>7</sup>, but since SSA requires extended resection to expose direct repeats, limiting DNA end processing is critical to promoting accurate DSB repair. How the degree of end resection is controlled is not well understood.

Resection takes place over several defined phases. It begins by the endo- and then exonuclease activity of MRE11-CtIP, and is extended by the Exo1 and BLM-DNA2 helicase/endonuclease complexes. The extensive ssDNA is bound by RPA, which is either exchanged for the recombinase RAD51, required for homology searching, strand invasion and gene conver-

sion, or the RPA bound sequences are annealed by RAD52 if homologous sequences are present in the resected ends<sup>4-6</sup>.

BRCA1, the breast and ovarian cancer predisposition gene product, and 53BP1, the p53 binding protein, are opposing regulators to the degree of DNA end resection. In the absence of BRCA1, resection is blocked by 53BP1 and its effector proteins, promoting NHEJ and suppressing HR repair (reviewed in<sup>8,9</sup>). BRCA1 overcomes the 53BP1-mediated block through interaction with the resection protein CtIP<sup>10</sup> and through its E3 ubiquitin ligase activity<sup>2</sup>. The N-termini of BRCA1 and BARD1 associate and establish an active E3 ubiquitin ligase<sup>11,12</sup>. The role the ligase activity plays in BRCA1 function has been controversial. Studies on the catalytically inactive Brca1-I26A mutant in murine cells suggest no effect on DNA repair<sup>13,14</sup>, whereas studies on RING-less Brca1 variants and another ligase deficient point mutant link loss of ligase function to genomic instability and defects in homologous recombination<sup>15-17,36</sup>. Synthetic viability of BRCA1 mutants and knock out strains with 53BP1 loss further suggests an important role in DNA repair pathway determination<sup>17-19</sup>.

Recently the target of BRCA1 E3 ligase activity has been identified as a specific group of lysines on H2A<sup>20</sup>, establishing a third specific ubiquitination site on H2A. K13/15 and K119 on H2A have previously been established as targets of RNF168 and polycomb complexes 1 (PRC1) respectively<sup>21,22</sup>. Ubiquitination of H2A by BRCA1 promotes resection and HR-repair through the recruitment and activity of the Swr1-like remodeler, SMARCAD1, which repositions the 53BP1 block and permits resection<sup>2</sup>. Conversely, in the absence of 53BP1, or its recruitment pathway, resection lengths are extended<sup>10,23-26</sup> and SSA becomes the dominant repair pathway<sup>26</sup>.

Deubiquitinating enzymes (DUBs) are able to counteract ubiquitination by cleavage of the isopeptide bond between ubiquitin's C-terminus and the target protein lysine. Several DUBs have been suggested to target H2A<sup>27-31</sup> but very little is known about their site specificity or their role in the different repair pathways. We wanted to investigate whether DUBs that act on H2Aub substrates show site specificity and whether known H2A DUBs would counteract the BRCA1-induced DNA damage response.

To find DUBs antagonizing BRCA1 E3 ligase activity we tested a panel of DUBs for site specific H2A deubiquitination. In this analysis USP48, previously identified as an interactor of ubiquitinated nucleosomes<sup>32</sup> but otherwise poorly characterized, appeared specific for the BRCA1 site and seems to need an auxiliary ubiquitin to be fully active. We show that in cells USP48 counteracts BRCA1 E3 ligase activity, restricting DNA end resection and RAD51 recruitment. Knock down of USP48 increases SSA and confers a survival benefit to cells treated with camptothecin. We propose USP48 as a novel regulator of the DNA damage response,

counteracting BRCA1 E3 ligase activity.

### 3

## Results

### Assessing site specificity of H2A DUBs

Each of the E3 ligases that modify H2A, specifically monoubiquitinates distinct groups of lysines. K125/127/129 are ubiquitinated by BRCA1/BARD1 ( $H2A^{BRCA1ub}$ ), K118/119 by PRC1 complexes ( $H2A^{PRC1ub}$ ) and K13/15 by RNF168 ( $H2A^{168ub}$ ). This site specificity is retained *in vitro*<sup>20-22</sup> and allows reconstitution of ubiquitinated nucleosomes. We wondered if there are DUBs specific for these three sites. We selected a subset of DUBs, previously suggested to deubiquitinate H2A (USP3, USP16, BAP1/ASXL1<sup>27-31</sup>) and/or being involved in the DNA damage response (USP1/UAF1, USP11, USP7, USP15, USP12/UAF1)<sup>33</sup>. We included USP48 because it has been identified as a potent binder of ubiquitinated nucleosomes<sup>32</sup>

We produced all the DUBs recombinantly and purified them for biochemical characterization (Figures S1a and b). Full kinetic analysis, done on minimal substrate ubiquitin-rhodamine ( $Ub^{Rho}$ ) in which ubiquitin is linked to a cleavable small peptide labeled with Rhodamine and the increase of fluorescence intensity due to liberation of free fluorescent Rhodamine from the quenched substrate is measured, show that all DUBs are active (Figure S1a and Supplemental Table 1).

We then designed an assay for site specific cleavage of ubiquitinated nucleosome core particles (NCPs) using a fluorescence based approach where a drop in the fluorescence polarization (FP) signal indicates cleavage (Figure 1a). We tested our panel of DUBs in this assay (Figures S1c, d) and the results indicate that most DUBs have no clear substrate preference. We normalized the observed rates from this assay to the activity of the respective DUBs on minimal substrate (Figure S1e) to assess if a nucleosomal substrate is preferred over the minimal substrate (Figure 1b). Of all DUBs tested USP3 and USP48 seem to prefer the nucleosomal substrate. USP48 has a preference for  $H2A^{BRCA1ub}$  over  $H2A^{168ub}$  and  $H2A^{PRC1ub}$ .

#### USP48 is specific for $H2A^{BRCA1ub}$

Analysis of USP48 cleavage time courses on western blot confirmed the observed preference for  $H2A^{BRCA1ub}$  over  $H2A^{168ub}$  or  $H2A^{PRC1ub}$  (Figure 1c). Surprisingly, USP48 only cleaves  $H2A^{BRCA1ub}$  efficiently if H2A is ubiquitinated on more than one lysine ( $H2A^{BRCA1ub3}$ ,  $H2A^{BRCA1ub2}$ ). To test if this reflects a general preference for multi-monoubiquitinated substrates or a site specificity for the BRCA1-site we created NCP substrates where we push the reaction equilibrium to enrich for  $H2A^{168ub2}$ ,  $H2A^{PRC1ub2}$  and  $H2A^{BRCA1ub2/3}$  (Figure S2a, "0" time points). Cleavage was analyzed on gel with fluorescently labeled ubiquitin as readout (Figure S2a). The

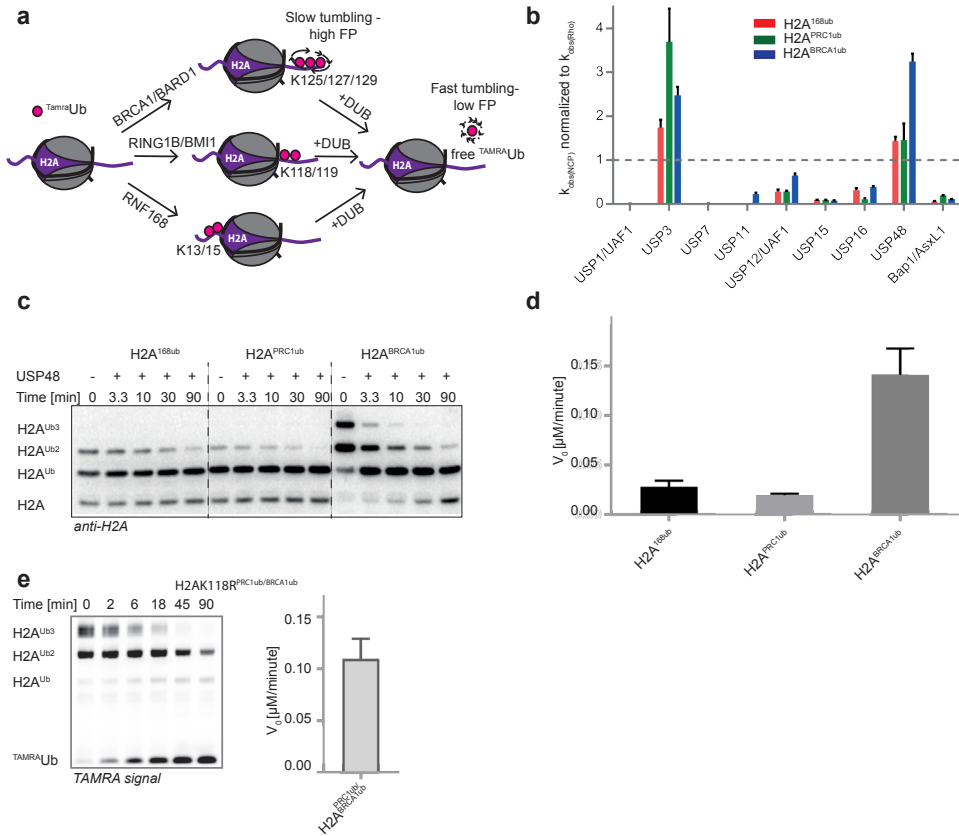


**Figure 1 USP48 specifically deubiquitinates H2A<sup>BRCA1ub</sup>**

**a** Schematics of the fluorescence polarization screen. Recombinant nucleosome core particles are site specifically ubiquitinated using the E3 ligase named and TAMRA-Ub. Upon addition of a DUB, cleavage can be followed by a decrease in FP signal.

**b** USP48 prefers nucleosomal substrates. Site specific cleavage of H2A<sup>168ub</sup>, H2A<sup>PRC1ub</sup> and H2A<sup>BRCA1ub</sup> in relation to activity on minimal substrate. Observed k values from the FP assay ( $k_{obs(NCP)}$ ) (Figure S1c) were normalized to observed k values on minimal substrate ( $k_{obs(Rho)}$ ) (Figure S1e). A value above one indicates that NCPs are the preferred substrate. Replicates of two experiments  $\pm$  SEM

**c** Time course of USP48 cleavage of H2A<sup>168ub</sup>, H2A<sup>PRC1ub</sup> and H2A<sup>BRCA1ub</sup>, anti-H2A western blot. USP48 only cleaves efficiently when more than one ubiquitin is present on the BRCA1-site.

**d** USP48 cleaves multi-monoubiquitinated H2A<sup>BRCA1ub</sup> faster than multi-monoubiquitinated H2A<sup>168ub</sup> and H2A<sup>PRC1ub</sup>. Quantification of the initial reaction velocity ( $V_0$ ) of USP48 measured by the liberation of free TAMRA-Ub. Gels used for quantification are shown in Figure S2A. Replicates of two experiments  $\pm$  SEM

**e** USP48 does not cleave H2A<sup>PRC1ub</sup> when H2A<sup>BRCA1ub</sup> is present. Left panel: Cleavage of NCPs, ubiquitinated on PRC1 site with unlabeled ubiquitin and on the BRCA1 site with TAMRA-Ub, by USP48 was followed on gel. The TAMRA fluorescence is used as readout. Right panel: Quantification of the initial reaction velocity ( $V_0$ ) measured by liberation of free ubiquitin. Replicates of two experiments  $\pm$  SEM

experiments show that USP48 can cleave all three substrates but shows a preference for H2A<sup>BRCA1ub</sup>. Comparison of the initial linear reaction rates revealed that H2A<sup>BRCA1ub</sup> is cleaved with an activated rate, roughly five times faster than on the other two sites (Figure 1d). We conclude that USP48 only cleaves H2A<sup>BRCA1ub</sup> efficiently if more than one ubiquitin is present

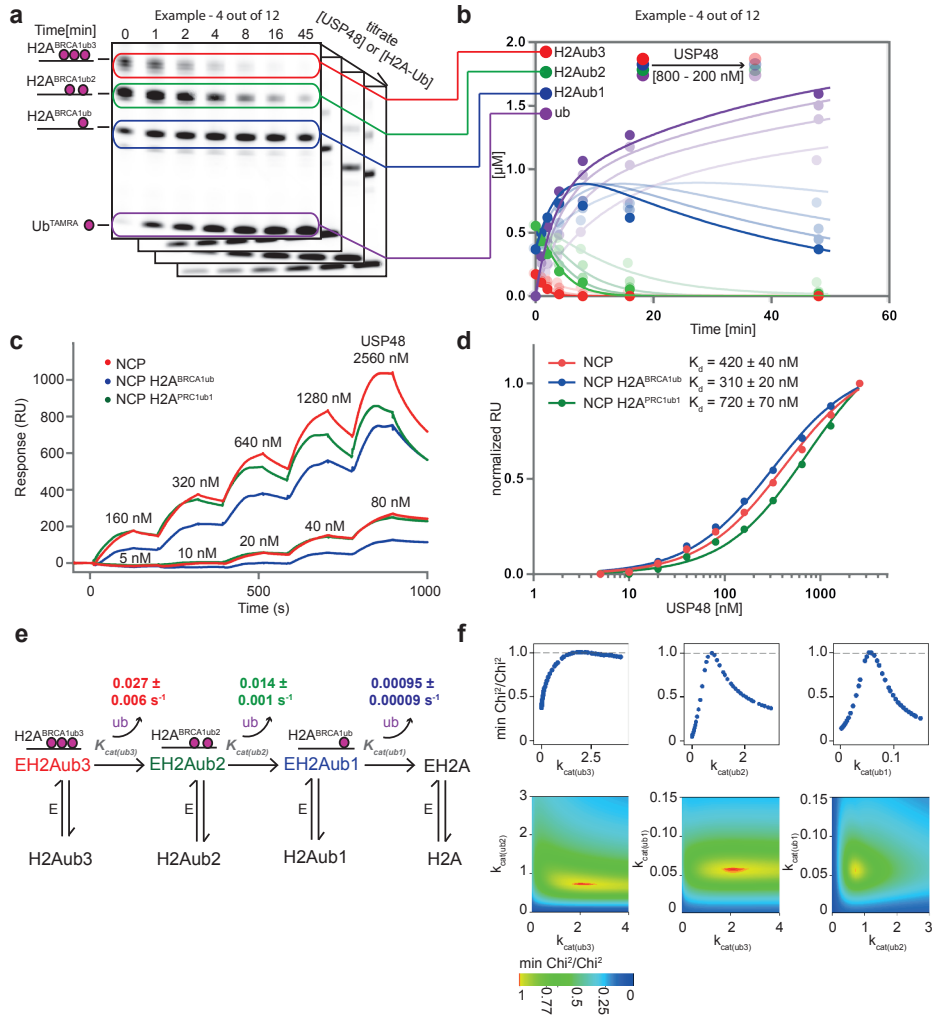


**Figure 2** USP48 cleavage rates on H2A<sup>BRCA1ub</sup> are modulated by an auxiliary ubiquitin

**a** An auxiliary ubiquitin activates USP48 processivity. Gel-based assay to measure USP48 cleavage of H2A<sup>BRCA1ub</sup>. TAMRA-Ub was used as readout. Cleavage was recorded under several different substrate and enzyme concentrations. Four (stacked) gels are shown as an example (Figure S3 for the full panel).

**b** Quantification of **a**. 4 out of 12 different conditions shown as an example (Figure S2 for full panel). Solid lines show fit obtained by global fitting of all 12 quantified time courses and binding data to the model defined in **e** using *Kintek Explorer*.

**c** Binding of USP48 to H2A<sup>BRCA1ub</sup>, H2A<sup>PRC1ub</sup> and unmodified nucleosomes measured by surface plasmon resonance. Nucleosomes were immobilized on the surface. 10 successive injections of different USP48 concentrations (indicated).

**d** USP48 binds nucleosomes of different ubiquitination status with similar affinities. Processed and fitted data from **c**.  $K_d$  and standard error of the fit are indicated.

**e** USP48 cleaves H2A<sup>BRCA1ub</sup> in nucleosomes 15-30 times faster than when auxiliary ubiquitin is present. Kinetic model describing USP48's cleavage pattern on H2A<sup>BRCA1ub</sup> with the fitted values for  $k_{cat}(ub3)$ ,  $k_{cat}(ub2)$  and  $k_{cat}(ub1)$  and the standard error of the fit.

**f** Parameters for  $k_{cat}(ub3)$ ,  $k_{cat}(ub2)$  and  $k_{cat}(ub1)$  in **e** are well constrained by the data. Evaluation of the goodness of fit. The upper three panels show how well defined the lower and upper boundaries are for the individual parameters. The lower panel shows how Chi<sup>2</sup> varies when two of the fitted variables are varied against each other. Red indicates a Chi<sup>2</sup> minimum.

on the site. We will refer to the additional ubiquitin needed for activity as the auxiliary ubiquitin because it aids USP48 cleavage but itself does not get cleaved.

We wondered how the observed preference for H2A<sup>BRCA1ub</sup> translates to a situation where multiple ubiquitination sites are available for cleavage on a single H2A. To test this we generated NCPs with an unlabeled ubiquitin conjugated to the polycomb site and a <sup>TAMRA</sup>Ub conjugated to the BRCA1 site. As expected, we find that USP48 cleaves these substrates with the activated rate (Figure 1e). Interestingly, no monoubiquitinated H2A with <sup>TAMRA</sup>Ub conjugated is observed, showing that the unlabeled ubiquitin on the PRC1 site is not cleaved as long as there is a labeled ubiquitin on the BRCA1 site. In other words, H2A<sup>PRC1ub</sup> will not get cleaved as long as H2A<sup>BRCA1ub</sup> is available, once again highlighting the specificity of USP48 for H2A<sup>BRCA1ub</sup>.

We next analyzed cleavage of all the possible di-ubiquitin linkages by USP48 (Figure S2b) and find that very little cleavage by USP48 takes place (USP16 serves as an unspecific positive control), further suggesting a certain degree of specificity for the nucleosome. Taken together our data suggests USP48 to be a DUB specific for multi-monoubiquitinated H2A<sup>BRCA1ub</sup>

### USP48 needs an auxiliary ubiquitin to be fully active

To investigate the effect of the auxiliary ubiquitin on USP48 rates we performed substrate binding assays combined with a detailed kinetic analysis. We quantified USP48 catalyzed cleavage of H2A<sup>BRCA1ub</sup> under different conditions, achieved by titrating either USP48 concentration while keeping substrate concentration fixed or vice versa (Figures 2a and b). We then tested affinities of USP48 for nucleosomes of different ubiquitination status and find that affinities are essentially the same for unmodified nucleosomes (NCP), monoubiquitinated nucleosomes (H2A<sup>PRC1ub1</sup>) and multi-monoubiquitinated nucleosomes (H2A<sup>BRCA1ub</sup>) (Figure 2c and d). We fitted these binding and kinetic data, using the software *KinTek Explorer*<sup>34,35</sup>, to the simplest model that could describe the observed USP48 H2A deubiquitination pattern (Figure 2e). We fixed the binding constants of the model to approximate the equilibrium constants determined by the Surface Plasmon Resonance (SPR) experiments (Figure 2d) and fitted the catalytic rates using the data from the quantified cleavage reactions (Figure S3a) as input. The obtained best fit values for  $k_{cat(ub3)}$ ,  $k_{cat(ub2)}$  and  $k_{cat(ub1)}$  describe the experimental data well (Figure 2b for example and Figure S3 for all experiments) and are well constrained (Figure 2f).  $k_{cat(ub1)}$  and  $k_{cat(ub2)}$  fall into a well-defined local minimum. For  $k_{cat(ub3)}$  the lower boundaries are well defined which allows the conclusion that  $K_{cat(ub3)}$  should always be faster than  $k_{cat(ub1)}$ . The kinetic modeling indicates increased processivity when an auxiliary ubiquitin is present. The rates for  $k_{cat(ub3)}$  ( $0.027 \text{ s}^{-1}$ ) and  $k_{cat(ub2)}$  ( $0.014 \text{ s}^{-1}$ ) are similar, whereas

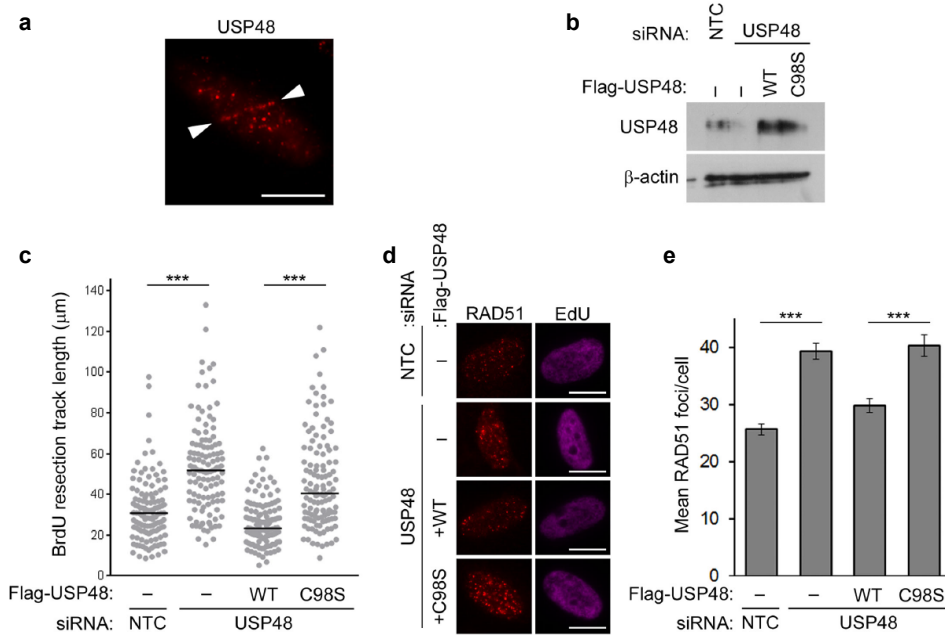


**Figure 3 USP48 deubiquitinase activity restrains resection.**

**a** USP48 recruits to sites of damage. BrdU sensitised HeLa cells were subjected to laser stripe irradiation followed by fixation after 1 hour and staining for endogenous USP48. White arrows mark the laser-induced damage stripe. Scale bar = 10  $\mu$ m.

**b** Expression levels of USP48 in stable HeLa FlpIn cell lines following depletion of USP48 and DOX-induced complementation of siResistant Flag-WT or Flag-C98S-USP48.

**c** USP48 knockdown increases resection length. Resection lengths were measured in HeLa cells depleted for USP48 and complemented as in B. Cells were treated with 10 mM BrdU for 24 hours with addition of 10  $\mu$ M Olaparib for the final 16 hours. Cells were lysed and DNA fibres spread before staining for BrdU-positive single-stranded DNA resection tracks. A minimum of 120 tracks were measured using ImageJ for each condition. Bars indicate median. \*\*\*  $p < 0.005$  Mann-Whitney test.

**d** USP48 knockdown increases Rad51 foci formation. Foci formation in S-phase (EdU positive) HeLa cells depleted for USP48 and complemented as in B. Cells were fixed at 2 hours post-5 Gy irradiation. Scale bars = 10  $\mu$ m.

**e** Graph shows quantification of mean number of RAD51 foci per S-phase cell ( $n=200$  cells from 3 independent experiments, error bars are S.E.M). \*\*\*  $p < 0.005$  Student's T-test.

$k_{\text{cat}(\text{ub1})}$  is roughly 15 times slower ( $0.00095 \text{ s}^{-1}$ ). These results can be explained by a catalytic activation in the presence of the auxiliary ubiquitin, possibly induced by a conformational change or reorientation, or the inability of USP48 to cleave one of the three ubiquitinated lysines efficiently.

We further asked if free ubiquitin could act as the auxiliary ubiquitin and increase USP48 processivity. To address this we performed  $\text{Ub}^{\text{Rho}}$  and  $\text{H2A}^{\text{BRCA1ub}}$  cleavage assays in the presence and absence of ubiquitin (Figures S3b and c). On both substrates the addition of free ubiquitin does not lead to activation of USP48. This indicates that the activating ubiquitin needs to be on the nucleosome and possibly in a defined orientation towards USP48 to cause activation. In our analysis we regarded affinities measured by SPR (Figure 2d) as actual



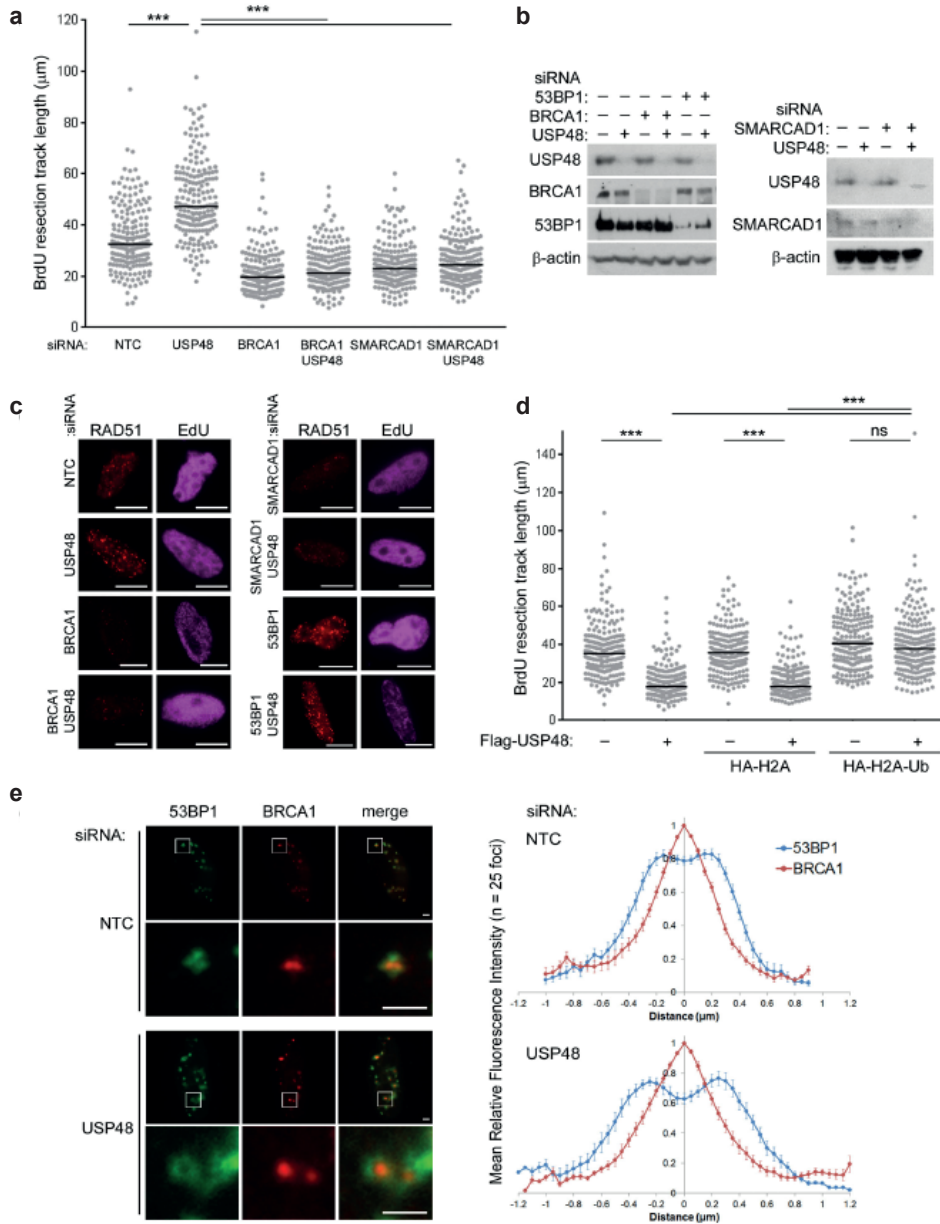


**Figure 4 USP48 antagonizes BRCA1-mediated resection.**

**a** USP48 knockdown only shows an effect if BRCA1 and SMARCAD1 are present. Resection lengths were measured in HeLa cells depleted as indicated. Cells were treated with 10 mM BrdU for 24 hours with addition of 10 µM Olaparib for the final 16 hours. Cells were lysed and DNA fibres spread before staining for BrdU positive single-stranded DNA resection tracks. 190 tracks were measured using ImageJ for each condition. Bars indicate median. \*\*\* p<0.005 Mann-Whitney test.

**b** Western blots to demonstrate protein expression levels following siRNA as indicated.

**c** Rad51 foci formation in S-phase (EdU positive) HeLa cells depleted as indicated. Cells were fixed at 2 hours post-5Gy irradiation. Scale bars = 10 µm.

substrate affinities. However, in order to engage the substrate (ubiquitin on H2A) a reorientation or conformational change of USP48 may occur on the nucleosome. This second step might be masked in our assays as binding is dominated by the affinities for the nucleosome. In the kinetic analysis such a possible conformational change would be reflected in the calculated  $k_{\text{cat}}$  values which include the rate for catalysis and the rate for any possible conformational change. Therefore the detailed analysis does not yet fully assign the role of the auxiliary ubiquitin, but it does firmly establish that some form of activation takes place.

In summary our biochemical analysis identified USP48 as a deubiquitinating enzyme specific for nucleosomes ubiquitinated by BRCA1/BARD1, identifying what is to our knowledge the first H2A DUB with in vitro specificity for the BRCA1-site. We also demonstrated the need of an auxiliary ubiquitin for USP48 to be fully active. We next sought to analyze USP48's importance in cells.

#### **USP48 deubiquitinating activity restrains resection.**

Since BRCA1/BARD1 is known to ubiquitinate H2A following DNA DSBs<sup>2,20</sup>, we sought to address whether USP48 is likely to have a role in the response to DSBs by first assessing USP48 localization to laser-induced lines of DNA damage. Endogenous USP48 was detected along the line of the laser indicating recruitment to sites of DNA damage (Figure 3a). The BRCA1:-BARD1 E3 Ub ligase activity promotes long-range resection<sup>2</sup>. To assess the possible role of a DUB capable of cleaving the BRCA1 H2A mark we next assessed DNA resection. Cells treated with USP48 and control siRNA were incubated with Bromodeoxyuridin (BrdU) exposed to olaparib and track-lengths of exposed BrdU epitope, indicative of ssDNA, were spread and measured. Median lengths of ssDNA were longer in cells treated with USP48 siRNA than in control cells (from 31.2  $\mu\text{m}$  in control cells to 51.7  $\mu\text{m}$  in USP48 depleted cells) (Figures 3b-c). Moreover expression of siRNA-resistant wild type (WT) USP48 restored shorter lengths to depleted cells (25.7  $\mu\text{m}$ ) whereas expression of USP48 in which the catalytic cysteine was mutated to serine (C98S) failed to do so (40  $\mu\text{m}$ )(Figures 3b-c).

The single-strand DNA binding protein RPA quickly loads on the resected, ssDNA and is then exchanged for RAD51 to enable subsequent strand invasion and gene conversion. We noted that cells depleted for USP48 showed an increase in the numbers of RAD51 foci compared

- **d** USP48 overexpression phenotypes can be rescued by co-expression of an uncleavable H2A-Ub fusion. Resection lengths were measured in HeLa cells depleted as indicated. Cells were prepared as in A and 210 tracks were measured using ImageJ for each condition. Bars indicate median. \*\*\*  $p < 0.005$ , ns=non-significant, Mann-Whitney test.
- e** USP48 restricts positioning of 53BP1 in damage foci. Images of BRCA1 and 53BP1 in cells treated with USP48 siRNA exposed to 2 Gy IR and fixed 8 hours later. Quantification of mean relative intensity profiles for co-localising foci.  $n=25$ , bars = S.E.M.

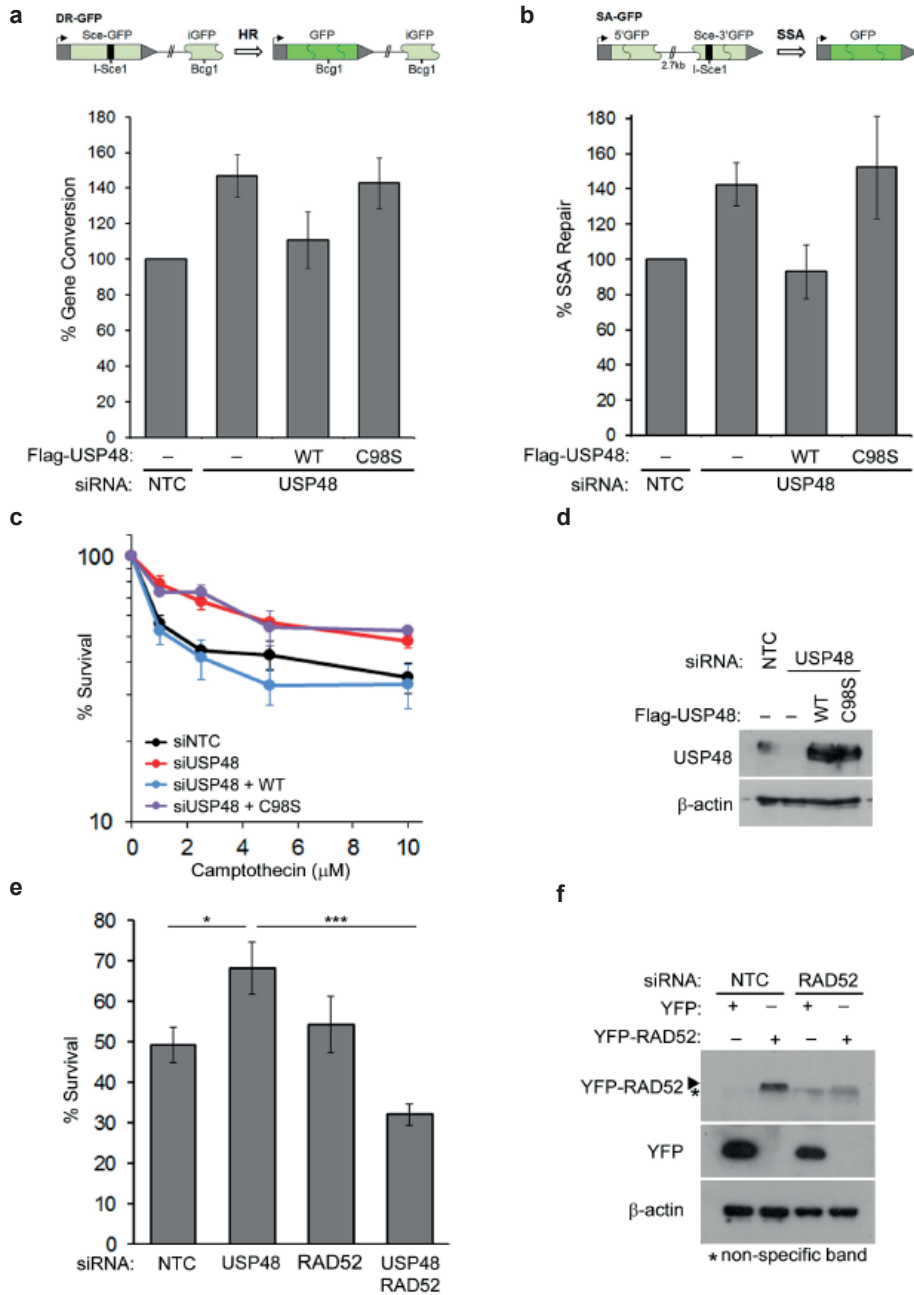


**Figure 5 USP48 restrains homology-directed repair mechanisms**

**a** Gene conversion (GC) was measured using U2OS DR3-GFP reporter cells as illustrated. Note functional GFP cannot be produced by SSA from this substrate as the template iGFP lacks the 5' and 3' regions of GFP<sup>38</sup>. Cells depleted for USP48 were transfected with RFP, Sce1 and either Flag-WT or Flag-C98S-USP48. GFP-positive cells were normalised to RFP-transfection efficiency. %-repair is given compared to NTC. Graph shows mean, n=5, error bars are S.E.M. **b** Single-strand annealing (SSA) was measured using U2OS SA-GFP reporter cells as illustrated. The two GFP fragments of the substrate share 266 nucleotides of homology. In principle GC with crossing over could also produce functional GFP, however these have been shown to be rare events<sup>38</sup>. Cells were treated and analysed as in **a**. Graph shows mean, n=3, error bars are S.E.M.

to control cells, as did those complemented with the siRNA-resistant catalytic mutant form of the enzyme (Figures 3d-e and S4a-b). In contrast, expression of siRNA-resistant wild-type (WT) enzyme brought the observed RAD51 foci down to levels similar to those seen in control cells (Figures 3d-e). Together these data indicate that the catalytic function of USP48 is required to restrain DNA resection lengths.

#### **USP48 antagonises the BRCA1-H2Aub-SMARCAD1 resection pathway.**

Resection promoted by the BRCA1-BARD1 E3 Ub ligase promotes SMARCAD1-mediated remodelling of chromatin-associated 53BP1<sup>2</sup>. To address whether USP48 is relevant to this pathway we tested whether the increased resection lengths observed on USP48 loss requires BRCA1 or SMARCAD1. As expected<sup>2</sup>, loss of BRCA1 or SMARCAD1 alone resulted in shortened ssDNA lengths (respectively 19.5 and 23.1  $\mu\text{m}$ , compared to 32.6  $\mu\text{m}$  in control cells Figures 4a-b). Significantly, loss of USP48 did not change the ssDNA lengths in BRCA1 or SMARCAD1 depleted cells (respectively 21.3 and 24.4  $\mu\text{m}$  in co-depleted cells compared to 47.1  $\mu\text{m}$  in USP48 depleted cells (Figure 4a), suggesting that repressing USP48 expression has little impact on resection if there is no ubiquitination to be cleaved or no reader to interpret that ubiquitination mark.

Consistent with the relationship between USP48 and BRCA1 and SMARCAD1 in resection RAD51 foci numbers remain decreased in cells co-depleted for BRCA1, or SMARCAD1 and USP48 (Figures 4c and S4c-e). Intriguingly loss of USP48 and 53BP1 have a similar impact on RAD51 foci numbers as loss of either protein alone (Figures 4c and S4c-e), suggesting the impact of USP48 loss on RAD51 nucleofilament formation is similar and in the same pathway as 53BP1 removal.

We<sup>2</sup> and others<sup>36</sup> have noted that expression of a fusion protein in which ubiquitin is genetically fused to the C-terminus of H2A can restore measures of gene conversion in BRCA1/BARD1 deficient cells. Such a fusion lacks an isopeptide bond and is resistant to proteases. To test the hypothesis that USP48 acts to cleave ubiquitin from the C-terminus of H2A in cells we addressed the impact of ectopic USP48 over-expression on resection lengths in cells expressing control H2A and an H2A-Ub fusion. (Note previous analysis has shown ectopic H2A and H2A-Ub are incorporated into chromatin<sup>2</sup>). Increased USP48 expression resulted in short ssDNA lengths (17.9  $\mu\text{m}$ , compared to 35.2  $\mu\text{m}$  in controls), consistent with the enzyme's ability to restrict resection (Figure 4d). This effect was unaffected by co-expression of

- **c** Camptothecin colony survival curves of HeLa cells depleted for USP48 and complemented with Flag-WT- or Flag-C98S-USP48. Graph shows mean % survival normalised to untreated controls, n=4,, error bars are S.E.M.
- d** Western blot shows USP48 expression levels.
- e** Camptothecin colony survival curves of HeLa cells depleted for USP48 and/or RAD52. Graph shows mean % survival normalised to untreated controls, n=6, error bars are S.E.M. \*\*\* p<0.005, \* p<0.05, Student's T-test.
- f** Western blot shows levels of YFP-RAD52 expression as a marker for RAD52 siRNA efficiency.

H2A (where they remained 17.8  $\mu\text{m}$ ). In contrast, when the H2A-Ub fusion was co-expressed increased USP48 expression did not result in short ssDNA lengths (lengths of 37.6  $\mu\text{m}$ ) (Figure 4d). Thus a protease-resistant H2A-Ub renders resection insensitive to the impact of USP48 overexpression, consistent with the enzyme's function in cleaving C-terminal H2A modifications.

These data are consistent with the notion that USP48 DUB activity acts to restrain resection through processing the H2A<sup>BRCA1ub</sup> and thus in turn restrains SMARCAD1-mediated remodeling. A consequence of BRCA1 ligase activity and SMARCAD1 function is the positioning of 53BP1 to the periphery of the IR foci<sup>2</sup>. To test the impact of USP48 on 53BP1 we measured the distribution of 53BP1 in foci associated with BRCA1 in USP48 depleted and control cells. 53BP1 accumulations exhibited a greater spread in USP48 depleted cells compared to controls (half peak intensity width  $\sim 1.1$   $\mu\text{m}$  in USP48 depleted cells compared to  $\sim 0.8$   $\mu\text{m}$  in control cells), and exhibited a larger 'hole' at foci cores (53BP1 peak to peak distance of  $\sim 0.5$   $\mu\text{m}$  within foci of USP48 depleted cells, compares to  $\sim 0.3$   $\mu\text{m}$  in control cells Fig 4e). Thus, consistent with its relationship with BRCA1, SMARCAD1 and H2A-Ub, USP48 appears to constrain 53BP1 repositioning at IRIF.

#### **USP48 restrains HR repair mechanisms.**

DNA end resection is the decision point committing cells to DSB repair by HR-mechanisms and inhibiting NHEJ. Incomplete resection results in IR sensitivity, and in reduced NHEJ repair, that can be rescued by inhibiting the initiation of resection<sup>37</sup>. USP48 depleted cells showed a slight reduction in NHEJ and slightly increased sensitivity to IR (Figures S4f-g). CtIP depletion restored IR-resistance in USP48 depleted cells (Figures S4h-i) suggesting that the sensitivity seen, is due to resection. This minor resection-dependent NHEJ impairment suggests USP48 contributes only in a small way to the decision between HR-mediated repair and NHEJ.

Long range resection creates stretches of ssDNA, quickly coated by RPA. In gene conversion RPA is exchanged for the RAD51 recombinase. Our data shows that USP48 loss increases resection and RAD51 nucleofilament foci numbers (Figures 4a-c). We also observed increased GFP products from an integrated substrate specific for gene conversion in cells transfected with I-Sce1<sup>38</sup> and depleted for USP48 or complemented with the catalytic mutant enzyme (Figure 5a). Taken together these data indicate USP48 activity restrains HR-repair by gene conversion. Since extended resection can reveal sequences that are substrates for SSA we also tested repair of an integrated reporter construct dependent on extensive resection and SSA for generation of a functional GFP (Figure 5b)<sup>38</sup>. USP48 depletion resulted in increased repair of this substrate which could similarly be suppressed by complementation with WT, but not with the catalytic mutant enzyme, consistent with the role of USP48 DUB activity

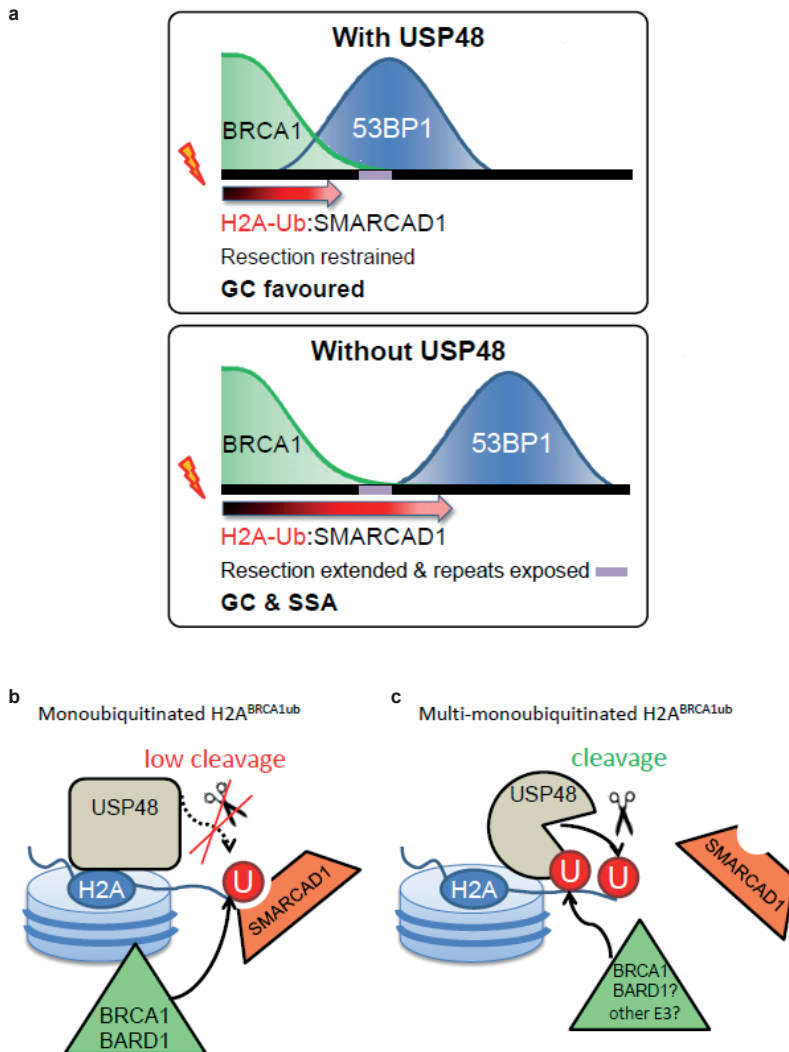


**Figure 6. Model of USP48 function in restricting extended DNA end resection.**

**a** USP48 cleaves the C-terminal Ub modification of H2A, limiting the extent of SMARCAD1 nucleosome remodelling and 53BP1 positioning. 53BP1 in turn restrains DNA end processing and consequently direct repeats are rarely exposed either side of the DSB, favoring GC (one side of the break is illustrated). Without USP48 activity H2A modification is unopposed and SMARCAD1 nucleosome remodeling is extended further from the break, resulting in 53BP1 positioning further from the break site. 53BP1 is unable to constrain extended resection, resulting in increased GC and, as repeats either side of the break are more often exposed, SSA is also increased.

**b** USP48 cannot cleave BRCA1-initiated H2A monoubiquitination efficiently, SMARCAD1 can bind and initiate downstream signaling

**c** A second ubiquitination on H2A can activate USP48, cleaving BRCA1-initiated ubiquitination, SMARCAD1 cannot engage with the nucleosome anymore and signalling is stopped.

restricting extended resection (Figure 3c).

To further assess the possible functional role of USP48 we addressed the consequences of its loss on survival of cells exposed to camptothecin, as repair of the DSB lesions produced relies on resection and HR-repair<sup>39</sup>. USP48 depleted cells, or cells complemented with cat-

alytically mutant enzyme, were more resistant to camptothecin than control cells or cells complemented with WT USP48 (Figures 5C-D). The annealing of flanking repeats in SSA requires RAD52<sup>40-42</sup>, to assess the contribution of RAD52-mediated mechanisms to the observed resistance we silenced RAD52 expression. Depletion of RAD52 alone had little impact on camptothecin sensitivity of control cells, but those in which USP48 was depleted RAD52 co-depletion dramatically increased sensitivity (Figures 5e-f). Thus a proportion of the camptothecin resistance seen on USP48 loss stems from a reliance of cells without the enzyme on HR-repair by SSA.

### Discussion

The data we present here establishes USP48 as a DUB that antagonises the BRCA1-dependent DNA resection. We show that USP48 specifically counteracts BRCA1-initiated H2A ubiquitination. By limiting the extent of this ubiquitination mark USP48 affects positioning of 53BP1 through SMARCAD1 and thus limits the length of resection. Its likely function is to fine tune resection length, to avoid over resection and prevent deleterious SSA. On a mechanistic level we show that USP48 needs an auxiliary ubiquitin on the substrate to be activated, possibly allowing cross-talk between different ubiquitination sites, generated by different ligases.

The FP assay we developed to measure site specific deubiquitination is a quick way to qualitatively assess site specificity of a panel of DUBs. Quantitation is complicated by the many variables influencing the FP signal: Some DUBs will bind free ubiquitin and change FP properties; additionally the ubiquitinated NCPs present a very heterogeneous substrate with a mix of mono-, di- and tri-ubiquitinated H2A, further complicating the analysis. Nevertheless, as a qualitative measure the assay proved to be useful and could be extended to other ubiquitinated substrates.

Under the conditions tested most DUBs do not show site specificity or a clear substrate specificity as they cleave both NCP and minimal substrate. In most cases the minimal substrate is cleaved more efficiently which suggests that nucleosomes are not the preferred target. With many other ubiquitinated proteins in the cell that are potentially better targets there might not be a need for clear cut substrate specificity as relative enzyme and substrate concentrations in a given situation will decide which target eventually gets cleaved. Participation in protein complexes and possible post-translational modifications will add another layer of regulation as reported for many other DUBs<sup>43</sup>.

Besides the enzymes tested there may be specific DUBs that were not included in this study, such as USP51, which has been reported to be specific for H2A<sup>168ub</sup><sup>44</sup>. Of the DUBs we did

test USP48 seems to be unique in showing clear intrinsic substrate specificity. Our biochemical analysis suggests that USP48 is specific for H2A ubiquitinated by BRCA1/BARD1.

Interestingly USP48 only reaches its full catalytic potential when more than one lysine on the BRCA1 site is ubiquitinated. A similar requirement for multiple ubiquitinations was reported for the proteasome associated DUB USP14<sup>45</sup>, which cleaves supernumerary chains. However, it is not clear whether USP14 cleaves any target with multiple sites ubiquitinated or only selected substrates, a question that can be extended to USP48. Our data suggest that USP48 is only fully active on H2A<sup>BRCA1ub</sup>, not on H2A<sup>PRC1ub</sup> nor H2A<sup>168ub</sup>, showing that it indeed only acts on a selected substrate. This suggests a two-fold regulatory switch for USP48: the first being the intrinsic target specificity for the BRCA1 site on the nucleosome, and the second the dependence on the auxiliary ubiquitin for full catalytic activation. While USP14 cleaves supernumerary chains marking targets for degradation, we show that USP48 can cleave signaling monoubiquitination highlighting that a similar regulatory mechanism is employed in two profoundly different pathways.

In cells we show that resection directed by BRCA1/BARD1 can be countered by the deubiquitinating activity of USP48. We show that manipulation of USP48 has striking consequences for DNA end resection. Without its activity cells exhibit increased DNA end processing which is dependent on BRCA1 and the remodeler SMARCAD1 and results in extended 53BP1 positioning around DNA break sites. Conversely, overexpression of USP48 drastically shortens resection lengths in a manner that can be reversed by expression of a protease resistant H2A-Ub fusion. These data suggest to us a model in which USP48-mediated removal of the BRCA1/BARD1 H2A-Ub mark on chromatin restrains subsequent SMARCAD1 function, thereby halting the mobilization of 53BP1, and bounding resection (Figure 6 a). In this model the opposing activities of BRCA1/BARD1 versus USP48 determine local H2A<sup>BRCA1ub</sup> modifications and consequently, in the presence of 53BP1, are capable of directing the degree of DNA end resection. We speculate that when USP48 is absent H2A-modification is sustained even at low levels of BRCA1/BARD1 accumulation so that SMARCAD1-mediated nucleosome sliding or H2A/B eviction<sup>46</sup> extends more widely than in control cells.

The observation that a H2A-Ub fusion rescues USP48 over-expression phenotypes is seemingly at odds with our biochemical data that suggests USP48 needs an auxiliary ubiquitin for efficient cleavage. The precise requirements for SMARCAD1's reading of the H2A-Ub C-terminus are not yet known. It is possible that the C-terminally linked ubiquitin fusion, due to its orientation and accessibility, can act as a more efficient signaling entity and thus alleviates the need, perhaps needed with endogenous substrate, for an additional ubiquitin to initiate signaling. Alternatively the results may indicate that one ubiquitin on the BRCA1 site is enough to initiate signaling but a second, auxiliary ubiquitin is needed to switch it off, through activa-



tion of USP48. This is an intriguing model given the recent data suggesting that BRCA1 activity is evolutionarily “underpowered”<sup>47</sup>, and thereby implying that too much activity may be toxic. Such a model would suggest two distinct ubiquitination sites: a signaling site responsible for SMARCAD1 recruitment and an auxiliary site, activating USP48 to cleave the ubiquitin on the signaling site. The auxiliary ubiquitin could be conjugated to one of the two unoccupied lysines on the BRCA1-site or may be placed by another E3 ligase on a different site, possibly by the PRC1 E3 ligase, at K118/119, providing a potential step in the observed crosstalk between DNA damage and transcriptional regulation (Figure 6 b & c)<sup>48–50</sup>.

Our data supports the idea of a continuum between increased resection that promotes GC and increased resection leading to SSA as we see both an increase in RAD51 foci and GC repair outcomes as well as increased SSA and RAD52 dependency when USP48 is inactive or reduced. While one model suggests ever longer ssDNA lengths may promote SSA over GC another possibility is that a proportion of increased resection does not reveal direct repeat sequences either side of the break, and thus encourages GC, while another exposes such sequences and SSA results. In contrast to our findings with USP48 loss, cells without 53BP1 exhibit a shift of HR repair dramatically to SSA<sup>26</sup>. A possible explanation for this difference is that in USP48 depleted cells, although 53BP1 is dramatically repositioned, it nevertheless restricts resection somewhat<sup>26</sup>.

Repetitive elements are numerous in the human genome so that restricting SSA would be expected to be significant in preventing large-scale rearrangements that cause deletions of sequences located between the repeats. High levels or activity of USP48 would be expected to decrease resection lengths and thus reduce GC, and phenocopy aspects of BRCA1 loss. In contrast USP48 loss or its decreased activity would be expected to increase resection lengths and favour SSA. Indeed, the occurrence of T-cell lymphoma in ATM-deficient mice is suppressed following Rad52 deletion and reduced SSA<sup>51</sup>, thus supporting a mutagenic role for SSA. In addition, cancers in individuals with increased RAD52 expression have been shown to be more aggressive<sup>52</sup>. We predict that an imbalance in the BRCA1/BARD1–USP48 circuit could have deleterious consequences for genome stability and be significant in the prevention or progression of cancer.

These data also suggest a further mode of resistance against PARP or topoisomerase inhibitor treatment in cancer therapy. However in contrast to 53BP1 loss, which can restore HR-repair to BRCA1 deficient tumours, USP48 loss is not an expected mechanism of tumour resistance in BRCA1 patients as hyper-resection following USP48 loss requires BRCA1 function. Nevertheless USP48 loss of function would be expected to increase the resistance of tumours in which the BRCA1-resection pathway is intact to agents that force a reliance on HR-mediated repair.

## Material and Methods

**Plasmids.** Flag-HA-USP48 isoform 2 was a gift from Wade Harper (Addgene plasmid # 22585). RNF168 RING domain (1-113) was cloned into pETNKI-His-SUMO2-LIC-kan. Plasmids for RING1b(1-159)/BMI1(1-109) RING domain expression were described in<sup>53</sup>. UBCH5C (UBE2D3) plasmid was a gift from P Jackson (Stanford University School of Medicine). BRCA1 and BARD1 constructs in pCOT7N vector were a gift from Rachel Klevit (University of Washington). USP15 and USP11 cDNA were a gift from Hidde Ploegh (Whitehead Institute for Biomedical Research). USP12 and UAF1 plasmids were a gift from Martin Cohn (University of Oxford). For recombinant protein expression in insect cells USP15, USP16, USP48 and BAP1 were cloned into pFastBacNKI-his-3C-LIC, USP1, USP3 and USP12 were cloned into the pFastBacHTb vector. UAF1 was cloned into pFastBac1. USP7 was cloned into pGEX6p-1 vector and expressed in *E. coli*. USP11 was cloned into pET-NKI His-3C-LIC<sup>54</sup> vectors and expressed in *E. coli*. For experiments in cells, human USP48 isoform 2 was cloned into pcDNA5/FRT/TO with addition of an N-terminal FLAG tag. Point mutations to generate siResistance and catalytic dead (C98S) versions were made by site-directed mutagenesis and all constructs were confirmed by sequencing (Source Biosciences). All primers used for mutagenesis are given in Supplemental Table 2. HA-H2A and HA-H2A-Ub (H2A-K13,15,118,119,125,127,129R-Ub-Kless) were described previously<sup>2</sup>. YFP-Rad52 was a kind gift from Claudia Lukas (University of Copenhagen, Denmark).

### Protein expression and purification

**hUBA1 and ubiquitin** hUBA1 and ubiquitin were purified from *E. coli* as described before<sup>53</sup>

**UBCH5C(UBE2D3)** Protein was expressed in *E. coli*. Cells were grown at 37 °C until an OD of 0.8 and then induced with 200 μM IPTG. Temperature was set to 18 °C and protein was expressed overnight. Cells were harvested in lysis buffer (50 mM TRIS pH7.5, 150 mM NaCl, 1 mM TCEP, 2mM Imidazole) with “Complete EDTA-free protease inhibitor” and lysed by sonication. Lysate was cleared by spinning down at 21000 x g and loaded on TALON beads (Clontech Laboratories, Inc). Beads were washed with 20 CV of lysis buffer + 6 mM Imidazole and eluted in lysis buffer + 300 mM Imidazole. His-tag was cleaved over night at 4 °C with 3C protease, dialyzing against gel filtration buffer (25 mM HEPES pH 8, 150 mM NaCl, 5 mM DTT). Protease and uncleaved protein were removed using TALON beads and sample was purified by size exclusion chromatography on a Superdex 75 16/60 column (GE).

**RNF168 RING domain (residues 1-113)** Protein was expressed in *E. coli* Cells were grown at 37 °C until an OD of 0.6 and the induced with 200 uM IPTG. Temperature was set to 18 °C and protein was expressed overnight. Cells were harvested in lysis buffer (50 mM TRIS pH 8,

500 mM NaCl, 1  $\mu$ M ZnCl<sub>2</sub>, 1 mM TCEP, 2 mM Imidazol) with “Complete EDTA-free protease inhibitor” and lysed by sonication. Lysate was cleared by spinning down at 21000 x g and loaded on TALON beads (Clontech Laboratories, Inc). Beads were washed with 20 CV of lysis buffer + 10 mM Imidazol and eluted in lysis buffer + 300 mM Imidazol. His-Sumo tag was cleaved overnight with SENP protease at 4 °C dialyzing against dialysis buffer (50 mM TRIS pH 8, 250 mM NaCl, 1  $\mu$ M ZnCl<sub>2</sub>, 1 mM TCEP). Protease, uncleaved sample and His-Sumo were removed with TALON beads. Sample was diluted to a salt concentration of 50 mM NaCl and loaded onto a Heparin column (GE). Sample was eluted with a salt gradient ranging from 50 mM to 1000 mM NaCl in 12 CV. Fractions containing RNF168 were combined and further purified by size exclusion chromatography using a Superdex 75 16/60 column (GE healthcare) in 50 mM TRIS pH 8, 150 mM NaCl, 1  $\mu$ M ZnCl<sub>2</sub> and 1 mM TCEP.

**RING1b/BMI1 RING domain** Purification of RING1b/BMI1 RING domain constructs has been described before<sup>53</sup>

**BRCA1/BARD1 RING domain** BRCA1 (1-303) and BARD1 (1-306) were co-expressed in *E.coli*. Cells were grown in LB at 37 °C until OD of 0.6 was reached and then induced with 100  $\mu$ M IPTG. Protein was expressed for 4 hours at 37 °C. Cells were harvested in lysis buffer (25 mM HEPES pH 7.5, 150 mM NaCl, 1mM TCEP, 5 mM Imidazole) and lysed by sonication. Lysate was cleared by spinning at 21000 x g and supernatant was loaded onto chelating sepharose beads (GE healthcare) charged with Ni<sup>2+</sup> in gravity flow columns. Beads were washed with 20 CV lysis buffer +30 mM Imidazole. Protein was eluted in lysis buffer +300 mM Imidazole. Salt concentration was diluted to 50 mM NaCl and sample was loaded on a Resource S cation exchange column (GE healthcare). Protein was eluted with a salt gradient (50 - 1000 mM NaCl, 25 mM HEPES pH7.5, 1mM TCEP) and fractions containing BRCA1/BARD1 were pooled. Pooled fractions were further purified by size exclusion chromatography on a Superdex 75 column (GE healthcare).

**USP1, USP12 and UAF1** Proteins were expressed and purified as described in<sup>55</sup>

**USP3** Same as USP48 but with 500 mM NaCl and 1  $\mu$ M ZnCl<sub>2</sub> in the lysis buffer and TEV protease was used to cleave the tag

**USP7** Protein was expressed in BL21(DE2)Rosetta2 cells. Cells were grown at 37 °C in TB until an OD of 1.8-2.0 and induced with 100  $\mu$ M IPTG. Temperature was set to 18 °C and protein was expressed overnight. Cells were lysed using Emulsiflex in lysis buffer (50 mM HEPES pH 7.5, 250 mM NaCl, 1 mM EDTA, 1mM DTT) + 0.1 mM PMSF and 1mg DNase1. Lysate was cleared by centrifugation at 20k x g and supernatant was loaded on Glutathione Sepharose 4B beads (GE healthcare) in gravity flow column. Beads were washed in lysis buffer and

eluted in lysis buffer + 15 mM reduced glutathione. GST-tag was cleaved overnight with 3C protease dialyzing against 10 mM HEPES pH 7.5, 50 mM NaCl, 1 mM EDTA, 1 mM DTT. Sample was purified using a ResourceQ anion exchange column (GE healthcare) using a salt gradient (50 to 500 mM NaCl, 10 mM HEPES pH 7.5, 1 mM DTT). USP7 containing fractions were pooled and further purified by size exclusion chromatography on a Superdex 200 column (GE healthcare).

**USP11** Protein was expressed in *E.coli* and purified as described before in<sup>56</sup>

**USP15, USP16 and USP48** Proteins were expressed in Sf9 insect cells for 48 – 72 hours. Cells were lysed by sonication in 25 mM HEPES pH7.5, 300 mM NaCl, 2 mM DTT and 5 mM Imidazole supplemented with Pierce EDTA-free protease inhibitor (Thermo Fischer). Lysate was cleared by centrifugation at 21000 x g at 4 °C and the supernatant was loaded on chelating sepharose beads (GE) charged with Ni<sup>2+</sup>. Beads were washed with 20 column volume of lysis buffer +30 mM Imidazole and then eluted in lysis buffer +300 mM Imidazole. The His-tag was cleared using His-tagged 3C protease over night at 4 °C while dialyzing against 25 mM HEPES 7.5, 150 mM NaCl, 1 mM DTT. The sample was then run over chelating sepharose beads charged with Ni<sup>2+</sup> to remove protease and uncleaved sample and subsequently purified by size exclusion chromatography using a Superdex S200 16/60 column (GE) in 25 mM HEPES 7.5, 150 mM NaCl, 1 mM DTT.

**BAP1/ASXL1 (1-390)** Protein was expressed and purified as described in<sup>57</sup>

**Nucleosome reconstitution.** Histones and 146bp DNA with Widom601 strong positioning sequence were purified, octamers folded and nucleosomes reconstituted by salt dialysis as described previously<sup>58,59</sup>

**Cell lines.** Flp-In™ Doxycyclin inducible HeLa parent cell lines were grown in DMEM (Sigma), 10 % Tetracycline-Free Foetal Calf serum (Clontech) supplemented with 1 % penicillin/streptomycin. All other cell lines were grown in DMEM supplemented with 10% foetal calf serum (Sigma) and 1 % penicillin/streptomycin. Mycoplasma testing was by Hoechst DNA staining. Stable doxycycline inducible cell lines were made by co-transfection of pcDNA5/FRT/TO-FlagUSP48-siResistant-WT or -C98S constructs with pOG44 recombinase into HeLa FlpIn cells. Clones were selected in hygromycin (400 µg/ml) and expanded. Flag-USP48 expression following 48-72 hour induction with doxycycline (1 µg/ml) was confirmed by western blot.

**Transfections.** siRNA transfections were performed using Dharmafect1 (Dharmacon) and DNA plasmids using FuGENE 6 (3 µl:1 µg FuGENE:DNA) (Promega) following the manufacturer's protocols. Cells were grown for 48 hours post-transfection before treatment and

harvesting. All siRNA sequences are given in Supplemental Table 3.

**Western Blots.** A full list of antibodies used for western blots can be found in Supplemental Table 4.

**Kinetics on minimal substrate Ubiquitin-Rhodamine.** Ubiquitin linked to a cleavable small peptide labeled with Rhodamine (Ub<sup>RHO</sup>, UbiQ) was used as a substrate. Reaction was followed through increase of fluorescence intensity at 590 nm due to liberation of free fluorescent Rhodamine from the quenched substrate upon cleavage by a DUB. The assays were done in 384-well plates (Corning, flat bottom, low flange) in a Pherastar plate reader (BMG labtech) at 30 °C using an assay buffer of 25 mM HEPES pH 7.5, 150 mM NaCl, 5 mM DTT and 0.05 % TWEEN-20. For full Michaelis-Menten analysis substrate was titrated starting from 30 μM in eight two-fold dilutions while enzyme concentration was kept constant. Enzyme concentrations are indicated in Figure S1. Cleavage was started by addition of the respective DUB. The initial velocity of the reaction was calculated from the slope of the linear phase of the curve and was plotted against the substrate concentration and fitted to the Michaelis-Menten equation using the program GraphPad Prism.

For single point assays (Figure 1D) 2 μM of substrate and different concentrations of enzyme were used. Assays were done at 30 °C. The different enzyme concentrations are indicated in the figure.

**Fluorescent labeling of ubiquitin.** Ubiquitin with a cysteine residue introduced at the N-terminus right after the methionine at position 1 was labeled using maleimide-linked TAMRA dye. 250 μM ubiquitin was labeled with 1500 μM TAMRA (5)-Maleimide (Setareh) at 4 °C overnight. Excess dye was removed by size exclusion chromatography using a Superdex 75 16/60 column (GE) in 50 mM TRIS pH7.5, 150 mM NaCl and 1 mM DTT.

**Ubiquitination assay.** Nucleosomes were ubiquitinated using 0.5 μM hUBA1, 1 μM Ubch5C (UBE2D3), 1 μM E3 RING domain (RNF168, RING1B/BMI1 or BRCA1/BARD1) 5 μM NCP, 20 μM ubiquitin or <sup>TAMRA</sup>Ub and 3 mM ATP in 25 mM HEPES pH7.5, 150 mM NaCl, 3 mM MgCl<sub>2</sub> and 1 mM DTT for 60 minutes at 30 °C. Substrates for figure 1C were ubiquitinated for 40 minutes, all the others for 60 minutes (as stated). Ubiquitinated NCPs were then gel filtered on a Superose 6 Increase column using the Akta micro purifier system (GE) in 25mM HEPES pH 7.5, 150 mM NaCl, 1 mM DTT.

**Double ubiquitination at polycomb and BRCA1 site.** NCPs containing the H2A K118R were used to assure only K119 is ubiquitinated by RING1B/BMI1. Mutant NCP were ubiquitinated with RING1B/BMI1<sup>RING</sup> and gel filtered on the Superose 6 increase using the Akta micro purifier system (GE healthcare). Purified NCP ubiquitinated at K119 were then ubiquitinated

a second time using BRCA1/BARD1<sup>RING</sup> and <sup>TAMRA</sup>Ub, generating NCP ubiquitinated on K119 with unlabeled ubiquitin and on the BRCA1 site with <sup>TAMRA</sup>Ub.

**Fluorescence polarization assay to measure DUB activity and normalization to minimal substrate.** FP assays were done in 384-well plates (Corning, flat bottom, low flange) in a Pherastar plate reader (BMG labtech) at 30 °C using an assay buffer of 25 mM HEPES pH 7.5, 150 mM NaCl, 5 mM DTT and 0.05 % TWEEN-20 (Sigma). NCPs ubiquitinated with <sup>TAMRA</sup>Ub on either of the three sites were used at 2 μM label concentration. 500 nM of the respective DUB was added to start the assay and reaction progression was followed by measuring FP signal at Excitation: 540 nm, Emission 590/590 nm. A reaction without DUB was run in parallel to subtract baseline drift from the experimental data. An exponential function, where  $FP_0 - FP$  is the signal of ubiquitinated substrate and  $FP_{min} - FP$  the signal of free <sup>TAMRA</sup>Ub, was fitted to determine  $k_{obs(NCP)}$  as a measure of the enzymes processivity. To normalize the data to the intrinsic DUB activity on minimal substrate cleavage of 2 μM Ub<sup>Rho</sup> was measured under the same conditions. The curve was fitted to obtain  $k_{obs(Rho)}$ .  $k_{obs(NCP)}$  was then normalized to  $k_{obs(Rho)}$  using the equation, where  $[E_{Rho}]$  is the concentration of the DUB in the reaction with minimal substrate and  $[E_{NCP}]$  is the concentration of the DUB in the reaction with NCP.

**Biotinylation, USP48 inactivation and SPR measurements.** Measurements were done on a Biacore T200 (GE). NCPs of different ubiquitination status at a concentration of 2 μM were biotinylated over night at 4 °C using EZ-link Sulfo-NHS-LC-Biotin (Thermo Fischer) with a 2:1 excess of NCP over biotin. Biotinylation was stopped by adding 1 mM TRIS pH7.5. USP48 at 30 μM was inactivated by incubating with 25 mM Iodoacetamide for 20 minutes at room temperature. Excess Iodoacetamide was removed using Zeba Spin Desalting Columns (Thermo Fischer) according to manufacturer's protocol. The buffer used for SPR experiments was 25 mM HEPES pH 7.5, 150 mM NaCl, 0.05% TWEEN-20, 1 mg/ml BSA, 1mg/ml Dextran. Biotinylated NCPs were immobilized on a (Series S SA chip, GE) to roughly 100 RU and inactivated USP48 was flown over at varying concentrations with two-fold dilutions starting at 2.56 μM. A reference flow cell without immobilized NCP was included to subtract unspecific binding. Data was processed using GraphPad Prism 7.0.

**USP48 cleavage reactions.** All cleavage reactions were done in reaction buffer 25 mM HEPES pH7.5, 150 mM NaCl, 5 mM DTT. NCPs ubiquitinated on either one of the H2A ubiquitination sites with <sup>TAMRA</sup>Ub were used and reaction was started by addition of USP48. Concentrations are indicated in the figures. Samples were taken at the indicated time points and reaction was stopped by addition of SDS-loading dye. Samples were separated on a NuPage 4-12 % Bis-TRIS SDS gel in MES buffer (Thermo Fischer) and the fluorescence signal was read out on a Typhoon FLA-9500 gel scanner (GE healthcare). Quantification of individual bands was achieved by measuring the fluorescence intensity and relating it to the total intensity

of each lane at a known concentration of dye used in the respective assay. This way each band represents a fraction of the concentration of dye used in the experiment. To convert to molar concentration of ubiquitinated histones the dye concentration was divided by the number of labeled ubiquitins present on the respective histone species (H2Aub3, H2Aub2, H2Aub1).

**USP48 kinetic modeling.** USP48 cleavage reactions as described before were done at varying substrate and enzyme concentration to allow subsequent kinetic modeling. Different conditions are indicated in figure S3 and S4. Concentrations of the different reaction species were quantified and quantified data were used to globally fit the three different catalytic rates defined in figure 2E,  $k_{\text{cat}(\text{ub}3)}$ ,  $k_{\text{cat}(\text{ub}2)}$  and  $k_{\text{cat}(\text{ub}1)}$ . Binding constants were fixed to  $k_{\text{on}} = 20 \mu\text{M}^{-1}\text{s}^{-1}$ , an order of magnitude we routinely observe in SPR experiments, and  $k_{\text{off}} = 10 \text{ s}^{-1}$  to reflect a Kd of 500 nM as approximated by SPR. Fitting was done using the software *KinTek Explorer Version 6.1.170209*.

**DNA repair reporter assays.** U2OS-DR3-GFP (gene conversion), U2OS-SA-GFP (Single-strand annealing) and U2OS-EJ5-GFP (Non-homologous end-joining) were a generous gift from Jeremy Stark (City of Hope, Duarte USA). U2OS reporter cell lines were simultaneously co-transfected with siRNA using Dharmafect1 (Dharmacon) and DNA (RFP, or Flag-USP48 and *I-Sce1* endonuclease expression constructs) using FuGene6 (Promega) respectively. After 16 hours the media was replaced and cells were grown for a further 48 hours before fixation in 2% PFA. RFP and GFP double positive cells were scored by FACS analysis using a CyAn flow cytometer and a minimum of 10000 cells counted. Data was analyzed using Summit 4.3 software. Each individual experiment contained 3 technical repeats and normalized to siRNA controls or to WT-complemented cells. Graphs shown are combined data from a minimum of 3 independent experiments and error bars show standard error.

**Colony Assays.** Cells were plated at  $2 \times 10^5$  cells/ml in a 24 well plate and treated as required. Cells were then trypsinized and plated at limiting dilution to form colonies and grown on for 10-14 days. Colonies were stained using 0.5% crystal violet (BDH Chemicals) in 50% methanol and counted. Each individual experiment contained 3 technical repeats and is normalized to untreated controls. Graphs shown are combined data from a minimum of 3 independent experiments and error bars show standard error.

**Laser Microirradiation.** Laser-microirradiation experiments were performed on BrdU-pre-sensitized cells (10  $\mu\text{M}$  BrdU, 24h) as described<sup>60</sup> using a Zeiss PALM MicroBeam equipped with a 355 nm UV-A pulsed-laser and the 40x objective with laser output at 40%, assisted by the PALMRobo-Software supplied by the manufacturer.



**Measurement of resection tracks (BrdU).** 24 hours before fixation cells were incubated with 10  $\mu$ M BrdU and then 10  $\mu$ M Olaparib for the last 16 hrs of treatment. Cells were trypsinized and resuspended in ice cold PBS to a concentration of  $10 \times 10^5$  cells/ml. In order to lyse the cells, 2  $\mu$ l of sample was placed on a slide and mixed with 7  $\mu$ l of spreading buffer (200 mM Tris pH 7.4, 50 mM EDTA, 0.5% SDS) and incubated for 2 mins. Slides were then placed at a shallow angle to cause the droplet to gradually run down the slide, ensuring constant movement of the droplet. Slides were fixed in 3:1 Methanol: Acetic Acid for 10 mins and then stored at 4°C. Slides were washed in PBS and Blocking solution (2 g BSA, 200  $\mu$ l Tween-20, 200 ml PBS) and then incubated with mouse anti BrdU primary antibody. Slides were washed in PBS before being incubated with AlexaFluor donkey anti mouse 488. Images were taken on the Leica DM6000B microscope and analysis performed using ImageJ software. Lengths were calculated using a scale bar to convert pixels to  $\mu$ m and this ratio, of 3.493 pixels per  $\mu$ m, was used to measure BrdU track lengths. >100 fibres per treatment were measured and plotted on a Whisker plot using Graphpad.

**Immunofluorescence.** HeLa FlpIn, HeLa-Flag-USP48 or HeLa-Flag-USP48-C98S cells were seeded onto coverslips and transfected with siRNA, expression constructs and/ or induced with doxycycline as described. Cells were labelled with 10  $\mu$ M EdU 10 minutes prior to irradiation using a Gamma-cell 1000 Elite irradiator (caesium-137 source). At 2 hours post-irradiation cells were washed briefly in CSK buffer (100 mM sodium chloride, 300 mM sucrose, 3 magnesium chloride, 10 mM PIPES pH 6.8) before fixation with 4 % Paraformaldehyde for 10 mins. For IF staining cells were permeabilized with 0.2% TritonX100 in PBS for 10 mins before blocking in 10 % FBS in PBS. EdU was visualised by Click-iT® chemistry according to the manufacturer's protocols (Life Technologies) with Alexa-647-azide. Cells were incubated with primary antibody for 1 hr, washed three times in PBS and incubated with secondary AlexaFluor antibodies for 1 hr. The DNA was stained using Hoechst at 1:20,000.

**Microscopy.** For 53BP1/BRCA1 foci analysis: Images of immunofluorescent staining were captured on the Zeiss 510 Meta confocal microscope, using three lasers to give excitation at 647, 555 and 488 nm wavelengths. Images at each wavelength were collected sequentially at a resolution of approximately 1024 x 1024 pixels, using the Plan-Apochromat 100x/1.4 Oil objective. All other immunofluorescent staining was imaged using the Leica DM6000B microscope using a HBO lamp with 100W mercury short arc UV bulb light source and four filter cubes, A4, L5, N3 and Y5 to produce excitations at wavelengths 360 488, 555 and 647 nm respectively. Images were captured at each wavelength sequentially using the Plan Apochromat HCX 100x/1.4 Oil objective at a resolution of 1392x1040 pixels.

**Statistics.** BrdU resection tracks which were analysed by one-sided Mann-Whitney test with centre values given as median. All other statistical analysis was by two-sided Students T-test



throughout. \* $p < 0.05$ , \*\* $p < 0.01$ , \*\*\* $P < 0.005$ . All centre values are given as the mean and all error bars are standard error about the mean (S.E.M). For kinetic modelling, data was fitted globally to the defined model by numerical integration and best-fit parameters were determined by finding minimum  $\text{Chi}^2$  values using *KinTek Explorer*. Quality of the fit was evaluated by calculating the *FitSpace* shown in Figure 2 E.

### Acknowledgements

Grant funding for this project was as follows. NWO-CW TOP 714.012.001, ERC 249997, Gravity CGC.nl, CRUK: C8820/A19062 (RMD). JRM is HEFCE funded. We thank J. Stark (City of Hope) for U20S-DR3, U20A-SA and U20S-EJ5 cells and *I-SCE1* plasmid and Claudia Lukas (University of Copenhagen) for YFP-RAD52. We thank the TechHub Facility at the University of Birmingham for Microscope and FACS support.

### Author Contributions

MU devised the screen and kinetic analysis and performed all in vitro assays, HHKW reconstituted NCPs, AF supervised kinetic analysis, RMD performed cell and biochemical experiments, designed experiments and interpreted data. TKS initiated the project and supervised MU, JRM contributed to data interpretation, directed the project and supervised RMD. MU, RMD, TKS and JRM contributed to writing the paper.

### References

1. Chapman, J. R., Taylor, M. R. G. & Boulton, S. J. Playing the End Game: DNA Double-Strand Break Repair Pathway Choice. *Molecular Cell* **47**, 497–510 (2012).
2. Densham, R. M. *et al.* Human BRCA1-BARD1 ubiquitin ligase activity counteracts chromatin barriers to DNA resection. *Nat. Struct. Mol. Biol.* **23**, 647–55 (2016).
3. Zimmermann, M. & De Lange, T. 53BP1: Pro choice in DNA repair. *Trends in Cell Biology* **24**, 108–117 (2014).
4. Ceccaldi, R., Rondinelli, B. & D'Andrea, A. D. Repair Pathway Choices and Consequences at the Double-Strand Break. *Trends in Cell Biology* **26**, 52–64 (2016).
5. Bhargava, R., Onyango, D. O. & Stark, J. M. Regulation of Single-Strand Annealing and its Role in Genome Maintenance. *Trends in Genetics* **32**, 566–575 (2016).

6. Bhattacharjee, S. *et al.* Choices have consequences: the nexus between DNA repair pathways and genomic instability in cancer. *Clin. Transl. Med.* **5**, 45 (2016).
7. Ivanov, E. L., Sugawara, N., Fishman-Lobell, J. & Haber, J. E. Genetic requirements for the single-strand annealing pathway of double-strand break repair in *Saccharomyces cerevisiae*. *Genetics* **142**, 693–704 (1996).
8. Panier, S. & Boulton, S. J. Double-strand break repair: 53BP1 comes into focus. *Nat. Rev. Mol. Cell Biol.* **15**, 7–18 (2014).
9. Jiang, Q. & Greenberg, R. A. Deciphering the BRCA1 tumor suppressor network. *Journal of Biological Chemistry* **290**, 17724–17732 (2015).
10. Escribano-Díaz, C. *et al.* A Cell Cycle-Dependent Regulatory Circuit Composed of 53BP1-RIF1 and BRCA1-CtIP Controls DNA Repair Pathway Choice. *Mol. Cell* **49**, 872–883 (2013).
11. Wu, L. *et al.* Identification of a RING protein that can interact in vivo with the BRCA1 gene product. *Nat. Genet.* **14**, 430–40 (1996).
12. Hashizume, R. *et al.* The RING heterodimer BRCA1-BARD1 is a ubiquitin ligase inactivated by a breast cancer-derived mutation. *J. Biol. Chem.* **276**, 14537–40 (2001).
13. Reid, L. J. *et al.* E3 ligase activity of BRCA1 is not essential for mammalian cell viability or homology-directed repair of double-strand DNA breaks. *Proc. Natl. Acad. Sci. U. S. A.* **105**, 20876–20881 (2008).
14. Shakya, R. *et al.* BRCA1 Tumor Suppression Depends on BRCT Phosphoprotein Binding, But Not Its E3 Ligase Activity. *Science (80-. )*. **334**, 525–528 (2011).
15. Drost, R. *et al.* BRCA1185delAG tumors may acquire therapy resistance through expression of RING-less BRCA1. *J. Clin. Invest.* **126**, 2903–2918 (2016).
16. Drost, R. *et al.* BRCA1 RING function is essential for tumor suppression but dispensable for therapy resistance. *Cancer Cell* **20**, 797–809 (2011).
17. Li, M. *et al.* 53 BP 1 ablation rescues genomic instability in mice expressing ‘RING-less’ BRCA 1. *EMBO Rep.* **17**, 1–10 (2016).
18. Bouwman, P. *et al.* 53BP1 loss rescues BRCA1 deficiency and is associated with triple-negative and BRCA-mutated breast cancers. *Nat. Struct. Mol. Biol.* **17**, 688–695 (2010).

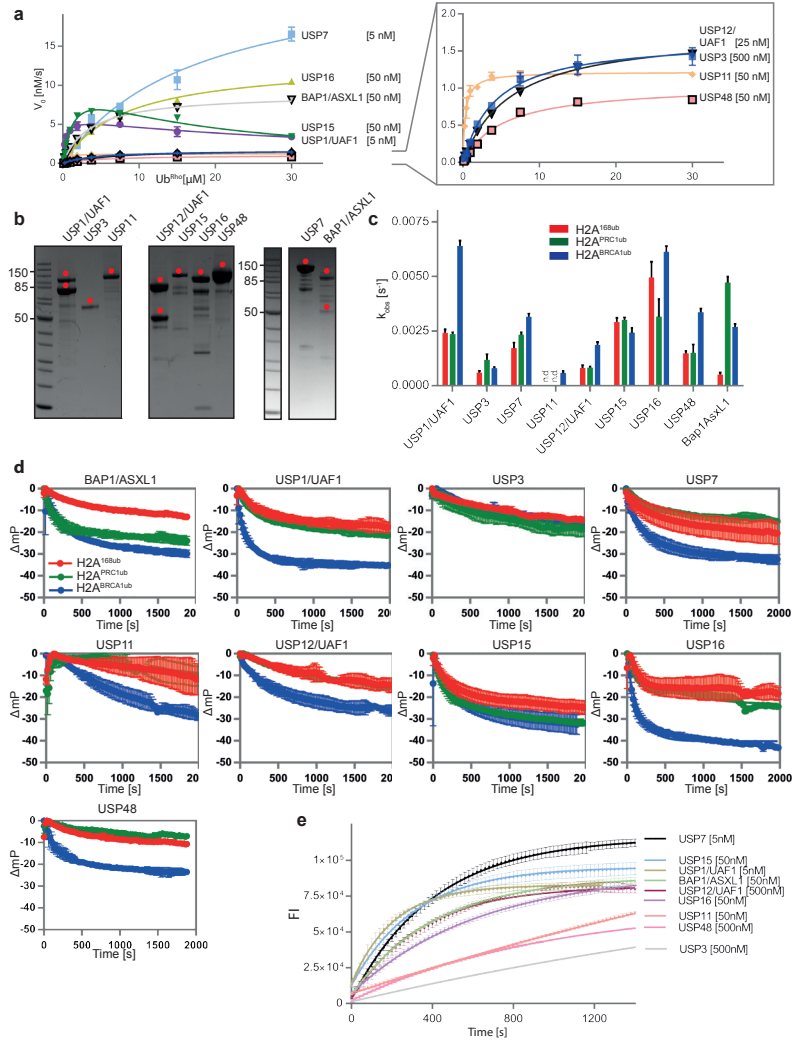
19. Cao, L. *et al.* A Selective Requirement for 53BP1 in the Biological Response to Genomic Instability Induced by Brca1 Deficiency. *Molecular Cell* **35**, 534–541 (2009).
20. Kalb, R., Mallery, D. L., Larkin, C., Huang, J. T. J. & Hiom, K. BRCA1 is a histone-H2A-specific ubiquitin ligase. *Cell Rep.* **8**, 999–1005 (2014).
21. Mattioli, F. *et al.* RNF168 ubiquitinates K13-15 on H2A/H2AX to drive DNA damage signaling. *Cell* **150**, 1182–1195 (2012).
22. Wang, H. *et al.* Role of histone H2A ubiquitination in Polycomb silencing. *Nature* **431**, 873–8 (2004).
23. Xie, A. *et al.* Control of sister chromatid recombination by histone H2AX. *Mol. Cell* **16**, 1017–1025 (2004).
24. Muñoz, M. C. *et al.* Ring finger nuclear factor RNF168 is important for defects in homologous recombination caused by loss of the breast cancer susceptibility factor BRCA1. *J. Biol. Chem.* **287**, 40618–40628 (2012).
25. Zhou, Y., Caron, P., Legube, G. & Paull, T. T. Quantitation of DNA double-strand break resection intermediates in human cells. *Nucleic Acids Res.* **42**, e19 (2014).
26. Ochs, F. *et al.* 53BP1 fosters fidelity of homology-directed DNA repair. *Nat. Struct. Mol. Biol.* **23**, 714–21 (2016).
27. Joo, H.-Y. *et al.* Regulation of cell cycle progression and gene expression by H2A deubiquitination. *Nature* **449**, 1068–1072 (2007).
28. Lancini, C. *et al.* Tight regulation of ubiquitin-mediated DNA damage response by USP3 preserves the functional integrity of hematopoietic stem cells. *J. Exp. Med.* **211**, 1759–77 (2014).
29. Nicassio, F. *et al.* Human USP3 Is a Chromatin Modifier Required for S Phase Progression and Genome Stability. *Curr. Biol.* **17**, 1972–1977 (2007).
30. Scheuermann, J. C. *et al.* Histone H2A deubiquitinase activity of the Polycomb repressive complex PR-DUB. *Nature* **465**, 243–7 (2010).
31. Sharma, N. *et al.* USP3 counteracts RNF168 via deubiquitinating H2A and  $\gamma$ H2AX at lysine 13 and 15. *Cell Cycle* **13**, 106–114 (2014).
32. Kalb, R. *et al.* Histone H2A monoubiquitination promotes histone H3 methylation in

- Polycomb repression. *Nat. Struct. Mol. Biol.* **21**, 569–71 (2014).
33. Nishi, R. *et al.* Systematic characterization of deubiquitylating enzymes for roles in maintaining genome integrity. *Nat. Cell Biol.* **16**, 1016–26, 1–8 (2014).
  34. Johnson, K. A., Simpson, Z. B. & Blom, T. FitSpace Explorer: An algorithm to evaluate multidimensional parameter space in fitting kinetic data. *Anal. Biochem.* **387**, 30–41 (2009).
  35. Johnson, K. A., Simpson, Z. B. & Blom, T. Global Kinetic Explorer: A new computer program for dynamic simulation and fitting of kinetic data. *Anal. Biochem.* **387**, 20–29 (2009).
  36. Zhu, Q. *et al.* BRCA1 tumour suppression occurs via heterochromatin-mediated silencing. *Nature* **477**, 179–184 (2011).
  37. Shibata, A. *et al.* Role of ATM and the Damage Response Mediator Proteins 53BP1 and MDC1 in the Maintenance of G2/M Checkpoint Arrest. *Mol. Cell. Biol.* **30**, 3371–3383 (2010).
  38. Stark, J. M., Pierce, A. J., Oh, J., Pastink, A. & Jasin, M. Genetic steps of mammalian homologous repair with distinct mutagenic consequences. *Mol. Cell. Biol.* **24**, 9305–16 (2004).
  39. Adachi, N., So, S. & Koyama, H. Loss of nonhomologous end joining confers camptothecin resistance in DT40 cells: Implications for the repair of topoisomerase I-mediated DNA damage. *J. Biol. Chem.* **279**, 37343–37348 (2004).
  40. Symington, L. S. Role of RAD52 epistasis group genes in homologous recombination and double-strand break repair. *Microbiol. Mol. Biol. Rev.* **66**, 630–70, table of contents (2002).
  41. Rothenberg, E., Grimme, J. M., Spies, M. & Ha, T. Human Rad52-mediated homology search and annealing occurs by continuous interactions between overlapping nucleoprotein complexes. *Proc. Natl. Acad. Sci. U. S. A.* **105**, 20274–9 (2008).
  42. Mortensen, U. H., Lisby, M. & Rothstein, R. Rad52. *Current Biology* **19**, R676–R677 (2009).
  43. Sahtoe, D. D. & Sixma, T. K. Layers of DUB regulation. *Trends in Biochemical Sciences* **40**, 456–467 (2015).

44. Wang, Z. *et al.* USP51 deubiquitylates H2AK13, 15ub and regulates DNA damage response. *Genes Dev.* **30**, 946–959 (2016).
45. Lee, B.-H. *et al.* USP14 deubiquitinates proteasome-bound substrates that are ubiquitinated at multiple sites. *Nature* **532**, 398–401 (2016).
46. Awad, S., Ryan, D., Prochasson, P., Owen-Hughes, T. & Hassan, A. H. The Snf2 homolog Fun30 acts as a homodimeric ATP-dependent chromatin-remodeling enzyme. *J. Biol. Chem.* **285**, 9477–9484 (2010).
47. Stewart, M. D., Duncan, E. D., Coronado, E., Brzovic, P. S. & Klevit, R. E. Tuning BRCA1 and BARD1 activity to investigate RING ubiquitin ligase mechanisms. *Protein Sci.* **26**, 475–483 (2016).
48. Shanbhag, N. M., Rafalska-Metcalf, I. U., Balane-Bolivar, C., Janicki, S. M. & Greenberg, R. A. ATM-Dependent chromatin changes silence transcription in cis to dna double-strand breaks. *Cell* **141**, 970–981 (2010).
49. Kakarougkas, A. *et al.* Requirement for PBAF in Transcriptional Repression and Repair at DNA Breaks in Actively Transcribed Regions of Chromatin. *Mol. Cell* **55**, 723–732 (2014).
50. Ui, A., Nagaura, Y. & Yasui, A. Transcriptional elongation factor ENL phosphorylated by ATM recruits polycomb and switches off transcription for DSB repair. *Mol. Cell* **58**, 468–482 (2015).
51. Treuner, K., Helton, R. & Barlow, C. Loss of Rad52 partially rescues tumorigenesis and T-cell maturation in Atm-deficient mice. *Oncogene* **23**, 4655–4661 (2004).
52. Delahaye-Sourdeix, M. *et al.* The 12p13.33/RAD52 Locus and genetic susceptibility to squamous cell cancers of upper aerodigestive tract. *PLoS One* **10**, e0117639 (2015).
53. Buchwald, G. *et al.* Structure and E3-ligase activity of the Ring-Ring complex of polycomb proteins Bmi1 and Ring1b. *EMBO J.* **25**, 2465–74 (2006).
54. Luna-Vargas, M. P. A. *et al.* Enabling high-throughput ligation-independent cloning and protein expression for the family of ubiquitin specific proteases. *J. Struct. Biol.* **175**, 113–119 (2011).
55. Dharadhar, S., Clerici, M., van Dijk, W. J., Fish, A. & Sixma, T. K. A conserved two-step

- binding for the UAF1 regulator to the USP12 deubiquitinating enzyme. *Journal of Structural Biology* **196**, 437–447 (2016).
56. Clerici, M., Luna-Vargas, M. P. A., Faesen, A. C. & Sixma, T. K. The DUSP-Ubl domain of USP4 enhances its catalytic efficiency by promoting ubiquitin exchange. *Nat. Commun.* **5**, 5399 (2014).
  57. Sahtoe, D. D., van Dijk, W. J., Ekkebus, R., Ovaa, H. & Sixma, T. K. BAP1/ASXL1 recruitment and activation for H2A deubiquitination. *Nat. Commun.* **7**, 10292 (2016).
  58. Luger, K., Rechsteiner, T. J. & Richmond, T. J. in *Chromatin Protocols* **119**, 1–16 (Humana Press, 1999).
  59. Lowary, P. . & Widom, J. New DNA sequence rules for high affinity binding to histone octamer and sequence-directed nucleosome positioning. *J. Mol. Biol.* **276**, 19–42 (1998).
  60. Lukas, C., Falck, J., Bartkova, J., Bartek, J. & Lukas, J. Distinct spatiotemporal dynamics of mammalian checkpoint regulators induced by DNA damage. *Nat. Cell Biol.* **5**, 255–260 (2003).

Supplemental Material



Supplemental Figure 1

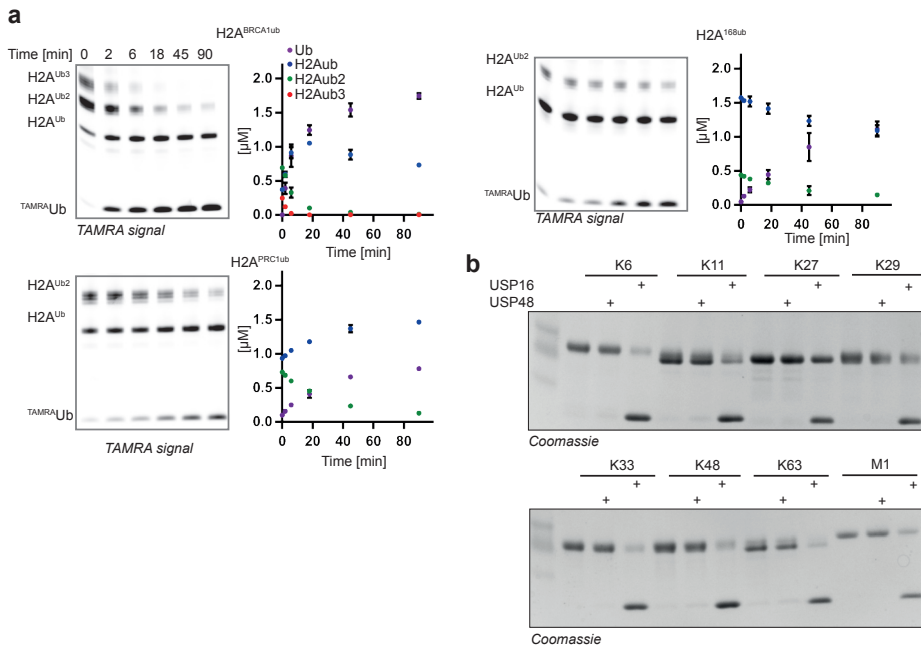
**a** Michaelis-Menten kinetics of the purified DUBs on minimal substrate Ub<sup>Rho</sup>. Different enzyme concentrations were used for different DUBs as indicated in the figure. The speed of the linear phase of the reaction is plotted at different substrate concentrations. The data were fit to the Michaelis-Menten equation using the program Graph-Pad Prism. See also supplemental Table 1. Replicates of two experiments ± SEM

**b** Purified DUBs used on in this study. \* Indicates bands corresponding to the respective DUB

**c** DUBs tested show no exclusive site specificity but rather preferential cleavage of H2A<sup>168ub</sup>, H2A<sup>PRC1ub</sup> and H2A<sup>BRC1ub</sup> in NCPs. Site specific reaction speed quantified for all DUBs tested. k<sub>obs</sub> values were obtained by fitting an exponential function to the traces in D). Replicates of two experiments ± SEM.

**d** Raw data of the FP assay to identify site specific DUBs. 2 μM of H2A<sup>168ub</sup>, H2A<sup>PRC1ub</sup> or H2A<sup>BRC1ub</sup> were cleaved by 500 nM of the indicated DUB. Different amplitudes are because the distance from the center of mass to the ubiquitination sites is different for differently modified NCP. Replicates of two experiments ± SEM

**e** Activity of the DUBs included in this study on minimal substrate. Cleavage of 2 μM minimal substrate Ub<sup>Rho</sup> using the same conditions as in the FP screen on nucleosomal substrates. Concentrations of the respective DUB used are indicated.

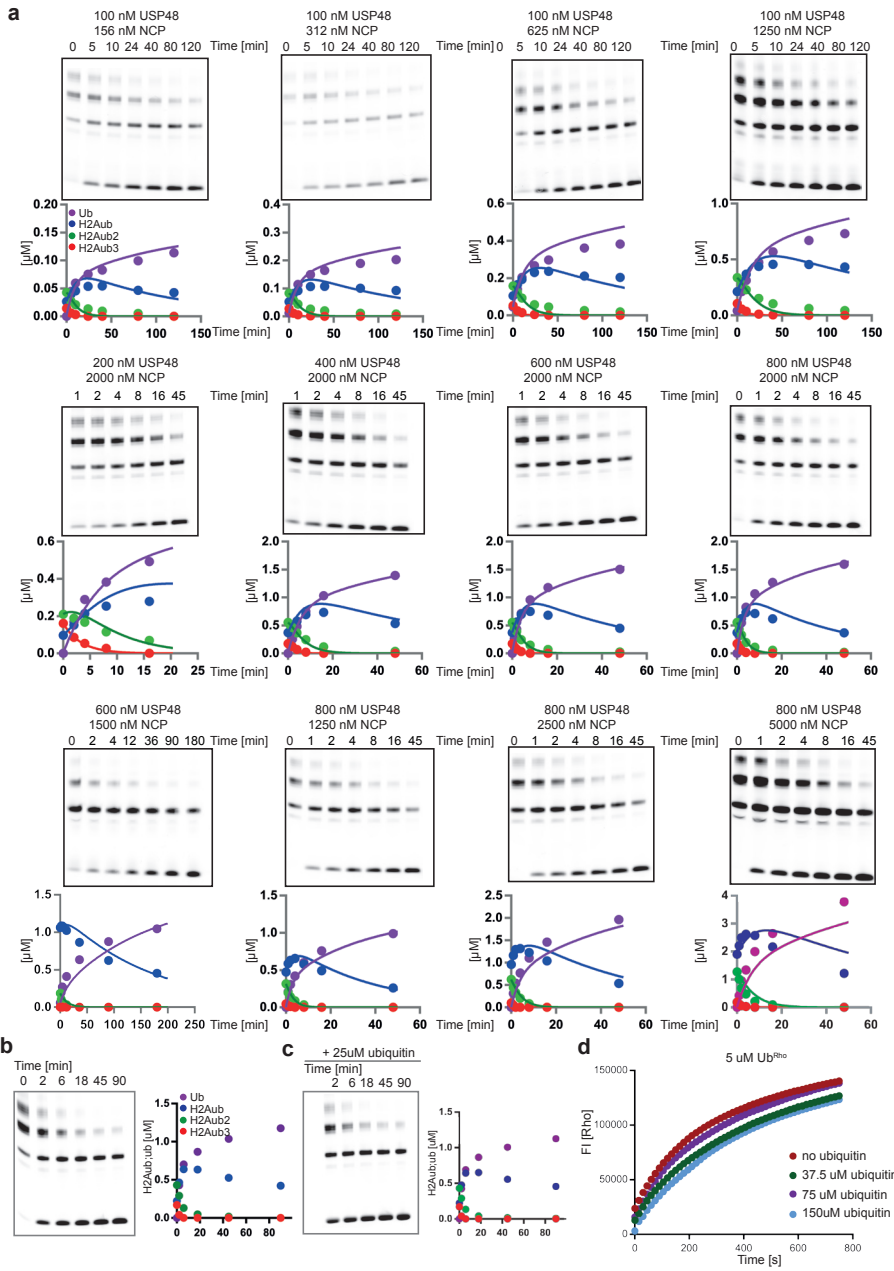


### Supplemental Figure 2

**a** Time course of cleavage of 2  $\mu\text{M}$  H2A<sup>168ub</sup>, H2A<sup>PRC1ub</sup> and H2A<sup>BRCA1ub</sup> in NCPs by USP48 (50 nM) on SDS-gel quantified using TAMRA<sup>Ub</sup>. Fluorescent gel scans and quantification of the individual reaction species are shown. Replicates of two experiments  $\pm$  SEM

**b** Cleavage of all the di-Ubiquitin linkages by USP48 (100 nM). USP16 (500 nM) serves as an unspecific positive control.





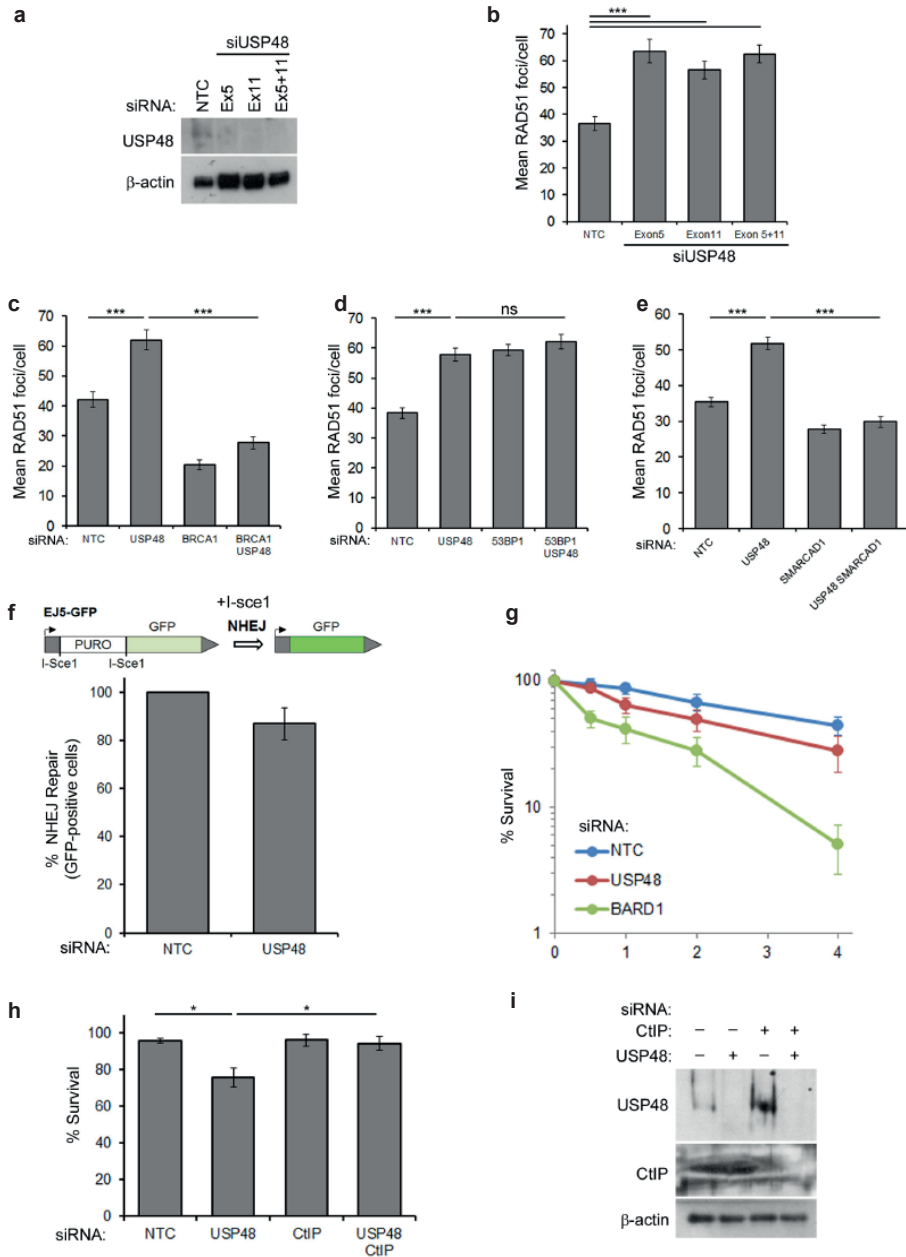
**Supplemental Figure 3**

**a** Gel based cleavage assay of H2A<sup>BRCA1ub</sup> kinetic analysis in Figure 2. TAMRAUb was used as readout and concentration of USP48 and H2A<sup>BRCA1ub</sup> were varied across the range indicated. Fluorescence readout of the gels and quantifications are shown including the fit obtained from fitting with *KinTek explorer*.

**b** USP48 binding to NCPs of different ubiquitination status. Raw traces from the SPR experiments fitted in Figure 2d.

**c** USP48<sup>so1</sup> cleavage of 2 μM H2A<sup>BRCA1ub</sup> in the absence and presence of 25 μM ubiquitin.

**d** Ubiquitin does not activate USP48. Cleavage of 2 μM Ub<sup>Bho</sup> by 50 nM USP48 in the presence of indicated ubiquitin concentrations.



**Supplemental Figure 4.**

**a** Western blot for USP48 expression levels with two independent siRNA sequences.

**b** Quantification of RAD51 foci in S-phase HeLa cells depleted for USP48 and fixed at 2 hours post 5 Gy IR. Graph shows mean RAD51 foci/cell, n >30 cells, errors = S.E.M. \*\*\* p<0.005 Student's T-test.

**c** Quantification of RAD51 foci in S-phase HeLa cells depleted for USP48 and BRCA1 and fixed at 2 hours post 5 Gy IR. Graph shows mean RAD51 foci/cell, n=60 cells, errors = S.E.M. \*\*\* p<0.005 Student's T-test.

**d** Quantification of RAD51 foci in S-phase HeLa cells depleted for USP48 and 53BP1 and fixed at 2 hours post 5 Gy IR. Graph shows mean RAD51 foci/cell, n=115 cells, errors = S.E.M \*\*\* p<0.005, ns=non-significant, Student's T-test.

**e** Quantification of RAD51 foci in S-phase HeLa cells depleted for USP48 and SMARCD1 and fixed at 2 hours post

- 5 Gy IR. Graph shows mean RAD51 foci/cell, n=145 cells, errors = S.E.M \*\*\* p<0.005 Student's T-test.
- f** Measures of non-homologous end-joining (NHEJ) are slightly decreased on USP48 depletion. Integrated NHEJ assay of cells treated with control (NTC) and USP48 siRNA. GFP-positive cells were normalised to the transfection efficiency (RFP) and %-repair is given compared to NTC. Graph shows mean of 5-independent experiments, error bars are S.E.M.
- g** Colony survival of HeLa cells depleted for USP48, BARD1 or treated with control siRNA and treated with ionising irradiation (IR). After treatment cells were plated at limiting dilutions and grown for 10-14 days to form colonies. Graph shows mean % survival normalised to untreated controls, n=4, error bars are S.E.M.
- h** Colony survival of HeLa cells depleted for USP48, CtIP and both USP48 and CtIP. Cells were treated with 1 Gy IR before plating out at limiting dilutions and grown for 10-14 days to form colonies. Graph shows mean % survival normalised to untreated controls, n=3, error bars are S.E.M. \* p<0.05 Student's T-test.
- i** Western blot of siRNA treated lysates probed for USP48 and CtIP.

**Supplemental table 1**

Best fit values for Michaelis-Menten kinetics from Figure S1A.

	Kcat (s <sup>-1</sup> )	Km (uM)	Kcat/Km (s <sup>-1</sup> uM <sup>-1</sup> )
<b>USP1/UAF1</b>	1.18 ± 0.06	0.34 ± 0.06	3.450
<b>USP3</b>	0.00360 ± 0.00006	6.29 ± 0.21	0.0006
<b>USP7</b>	0.51 ± 0.04	17.50 ± 2.52	0.029
<b>USP11</b>	0.020 ± 0.001	0.31 ± 0.03	0.076
<b>USP12/UAF1</b>	0.064 ± 0.002	4.31 ± 0.45	0.079
<b>USP15</b>	0.23 ± 0.02	1.61 ± 0.21	0.143
<b>USP16</b>	0.26 ± 0.006	8.20 ± 0.49	0.032
<b>USP48</b>	0.02 ± 0.0007	5.14 ± 0.53	0.004
<b>BAP1/ASXL1</b>	1.78 ± 0.031	3.57 ± 0.19	0.499



## Chapter 4

### **The nucleosome acidic patch plays a critical role in RNF168-dependent ubiquitination of histone H2A**

Francesca Mattioli<sup>1\*</sup>, Michael Uckelmann\*, Danny D. Sahtoe, Willem J. van Dijk, Titia K. Sixma

*Division of Biochemistry and Center for Biomedical Genetics, Netherlands Cancer Institute, Plesmanlaan 121, 1066 CX Amsterdam, The Netherlands. <sup>1</sup>Current address: Howard Hughes Medical Institute and Department of Molecular and Radiological Biosciences, Colorado State University, 1870 Campus Delivery, Fort Collins, CO 80523.*

*\* These authors contributed equally to this work.*

*Nature Communication 2014;5:3291*

## ABSTRACT

During DNA damage response, the RING E3 ligase RNF168 ubiquitinates nucleosomal H2A at K13-15. Here we show that the ubiquitination reaction is regulated by its substrate. We define a region on the RING domain important for target recognition and identify the H2A/H2B dimer as the minimal substrate to confer lysine specificity to the RNF168 reaction. Importantly, we find an active role for the substrate in the reaction. H2A/H2B dimers and nucleosomes enhance the E3-mediated discharge of ubiquitin from the E2 and redirect the reaction towards the relevant target, in a process that depends on an intact acidic patch. This active contribution of a region distal from the target lysine provides regulation of the specific K13-15 ubiquitination reaction during the complex signaling process at DNA damage sites.

## INTRODUCTION

Ubiquitin conjugation is a regulatory post-translational modification employed by the cell in a variety of processes<sup>1</sup>. A three step cascade of E1, E2 and E3 enzymes is required for the reaction and the molecular mechanism of the ubiquitination process varies with the target and the enzymes involved.

Target specificity in the ubiquitination reaction is regulated in most cases by the E3 ligases<sup>2</sup> that can mono-, multi- or poly-ubiquitinate their substrates. The vast majority of these proteins function through a structurally conserved RING domain that is able to allosterically activate the E2~ubiquitin complex to release the ubiquitin moiety directly onto the lysine residue of the selected substrate<sup>3</sup>.

In some cases, the modification site on the substrate is relatively undefined (for example, on p53, p27 and DDB2)<sup>4-6</sup>. In other cases, E3 ligase reactions are highly specific for a single residue (for example, PCNA, IκB, H2B and H2A)<sup>7-16</sup>. The difference in the stringency of the site-specificity of the E3 reactions highlights the diversity of signals generating from ubiquitination events. Some ubiquitin signals do not require a specific attachment site on the substrate, as they signal primarily through the ubiquitin moieties (for example, K48 chains for proteasomal degradation). However, in those cases where ubiquitination stimulates a specific molecular signal, the choice of target lysine must be restricted, resulting in a highly selective E3 reaction. Examples include the site-specific mono-ubiquitination of PCNA, H2B and H2A, which are recognized by specific interacting proteins, thus providing a selective signaling response<sup>17-21</sup>.

How RING E3 ligases determine target selection is highly variable. In some classes of RING E3s components outside the RING domain are responsible for target selection. For instance,

in the family of Cullin-RING Ligases (CRLs) substrate recognition involves a separate molecule besides the subunit carrying the RING domain<sup>22</sup>. Similarly, for some RING E3s not belonging to the CRL family (for example, CHIP and c-Cbl)<sup>23,24</sup>, domains outside the RING motif are required for target recognition.

In other cases, the isolated RING domains appear to be sufficient for lysine specificity<sup>13,14,25</sup>. In these instances, a selective RING/E2~Ub-substrate interaction must occur to orient the ubiquitination machinery to the correct lysine. However, the RING is situated at least 20-30 Å away from the active site cysteine on the E2 enzyme where the C-terminal end of ubiquitin forms a thioester bond, ready to be attacked by the amino group of the target lysine. This implies that a region of the substrate, relatively far from the target lysine, may be involved in the ubiquitination reaction.

The molecular mechanism of activation of the E2~Ub complex by the RING domain of E3s has recently been clarified by several studies<sup>26-28</sup>. These show how the RING domain and the ubiquitin-charged E2 form a trimeric complex that positions ubiquitin in a conformation proficient for efficient release onto the substrate lysine. In this orientation, the donor ubiquitin makes contact with the E2 via the I44 hydrophobic patch and a salt bridge via its R42, but also engages interactions with the E3 via residues of the I36 hydrophobic patch<sup>26-30</sup>. Stabilization of this state is a largely conserved mechanism among different RING-mediated reactions and mutation of these residues on ubiquitin affects E2 discharge and target modification. However, in this rather detailed mechanistic description of the ubiquitination reaction by RING domains, the role of the target molecule has thus far been poorly defined. Molecular insights on the potential catalytic roles of targets so far have been restricted to ubiquitin itself as a substrate during the formation of specific chain types by E2 conjugating enzymes<sup>29,30</sup>.

Here, we investigate the relative contributions of E3 and substrate during histone H2A ubiquitination by RNF168. H2A is one of the histone proteins composing the nucleosome core. H2A is abundantly modified on its C-terminal tail at K119 by the RING E3 ligases present in the Polycomb repressive complex 1 (PRC1), where RING1B/BMI1 is the most studied E3 dimer<sup>12,13,31,32</sup>. Recently, the E3 ligase RNF168 has been described to target the N-terminal residues K13-15 during DNA double-strand break signaling<sup>14,15</sup>.

RNF168 is a monomeric E3 ligase that is recruited to sites of DNA damage by interaction of its conserved ubiquitin interaction motives with ubiquitin chains<sup>33-37</sup>. Its recruitment depends on the signaling of a large number of other proteins that are localized at damage sites with faster kinetics<sup>35-37</sup>. Once RNF168 is localized at these sites, its ability to target K13-15 on H2A is required for a functional response cascade<sup>14,20</sup>. This ubiquitination reaction is

highly selective for K13-15 in cells and interestingly the RING domain of the E3 is sufficient to confer target specificity *in vitro* with the E2 Ubch5c<sup>14,20</sup>. This provides a useful system for mechanistic studies of the molecular determinants on the E3 and the substrate that regulate this specificity.

In this study we identify the region on the RING domain of RNF168 that interacts with its targets, namely the nucleosomes and H2A/H2B dimers. We find that these substrates activate the RNF168-dependent reaction and this effect is dependent on a conserved acidic patch present on the H2A/H2B surface. These findings indicate that RNF168-dependent K13-15 modification is regulated by a region located distally to the target lysines. In addition, they highlight the importance of accessibility to the acidic patch by the ubiquitination machinery during DNA damage signaling.

## RESULTS

### RNF168 can site-specifically modify H2A/H2B dimers

We previously showed that the E3 ligase RNF168 is specific for K13 and K15 on H2A in oligonucleosomes *in vivo* and *in vitro*<sup>14</sup>. Here, by using recombinant nucleosome core particles (NCPs) carrying lysine mutations on H2A we find that, although eventually other lysines are also modified, the RING domain of RNF168 is sufficient to favour modification of the K13-15 lysines *in vitro* (Supplementary Fig 1a). As we use a RNF168 construct (R; residues 1-189), carrying not only the RING domain but also the MIU1 and UMI motives<sup>33-37</sup> we wondered if specificity for the K13-15 site is affected upon deletion of these ubiquitin-binding regions (Supplementary Fig. 1b). With a minimal RING domain construct (residues 1-113) we observe a decrease in activity towards H2A in NCPs but the specificity for K13-15 is retained (Supplementary Fig. 1c), confirming that the short RING domain provides the observed lysine specificity<sup>20</sup>.

Next, we investigated the minimal substrate requirements for RNF168 activity. As previously shown<sup>14</sup>, RNF168 can target the isolated histone H2A *in vitro* in an aspecific manner, as the K13-15R mutant is modified at similarly low levels as WT H2A (Fig. 1a). This is not surprising as the histone in isolation is mostly unfolded.

In contrast, when a reconstituted dimer of H2A and H2B is provided as substrate, the RING domain of RNF168 can modify the WT protein efficiently, but not the K13-15R variant, indicating that the reaction becomes specific for these lysines on H2A (Fig. 1b). These findings indicate that the isolated H2A/H2B dimer is sufficient to provide H2A lysine specificity for the RNF168 RING domain reaction.

When we compare the activity of RNF168 towards H2A, the H2A/H2B dimer and NCPs, we



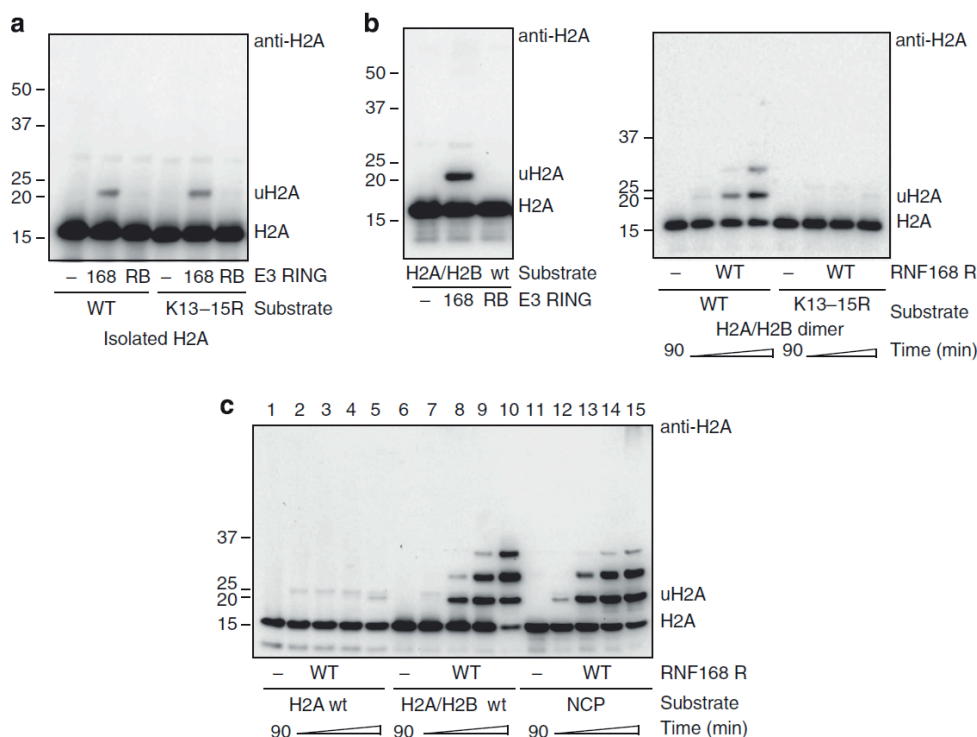


**Figure 1 The H2A/H2B dimer is specifically modified at K13-15 by the RNF168 RING domain**  
**a)** RNF168 targets H2A in isolation in an inefficient manner and its activity is not specific for K13-15. RING1B/BMI1 are inactive towards the histone protein alone. Ubiquitination assay performed in presence of H2A WT or K13-15R in isolation. **b)** RNF168 targets H2A specifically on K13-15 within the H2A/H2B dimer. Ubiquitination assays performed in presence of WT or K13-15R H2A in H2A/H2B dimer. Single time point assay, where RING1B/BMI1 were used as negative control. Time course assay (10-30-60-90 minutes) in presence of WT or K13-15R dimers (assays performed at 200 mM NaCl). **c)** RNF168 has comparable activity for H2A in dimers and in nucleosomes, while isolated H2A is targeted with low efficiency. Time course assay (10-30-60-90 minutes) to compare activity of RNF168 RING domain towards H2A alone, H2A/H2B dimers and NCPs.

observe that rates of modification for dimer and NCP are very similar and much higher than on H2A alone (Fig. 1c), showing that the histone dimer contains the minimal molecular features that define the relevant substrate for RNF168 activity.

**RNF168 RING uses a charged region for nucleosome recognition**

To understand how the RNF168 RING domain recognizes its substrate, we first set out to identify the region on the RING domain involved in nucleosome interactions. We have previously shown that a charged residue located adjacent to the second Zn ion in the RNF168 RING domain (R57, Fig. 2a) is important for nucleosomal H2A ubiquitination but not for targeting the isolated histone or making ubiquitin chains<sup>14</sup>.

First, we observed that the R57D RING domain mutant has lost activity towards H2A in the H2A/H2B dimer (Fig. 2b), indicating that the function of this residue is retained when only H2A and H2B are present. Additionally, we tested an RNF168 R57A mutant RING domain.

This protein also inhibits the E3 ligase function towards the histone dimer (Fig. 2c), excluding the possibility that the observed effect is caused by electrostatic repulsion of the aspartate mutant.

To further explore this region on the RING domain we analyzed the importance of a helix adjacent to this site in RNF168, rich in positively charged residues. We replaced this helix (residue 58-72, Fig. 2a) with a shorter loop that is present on RNF8, an E3 ligase that is inactive towards nucleosomal H2A<sup>14</sup> (residues 444-449, Fig. 2a). The constructs include either the helix alone (8loopR) or the helix and the R57D mutation (8loopD). Neither of these mutants is affected in its ability to promote ubiquitin chain formation (Fig. 2d). Nevertheless, both of these have lost the ability to modify H2A within the H2A/H2B dimer (Fig. 2b). Overall, these results show that both R57 and the adjacent helical region on the RING domain of RNF168 are required for H2A modification.

To test whether this region is involved in direct interaction with the substrate, we analyzed binding of the RNF168 RING domain to recombinant NCPs using native gel-shift assays and to H2A/H2B dimers using fluorescence polarization (FP) experiments. The RING domain of RNF168 binds to H2A/H2B dimers with an apparent dissociation constant ( $K_d$ ) of  $\sim 1 \mu\text{M}$  (Fig. 2e) and it can shift NCPs on a native gel (Fig. 2f). In contrast, the R57D mutant shows impaired binding to both substrates (Fig. 2e,f), indicating a role for this site in direct interaction with the H2A/H2B dimer and the NCPs.

In the RING domain of RING1B (Fig. 2a), the structurally analogous region to this C-terminal helix is involved in DNA binding and thereby in target recognition<sup>25</sup>, therefore we tested the DNA binding capacity of the RING domain of RNF168. In a buffer containing 50 mM NaCl, RING1B/BMI1 binds a double-strand 15mer DNA ( $K_d = 1\text{-}1.5 \mu\text{M}$ , Fig. 2g)<sup>25</sup>. In contrast, even at this low salt concentration, RNF168 shows very weak interaction with DNA ( $>10 \mu\text{M}$ , Fig. 2g). At higher salt concentrations no binding is observed. This indicates that RNF168 doesn't recognize NCPs through DNA interactions, in line with the observation that the H2A/H2B dimer is sufficient to provide an efficient substrate.

Overall, these data show that RNF168 RING domain binds the H2A/H2B dimer and the nucleosomes. The charged region at the C-terminal end of the RING domain of RNF168 is involved in this binding and thereby in substrate selection. Mutations in this positively charged region impair the RNF168-mediated H2A modification by disrupting the binding to its substrate, the NCPs. Notably, the intrinsic free ubiquitin chain forming activity of RNF168 is not affected in these mutants (Fig. 2d).

### **H2A modification requires an intact nucleosomal acidic patch**

We next investigated how the H2A/H2B dimer confers selectivity to the RNF168-driven reaction. The H2A/H2B dimer is known to form an acidic patch on the surface of the nucleosome core, by clustering several glutamate residues from H2A and H2B (Fig. 3a). This

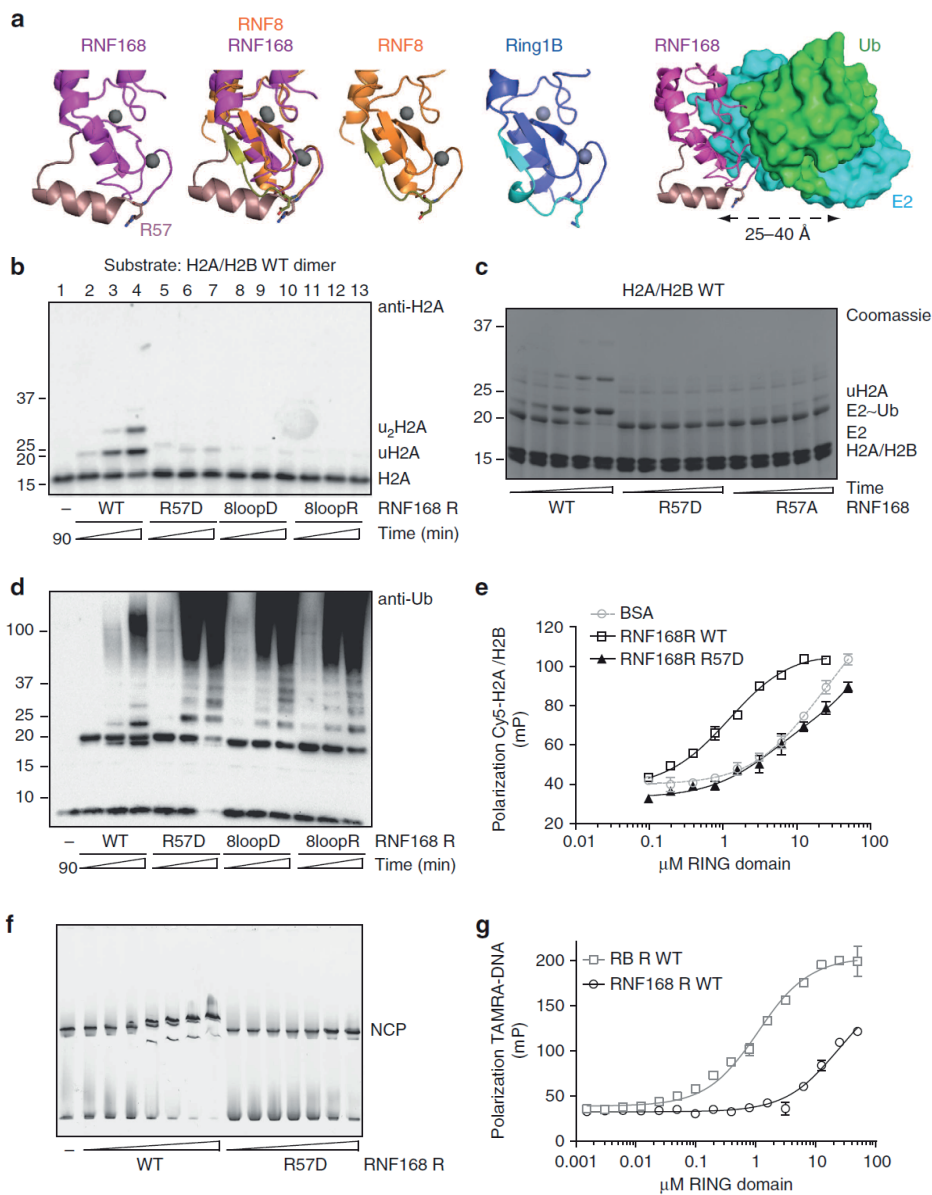


**Figure 2**

**RNF168 RING domain interacts with the target through a charged region**

**a)** Position of the targeting region on the RNF168 RING domain: 8loopD: replacement of residues 57-72 on RNF168 (PDB-code:3L11<sup>54</sup>, in magenta) with residues 443-449 of RNF8 (PDB-code: 4AYC<sup>14</sup>, in orange). 8loopR: replacement of residues 58-72 on RNF168 with residues 444-449 of RNF8: R57 is present in this RING domain mutant. The residues in RNF8 used in the 8loopD mutant are highlighted in olivegreen (D443 in sticks). Position of the targeting region relative to E2 binding (Model based on the RNF4/UbcH5a~Ub structure PDB-code: 4AP4<sup>27</sup>) **b)** H2A/H2B dimer targeting by RNF168 requires both the helix (58-72) and R57. Anti-H2A blots of time course experiment (30-60-90 minutes) performed in presence of H2A/H2B WT dimer (5 μM) and different mutants of RNF168 RING domain (1 μM). Anti-ubiquitin blot of these samples are shown in panel **d**. **c)** Mutation of R57 to A or D inhibits the activity of the RING domain towards H2A/H2B dimers. Time course single turnover assay (1,2,4,8,16 minutes) ▶

acidic patch is employed by a variety of proteins, including the H4 tail, for binding to the nucleosomes in different processes<sup>38</sup>. To investigate a potential role for this patch in the RNF168 reaction, we assembled H2A/H2B dimers with mutant histones (E61,64,91A on H2A and/or E102,110A on H2B). These mutations do not affect the formation of the H2A/H2B dimers (Supplementary Fig. 2a), but they prevent RNF168-dependent H2A ubiquitination (Fig. 3b). Similar results were obtained when we reconstituted NCPs with all five glutamates mutated (NCP EA) indicating that the integrity of this patch is required for productive ubiquitination by RNF168 (Fig. 3c).

To confirm these findings, we performed ubiquitination assays using wild-type NCPs in presence of a peptide known to bind on the acidic patch (LANA)<sup>39</sup>. In these experiments, increasing amounts of LANA peptide were found to inhibit the ubiquitination of nucleosomal H2A. Using a mutant variant of this peptide (LRS), unable to bind the nucleosome<sup>39</sup>, did not affect the reaction (Fig. 3d). This supports the hypothesis that the acidic patch on the nucleosome is required for activity of the RNF168/UbcH5c ubiquitination machinery.

#### The acidic patch is not involved in binding by RNF168/UbcH5c

To analyze the importance of the acidic patch for recruitment of the E3, we compared binding of the RNF168 RING domain to wild-type or EA mutant NCPs and H2A/H2B dimers. Surprisingly, the presence or absence of the acidic patch does not affect the binding of RNF168 RING domain to these substrates (Fig. 4a-b). Moreover, binding of the RNF168 RING domain on wild-type NCPs cannot be competed out by the LANA peptide (Fig. 4c) although this does inhibit ubiquitination activity (Fig. 3d).

These observations indicate that, in contrast to the RNF168 R57 site, the acidic patch on the target is not involved in the direct interaction with the E3 ligase. Since simple recruitment of the E3 ligase to the substrate does not explain the importance of the acidic patch for RNF168 activity, a different step in the ubiquitination reaction must be affected. We wondered whether the acidic patch would affect the formation of the NCP-E3-E2~Ub complex.

We used a mutant UbcH5c where the active site cysteine is mutated to lysine (C85K) to form a stable isopeptide linkage with the C-terminal tail of ubiquitin<sup>27</sup>, preventing the release of the ubiquitin in presence of the E3 and the substrate. With this stable E2~Ub complex we could assess how the RING/E2~Ub complex binds to NCPs in gel-shift assays.

- **coomassie staining of SDS-PAGE gel.** Appearance of ubiquitinated H2A is visible only in presence of WT RNF168. Experimental conditions as in Fig. 5b-c (100 nM E3). E2~Ub discharge occurs only in presence of a targetable substrate. **d)** Mutation of the helix (58-72) and R57 do not inhibit ubiquitin chain formation by RNF168 RING domain. Anti-ubiquitin blot of the samples shown in panel **b**. **e)** RNF168 RING domain interacts with H2A/H2B dimers via the R57 site. Fluorescence Polarization (FP) assay using <sup>15</sup>N-H2A/H2B dimers (10 nM) and increasing amounts of RNF168 RING domain WT or R57D mutant. BSA is shown as a control to assess the effect of protein crowding in the reactions. Mean and SEM are shown, calculated on at least two independent experiments. **f)** RNF168 RING domain interacts with NCPs via the R57 site. Gel shift assay performed in presence of WT NCPs (100 nM) and increasing concentrations of RNF168 RING domain WT or R57D (0.77-1.55-3.1-6,2-12,5-25-50 μM). **g)** RNF168 RING domain binds DNA with very low affinity at 50 mM NaCl, compared to the RING domains of RING1B/BMI1 (RB R). DNA binding measured by FP assay of TAMRA-labeled 15mer DNA. Mean and SEM are shown, calculated on two replicates.

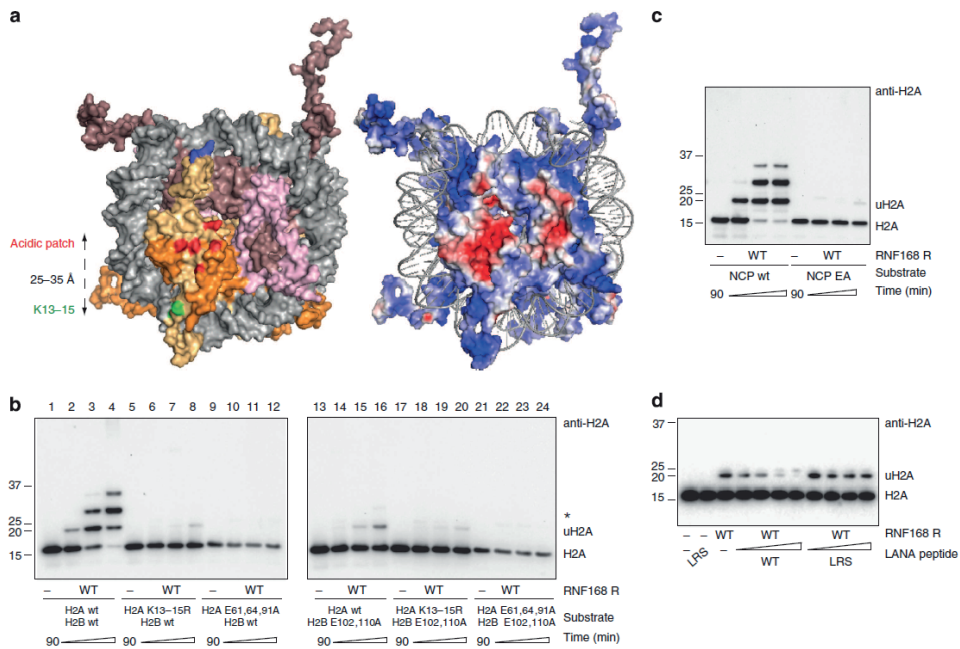


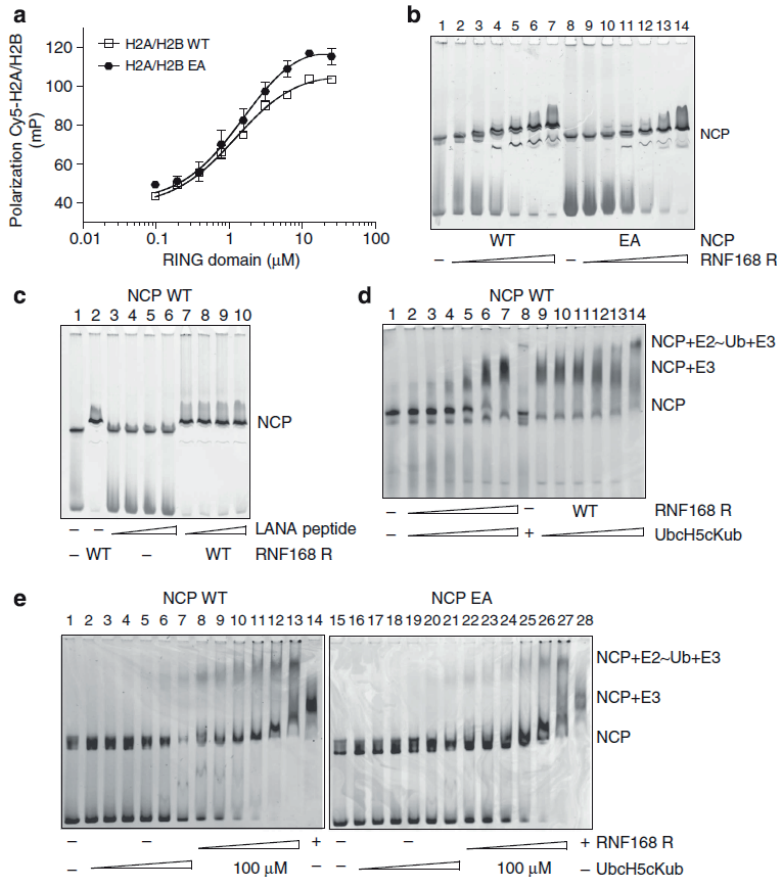
**Figure 3**  
**Targeting H2A requires an intact and accessible acidic patch** **a)** Position of the acidic patch within the nucleosome. NCP structure (1KX5<sup>55</sup>) where H2B is shown in orange, H2A in yellow-orange, H3 in light-pink and H4 in violet. K118-119 on H2A are highlighted in blue, K13-15 are in green and the glutamate residues of the acidic patch are shown in red. Distance between K13-15 and the acidic patch are indicated on the left. Electrostatic potential (red is negative, blue is positive) of the histone core in the NCP highlights the acidic patch on the surface of the H2A/H2B dimer. **b)** Mutations in the acidic patch on H2A or H2B impair H2A ubiquitination in H2A/H2B dimers. Time course experiment (30-60-90 minutes) following activity of RNF168 RING domain towards H2A in the different H2A/H2B mutant dimers. **c)** Acidic patch mutations prevent ubiquitination of NCPs. Time course experiment (30-60-90 minutes) to investigate the activity of RNF168 RING domains towards H2A in nucleosome WT or EA (H2A E61,64,91A and H2B E102,110A). **d)** Binding of a LANA peptide, but not a mutant LRS variant, to the nucleosome competes with RNF168-dependent ubiquitination of NCPs. Ubiquitination assay with 3-10-30-100 μM peptide. Note that E91 on H2A is part of the epitope recognized by the anti-H2A antibodies, therefore there is reduced signal on western blots when the E91A mutation is introduced.

In these assays the E2~Ub complex alone does not bind to NCPs (Fig. 4d, lane 8 and 4e, lanes 1-6) but it causes an additional shift of the E3-NCP complex when E2~Ub is present at high concentrations (>25 μM) (Fig. 4d). This shows that a trimeric complex can assemble on NCPs containing E3/E2~Ub, although the E2~Ub component does not significantly alter the affinity of the RING for NCPs.

Interestingly the trimeric complex is observed for both WT and EA NCPs with the charged E2 complex (Fig. 4e). This implies that its assembly takes place independently of the integrity of the acidic patch. We conclude that binding of the ubiquitination machinery to the substrate does not rely on the nucleosomal acidic patch.

**The acidic patch is critical for H2A ubiquitination by RNF168**

Since the importance of the acidic patch for activity (Fig. 3) is not explained by a role in binding (Fig. 4), we postulated that these negative charges on the nucleosome core may

**Figure 4****The nucleosome interacts with the E2~Ub/E3 complex independently of the acidic patch**

**a)** Mutation of the acidic patch on H2A/H2B dimers does not affect RNF168 RING domain binding. Fluorescence Polarization (FP) assay using Cy5-labelled H2A/H2B dimers (10 nM) and increasing amounts of RNF168 RING domain WT. Mean and SEM are shown, calculated on at least two independent experiments. **b)** The RNF168 RING domain binds equally well to NCPs with (WT) and without acidic patch (EA). Gel-shift assay with NCPs WT and EA (100 nM) and RNF168 RING domain (1.55-3.1-6.2-12.5-25-50 μM). **c)** Binding to NCPs does not rely on the accessibility of the acidic patch. Gel-shift assay where NCPs WT (100 nM) are assessed for binding by RNF168 RING domain (25 μM) with increasing concentration of LANA peptide WT (12-25-50-100 μM). **d)** The E2~Ub thioester shifts the E3-NCP complex at high concentrations. Gel-shift assay where WT NCPs (100 nM) are assessed for binding by RNF168 RING domain (3.1-6.2-12.5-25-50-100 μM, lanes 2-7) and/or UbcH5c~Ub (3.1-6.2-12.5-25-50-100 μM, lanes 9-14). In lanes 9-14 the E3 concentration was kept constant to 100 μM. **e)** Both WT and EA NCPs can form a E2~Ub/E3/target complex. Gel-shift assay where NCPs WT (100 μM, lane 1-14) and EA (100 nM, lane 15-28)) are assessed for binding by UbcH5c~Ub (3.1-6.2-12.5-25-50-100 μM, lanes 2-7/15-21) or for binding of RNF168 RING domain (3.1-6.2-12.5-25-50-100 μM, lane 8-13/22-27) in the presence of 100 μM UbcH5c-Ub.

have a role in the actual catalysis by the RNF168 RING domain and the E2 UbH5c.

To address this point we performed single turnover assays following the rate of ubiquitin discharge from UbH5c in presence of RNF168 and of the different substrates.

In these reactions, when the E3 concentration is low (100 nM), RNF168 is hardly capable to activate ubiquitin discharge (Fig. 5a, lanes 4-5-6), compared to conditions where we use 1 μM E3 concentrations (Fig. 5a, lanes 10-11-12). Nevertheless, when substrate (NCPs) was added to the reactions, we observed a drastic activation of the discharge rate even



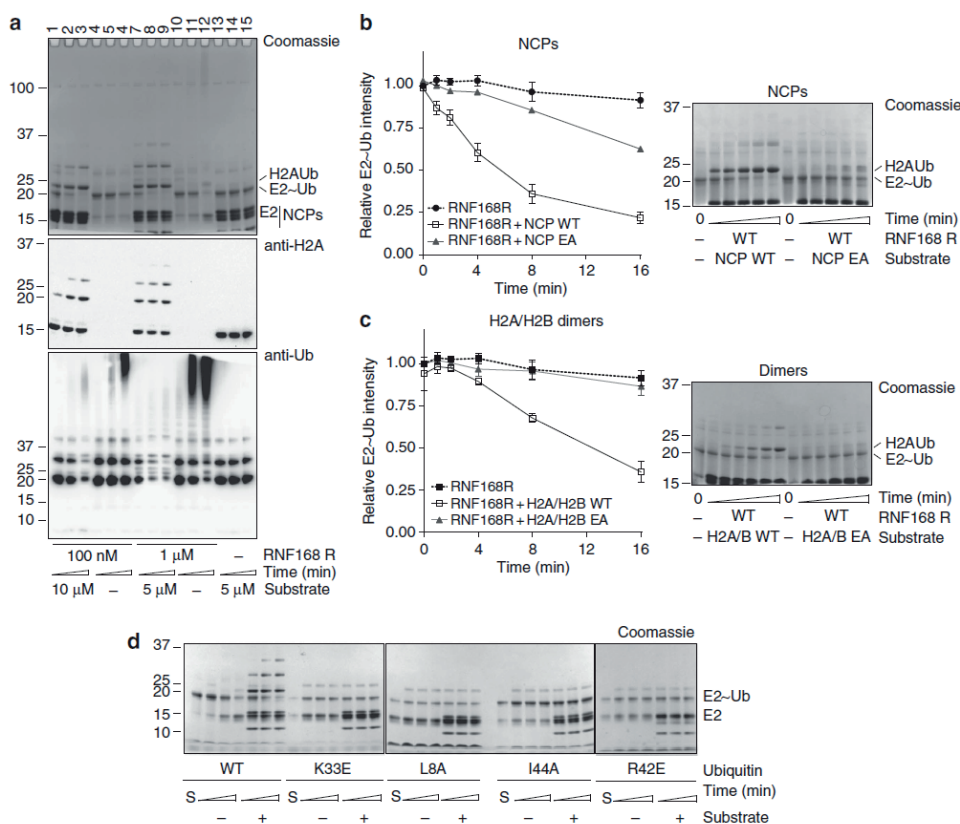


**Figure 5**

**The active role of the substrate in the reaction depends on the acidic patch.**

**a)** The substrate activates the discharge of ubiquitin from the E2 by RNF168 RING domain. Single turnover experiment performed at different E3 concentration shows that in presence of NCPs, there is activation of the enzymatic activity of RNF168 RING domain. The NCPs alone, in absence of RNF168, (lanes 13-15) are unable to stimulate E2 discharge. **b-c)** NCPs (**b**) and H2A/H2B dimers (**c**) further stimulate E2 discharge by RNF168. In the absence of the charges on the acidic patch the substrate-dependent activation is not taking place. Quantification of time course single turnover assays (1,2,4,8,16 minutes), where peak height of the E2~Ub band was used from Coomassie stained SDS-PAGE gels. Example gels are shown, the gels were run for longer time to increase the separation between the E2~Ub and the H2Aub bands. The samples at time 0 were used for the normalization. At least two independent experiments per time point and condition were used for quantification. Mean and SEM are shown. 100 nM E3 was used in these reactions. **d)** Ubiquitin residues required for E3 allosteric activation are important in the reaction towards the substrate. Single turnover assays in presence and absence of NCPs performed with 20 μM E2~Ub and 1 μM E3 and 5 μM substrate, time course 1,5-3-4-6-8 minutes. The R42E ubiquitin mutant samples were run using oligonucleosomes and not recombinant NCPs.

at these low RNF168 concentrations (Fig. 5a, lanes 1-2-3). This effect was only observed in presence of RNF168 (Fig. 5a, lanes 13-14-15), confirming that the NCPs alone do not promote discharge of the E2~Ub complex.

As quantified in Fig. 5b-c, the activating contribution of the substrate to the RNF168 reaction was observed both for NCPs and H2A/H2B dimers (Fig. 5b-c, solid black lines). Moreover, in these experiments we also noticed that the substrate seems to redirect the ubiquitination from chain formation to target protein modification. While the sole addition of the RNF168 RING domain increases the amount of ubiquitin conjugates in the reaction as expected

(Fig. 5a, lanes 4-5-6-10-11-12 and Supplementary Fig 3a-b, lane 7 to 11), the concomitant addition of the substrate NCP or H2A/H2B dimer strongly reduces the formation of high molecular weight ubiquitin species in favor of H2A modification (Fig. 5a, lanes 1-2-3-7-8-9 and Supplementary Fig 3a, lanes 12 to 16 and 3b, lanes 13 to 17). This suggests that the substrate is actively involved in catalysis by directing the E2/E3 activity towards the target lysine on H2A.

Interestingly, when we used NCPs or H2A/H2B dimers with mutation of the acidic patch (EA), the activation of the E2~Ub discharge due to the presence of the substrate was lost (Fig. 5b-c, solid gray lines) and the high molecular weight ubiquitin chains were formed in similar amounts compared to the reactions where the substrate is not present (Supplementary Fig. 3a, lanes 17-21 and 3b, lanes 18-22). These findings show that the acidic patch residues are critical for catalysis by RNF168/UbcH5c, without being involved in the interaction between the ubiquitination machinery and the target (Fig. 4).

In previous studies of the RING E3 mechanism it became clear that an important step in the reaction can be the positioning of ubiquitin for catalysis<sup>26-30</sup>. A possible function of the substrate in these reactions may cause a different catalytic mechanism by forcing a different orientation of ubiquitin in respect to the E3/E2 machinery to enhance the ubiquitin transfer. We investigated if mutation of key residues critical in RING-dependent stabilization of an E2~ubiquitin complex<sup>26-28</sup> could affect the RNF168 reactions in presence or absence of the target. In these assays the I44, L8, R42 and K33 sites are required for both substrate-independent and -dependent reactions (Fig. 5d), indicating that RNF168-dependent catalysis is likely to utilize a similar mechanism as previously described<sup>26-28</sup> both in presence and in absence of the substrate. This suggests that the acidic patch effect during the RNF168 reaction is not due to a repositioning of the ubiquitin moiety in the ubiquitination complex. Moreover, since mutation of the residues forming the acidic patch on either H2A or H2B individually has comparable effects (Fig. 3a), it seems likely that the role of the acidic patch is not mediated by a single glutamate residue involved in catalysis, but rather that the nucleosomal negative surface at this region influences the reaction by RNF168/UbcH5c, either by orienting the machinery or by long-range effects on the catalysis (Fig. 6a).

## DISCUSSION

The mechanism of RING-dependent ubiquitination reactions is complex and does not involve enzymes with conventional catalytic properties. Recent studies have highlighted how RING domains allosterically activate the release of ubiquitin from the E2<sup>26-28</sup>, but relatively little is known about the influence of the substrate on the reaction.

H2A ubiquitination is particularly interesting because the RING domains of the respective E3 ligases can provide lysine specificity to the *in vitro* reactions with the same E2 enzyme, UbcH5c. Therefore the RING domains of PRC1 and RNF168 must contain the molecular



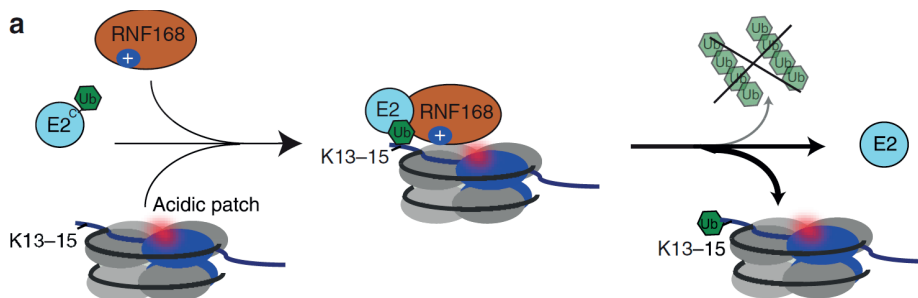


**Figure 6**

**The nucleosomal acidic patch is critical for RNF168 reaction**

**a)** The ubiquitination of K13-15 on H2A in nucleosomes requires a positive patch on RNF168 for recruitment of the E3 ligase to the H2A/H2B dimer and the nucleosome. The negatively charged acidic patch formed by H2A and H2B activates and redirects the reaction from chain formation to selective H2A modification.

requirements to orient themselves, providing a minimal system for studying substrate recognition and its role in the catalytic process.

This study focuses on the recently described K13-15 ubiquitination of H2A by RNF168, which has roles in the DNA damage signaling. We showed that the isolated H2A/H2B dimer is the minimal relevant substrate required for an efficient and specific reaction. Then we identified a region on the RING domain of the E3 involved in substrate binding. Next, we found that the substrate is able to accelerate the reaction catalysed by RNF168/UbcH5c, redirecting ubiquitination activity towards the physiologically relevant lysines on H2A. These effects are highly dependent on an intact acidic patch on the H2A/H2B dimer within the nucleosome.

The actual mechanism used by these substrates to regulate catalysis and the selectivity for specific lysines require further analysis. Particularly the target lysines (K13-15) are likely to play a role in this mechanism, but we have not succeeded in uncoupling the contribution of these residues, because the lysine mutants are still modified in these *in vitro* reactions.

Nevertheless, our results are important for understanding the mechanistic aspects of the RNF168 reaction as well as its functional requirements in the biological context of DNA damage signaling. The acidic patch is located far from the target lysine, providing the first distal substrate region with a direct role in ubiquitination catalysis beyond mere binding. This proposes a novel role for substrates in ubiquitination reactions that may well be more general, although it is unlikely that all ubiquitination targets will contribute to ubiquitination reactions in this manner. When the target is non-specific and it is not important which lysine is modified, as proposed for example for Cullin-mediated reactions<sup>40</sup>, such an involvement is less likely. For cases where the lysine location is a critical signal, however, the catalytic involvement of the substrate can provide an important step in optimizing selectivity and efficiency of the ubiquitination reaction, with unique aspects. Such a complex mechanism ensures that modification takes place only when sufficient E3/E2~Ub is available that contacts the substrate in a specific configuration, where two conditions are met: the lysine

is available in proximity to the E2-ubiquitin thioester and the machinery can cross-talk to a distal region involved in the activation. Active involvement of the substrate may explain the low affinity interactions that are observed between RING E3s and their substrates, since it adds a regulatory step additional to proper target recognition.

Our data shows that RNF168 requires accessibility to the acidic patch on nucleosomes to target H2A. A large number of proteins are known to bind to this site, and RNF168 will have to compete with those to exert its function at DNA double-strand breaks sites. RNF168 is recruited to damaged chromatin by binding to ubiquitin chains, controlling the local concentration. The low affinity we measure for the E3 to the substrate ensures a dependence on the recruitment step and prevents premature action of RNF168. Here we propose that RNF168 reaction can only progress after adequate preparation of the chromatin fibers around the site of damage, where the acidic patch will be exposed. Many proteins are known to act upstream of RNF168, including E3 ligases such as RNF8 and HERC2 and other enzymes, for example, ATM and chromatin remodelers<sup>35-37,41-46</sup>. Some of these are required to recruit RNF168, but it is plausible that others are necessary to create the proper chromatin conformation around the damage that allow access to the acidic patch and hence promote ubiquitination of H2A. In addition, our study highlights that different histone H2A variants with alterations to the acidic patch residues may be treated differently by RNF168, for example, H2A.Bbd and H2A.Z<sup>47,48</sup>.

Overall, our findings contribute to the understanding of the molecular requirements necessary for proper RNF168 activity on nucleosomal H2A and to the clarification of the necessary steps required for DNA damage signaling in response to DNA double-strand breaks.

## METHODS

### Protein Expression and Purification

E1 was purified using His-tag affinity purification, PorosQ and gel-filtration columns<sup>49</sup>. UbcH5c was purified by GST-tag affinity purification and gel filtration after tag cleavage; untagged ubiquitin was purified by perchloric acid precipitation, Sepharose SP and Superdex 75 columns<sup>13,14</sup>. RNF168 (1-189) and RING1B/BMI1 RING domains were purified using a His-SUMO tag and a GST- and His-tags respectively, after cleavage of the tag, the proteins were run on a Superdex 75 column<sup>13,14</sup>. Oligonucleosomes were purified from HEK-293T cells<sup>13,14</sup>. Histone proteins were purified in denaturing conditions<sup>50</sup>. All point mutants, the RING loop substitutions and the acidic patch mutants were generated using the quickchange site directed mutagenesis kit (Stratagene). RNF168 (1-113) was cloned into a pGEX6p vector and it was expressed in E.coli with an overnight induction with 0.2 mM IPTG at 16°C. After lysis in buffer containing 30 mM Hepes 8.0, 500 mM NaCl, 10% glycerol, 1 μM ZnCl<sub>2</sub>, 1 mM TCEP, the

protein was purified using GSH beads (GE healthcare) and eluted with 50 mM glutathione. The tag was cleaved by GST-3c overnight in dialysis with lysis buffer. After removal of the protease, the uncleaved protein and the GST with GSH beads, the protein was loaded into a Superdex 75 column (GE healthcare) in 30 mM Hepes 8.0, 250 mM NaCl, 1  $\mu$ M ZnCl<sub>2</sub>, 1 mM TCEP. The fractions containing the protein were concentrated and stored at -80°C. SDS-PAGE of the final sample is shown in Supplementary Fig. 1b. Histone dimers were prepared by mixing H2A and H2B proteins in denaturing buffer. After refolding in dialysis tubes against 20 mM HEPES pH 7.5, 2M NaCl and 0.5 mM EDTA and 0.5 mM TCEP at 4°C overnight, the dimer was purified by gel-filtration on a S200 column (GE Healthcare) in 20 mM HEPES pH 7.5, 2 M NaCl and 0.5 mM EDTA and 0.5 mM TCEP, then concentrated and stored at -80°C. To minimize the NaCl contribution in the assays containing dimers, gel filtration in presence of buffer containing 500 mM NaCl was performed. The elution profile of the dimers in this condition remained unaltered. Assays shown in Fig. 5 and 3 were performed with dimers stored at 500 mM NaCl. Nucleosome core particles were prepared using a KCl gradient (2-0.15M)<sup>51,52</sup>. DNA used for the reconstitution was the 167 bp Widom 601 sequence<sup>53</sup>. The final purification step was a DEAE ion exchange column instead of preparative gel electrophoresis. After the linear salt gradient, NCPs were stored at 4°C in 20 mM HEPES pH 7.5, 200 mM KCl, 0.5 mM EDTA and 0.5 mM TCEP, for longer storage at -80°C a final concentration of 20% glycerol was added to the samples. Mutant proteins were treated and prepared as wild-type.

### ***In vitro* ubiquitination assays**

All *in vitro* ubiquitination assays (except those involving discharge assays in Fig. 2c, 5 and Supplementary Fig. 3r ) were done as follows: E1 (0.2  $\mu$ M) was mixed with UbcH5c (0.5  $\mu$ M), E3 ligase (0.5-1  $\mu$ M), ubiquitin (3-5  $\mu$ M), ATP (3mM) and 1  $\mu$ M of histone H2A, H2A/H2B dimer or NCPs. The reactions were incubated at 32 °C for 90 minutes (unless otherwise stated) in buffer 50 mM Tris/HCl pH 7.5, 100 mM NaCl, 10 mM MgCl<sub>2</sub>, 1  $\mu$ M ZnCl<sub>2</sub>, 1 mM TCEP. Final salt concentration in the assays was normally around 150 mM, unless otherwise stated. Western blot analysis was performed using anti-H2A (Millipore 07-146, 1:1000 dilution) or anti-ubiquitin (Santa Cruz P4D1, 1:1000 dilution) antibodies, followed by secondary HRP-conjugated anti-rabbit or anti-mouse antibodies respectively (BioRad, 1:10000 dilution).

### **E2 discharge assays**

For the single turnover assays, the E2 was pre-charged with ubiquitin. Concentrations are given for Fig. 5 and 2c, in brackets for Fig. 5 and Supplementary Fig. 3. To load the E2, E1 at 0.5  $\mu$ M was mixed with 100  $\mu$ M (70  $\mu$ M) UbcH5c in presence of 100  $\mu$ M (70 $\mu$ M) ubiquitin Mg<sup>2+</sup> and 3 mM ATP in buffer 50 mM Tris/HCl pH 7.5, 100 mM NaCl, 10 mM MgCl<sub>2</sub>. The sample was incubated 30-60 minutes at room temperature. Reaction was stopped with

50 mM EDTA final concentration and incubation on ice for 2 minutes. This mixture was then used for the discharge reactions, a final concentration of 15  $\mu$ M (20  $\mu$ M) E2~Ub was incubated at 32°C with 100 nM (1  $\mu$ M) of RNF168 RING domain alone or in presence of 10  $\mu$ M (5  $\mu$ M) NCPs or 20  $\mu$ M (5  $\mu$ M) dimers. Samples were stopped at given times and were analyzed by Coomassie staining on SDS-PAGE in non-reducing conditions and subsequently western blot analysis was carried out using anti-H2A (Millipore,07-146) or anti-Ub (Santa Cruz, P4D1) antibodies. Samples were run on either 12% or 4-12% NuPAGE gels in MOPS buffer (Life Technologies). Images were taken using ChemiDoc XRS system (BioRad) and ImageLab program. Quantifications were done using the peak height value of the E2~Ub band on Coomassie gels in ImageLab and GraphPad was used to prepare graphs.

#### Fluorescence Polarization (FP) assay

DNA binding reactions were carried out with 5 nM TAMRA-labeled DNA (TAACCCTAACCCCTA), 25 mM HEPES pH 7.4, 50 mM NaCl, 0.5% (w/v) BSA, 0.5% (v/v) Triton X-100. The RING domain protein solutions with the highest concentration were prepared in this buffer and subsequent dilutions were achieved by serial 1:1 dilutions in two repeats. The reaction was incubated for 15 min at room temperature before the measurements.

For H2A/H2B dimer affinity studies an H2A mutant, carrying an additional cysteine at the N-terminus was engineered using PCR site directed mutagenesis. The cysteine was labeled with a Cy-5 maleimide dye (GE Healthcare) using a 1:5 excess of dye over protein. The labeling reaction was carried out for 8 hours at room temperature and stopped with 10 mM DTT. This mutant was used to prepare <sup>Cy-5</sup>H2A/H2B dimers, following the same protocol used to prepare wild-type dimers.

To assess binding of RNF168 to <sup>Cy-5</sup>H2A/H2B dimer 10 nM of labeled dimer was titrated with increasing concentrations of RNF168 RING domain in a buffer containing 50 mM Tris pH 7.5, 100 mM NaCl, 10 mM MgCl<sub>2</sub>, 1 mM TCPE and 0.05% TWEEN20. The reaction was incubated for 5 minutes at room temperature prior to the measurement.

Fluorescence polarization was measured in 384-low volume plates (Corning) using a PHERAstar plate reader (BMG Labtech) with a FP filter module, with excitation filter 540 nm and emission filter 590 nm for <sup>TAMRA</sup>DNA and Ex 590 nm, Em 675 nm for <sup>Cy-5</sup>H2A/H2B. The data was analyzed with GraphPad and fitted to a one site binding model ( $Y=B_{max} * X / (K_d + X) + offset$ ).

#### UbCH5c C85K loading

The C85K mutation was inserted in pGEX6p, UbCH5c; the protein was expressed in E.coli with an overnight induction at 16°C with 0.2 mM IPTG. After lysis in buffer containing 50 mM Hepes pH 8, 150 mM NaCl, 0.5 mM TCEP the protein was purified using GSH beads (GE

healthcare) and eluted with 50 mM glutathione. The tag was cleaved by GST-3c overnight in dialysis with lysis buffer. After removal of the protease, the uncleaved protein and the GST with GSH beads, the protein was loaded into a S75 column in 20 mM Hepes 8.0, 150 mM NaCl, 1 mM TCEP. The fractions containing the protein were concentrated and stored at -80°C. The mutant E2 was loaded in a reaction containing 200 μM UbcH5c C85K, 200 μM ubiquitin, 1 μM Uba1 and 50 mM Tris pH 9.5, 150 mM NaCl, 0.8 mM TCEP, 3 mM ATP, 5 mM MgCl<sub>2</sub><sup>27</sup>. The reaction was incubated at 35°C for ~20 hours. The E2~Ub complex was purified on a S75 gel-filtration column and the fractions containing only the loaded E2 were concentrated and used for the gel-shift analysis shown in Fig. 4d-e.

### Gel Shift experiments

Gel shift assays were performed using native gelelectrophoresis on 4-12% Pre-Cast Tris-Glycine gels (Life Technologies), pre-run for at least 1 hour at 125V in Novex Tris-Glycine buffer. 100 nM NCPs were incubated with increasing amounts of E3 and/or E2~Ub in Shift Buffer (50mM Tris pH 7.5, 150 mM NaCl, 2mM arginine, 0,01% CHAPS, 0,01% Nonidet P-40). 5x Loading buffer containing 40% Sucrose and 0.25% Bromophenol Blue was added to the sample and 5 μl of the samples were loaded and the gel was run for 90 minutes at 125 V. Gels were stained with GelRed and visualized using the ChemiDoc XRS and ImageLab.

### REFERENCES

- 1 Hochstrasser, M. Origin and function of ubiquitin-like proteins. *Nature* **458**, 422-429, (2009).
- 2 Deshaies, R. J. & Joazeiro, C. A. RING domain E3 ubiquitin ligases. *Annu Rev Biochem* **78**, 399-434, (2009).
- 3 Budhidarmo, R., Nakatani, Y. & Day, C. L. RINGs hold the key to ubiquitin transfer. *Trends Biochem Sci* **37**, 58-65, (2012).
- 4 Rodriguez, M. S., Desterro, J. M., Lain, S., Lane, D. P. & Hay, R. T. Multiple C-terminal lysine residues target p53 for ubiquitin-proteasome-mediated degradation. *Mol Cell Biol* **20**, 8458-8467, (2000).
- 5 Skaar, J. R. & Pagano, M. Control of cell growth by the SCF and APC/C ubiquitin ligases. *Curr Opin Cell Biol* **21**, 816-824, (2009).
- 6 King, R. W., Deshaies, R. J., Peters, J. M. & Kirschner, M. W. How proteolysis drives the cell cycle. *Science* **274**, 1652-1659, (1996).
- 7 Hoegge, C., Pfander, B., Moldovan, G. L., Pyrowolakis, G. & Jentsch, S. RAD6-dependent DNA repair is linked to modification of PCNA by ubiquitin and SUMO. *Nature* **419**, 135-141, (2002).
- 8 Parker, J. L. & Ulrich, H. D. Mechanistic analysis of PCNA poly-ubiquitylation by the

- ubiquitin protein ligases Rad18 and Rad5. *Embo J* **28**, 3657-3666, (2009).
- 9 Hwang, W. W. *et al.* A conserved RING finger protein required for histone H2B monoubiquitination and cell size control. *Mol Cell* **11**, 261-266, (2003).
- 10 Winston, J. T. *et al.* The SCFbeta-TRCP-ubiquitin ligase complex associates specifically with phosphorylated destruction motifs in I $\kappa$ B and beta-catenin and stimulates I $\kappa$ B ubiquitination in vitro. *Genes Dev* **13**, 270-283, (1999).
- 11 Wu, G. *et al.* Structure of a beta-TrCP1-Skp1-beta-catenin complex: destruction motif binding and lysine specificity of the SCF(beta-TrCP1) ubiquitin ligase. *Mol Cell* **11**, 1445-1456, (2003).
- 12 Wang, H. *et al.* Role of histone H2A ubiquitination in Polycomb silencing. *Nature* **431**, 873-878, (2004).
- 13 Buchwald, G. *et al.* Structure and E3-ligase activity of the Ring-Ring complex of polycomb proteins Bmi1 and Ring1b. *Embo J* **25**, 2465-2474, (2006).
- 14 Mattioli, F. *et al.* RNF168 Ubiquitinates K13-15 on H2A/H2AX to Drive DNA Damage Signaling. *Cell* **150**, 1182-1195, (2012).
- 15 Gatti, M. *et al.* A novel ubiquitin mark at the N-terminal tail of histone H2As targeted by RNF168 ubiquitin ligase. *Cell Cycle* **11**, 2538-2544, (2012).
- 16 Sun, Z. W. & Allis, C. D. Ubiquitination of histone H2B regulates H3 methylation and gene silencing in yeast. *Nature* **418**, 104-108, (2002).
- 17 Bienko, M. *et al.* Ubiquitin-binding domains in Y-family polymerases regulate translesion synthesis. *Science* **310**, 1821-1824, (2005).
- 18 Papouli, E. *et al.* Crosstalk between SUMO and ubiquitin on PCNA is mediated by recruitment of the helicase Srs2p. *Mol Cell* **19**, 123-133, (2005).
- 19 Lee, J. S. *et al.* Histone crosstalk between H2B monoubiquitination and H3 methylation mediated by COMPASS. *Cell* **131**, 1084-1096, (2007).
- 20 Fradet-Turcotte, A. *et al.* 53BP1 is a reader of the DNA-damage-induced H2A Lys 15 ubiquitin mark. *Nature* **499**, 50-54, (2013).
- 21 McGinty, R. K., Kim, J., Chatterjee, C., Roeder, R. G. & Muir, T. W. Chemically ubiquitylated histone H2B stimulates hDot1L-mediated intranucleosomal methylation. *Nature* **453**, 812-816, (2008).
- 22 Petroski, M. D. & Deshaies, R. J. Function and regulation of cullin-RING ubiquitin ligases. *Nat Rev Mol Cell Biol* **6**, 9-20, (2005).
- 23 Dou, H. *et al.* Structural basis for autoinhibition and phosphorylation-dependent activation of c-Cbl. *Nat Struct Mol Biol* **19**, 184-192, (2012).
- 24 Zhang, M. *et al.* Chaperoned ubiquitylation--crystal structures of the CHIP U box E3 ubiquitin ligase and a CHIP-Ubc13-Uev1a complex. *Mol Cell* **20**, 525-538, (2005).
- 25 Bentley, M. L. *et al.* Recognition of UbcH5c and the nucleosome by the Bmi1/Ring1b ubiquitin ligase complex. *Embo J* **30**, 3285-3297, (2011).

- 26 Dou, H., Buetow, L., Sibbet, G. J., Cameron, K. & Huang, D. T. BIRC7-E2 ubiquitin conjugate structure reveals the mechanism of ubiquitin transfer by a RING dimer. *Nat Struct Mol Biol*, (2012).
- 27 Plechanovova, A., Jaffray, E. G., Tatham, M. H., Naismith, J. H. & Hay, R. T. Structure of a RING E3 ligase and ubiquitin-loaded E2 primed for catalysis. *Nature*, (2012).
- 28 Pruneda, J. N. *et al.* Structure of an E3:E2 approximately Ub Complex Reveals an Allosteric Mechanism Shared among RING/U-box Ligases. *Mol Cell*, (2012).
- 29 Petroski, M. D. & Deshaies, R. J. Mechanism of lysine 48-linked ubiquitin-chain synthesis by the cullin-RING ubiquitin-ligase complex SCF-Cdc34. *Cell* **123**, 1107-1120, (2005).
- 30 Wickliffe, K. E., Lorenz, S., Wemmer, D. E., Kuriyan, J. & Rape, M. The mechanism of linkage-specific ubiquitin chain elongation by a single-subunit E2. *Cell* **144**, 769-781, (2011).
- 31 Cao, R., Tsukada, Y. & Zhang, Y. Role of Bmi-1 and Ring1A in H2A ubiquitylation and Hox gene silencing. *Mol Cell* **20**, 845-854, (2005).
- 32 Endoh, M. *et al.* Histone H2A Mono-Ubiquitination Is a Crucial Step to Mediate PRC1-Dependent Repression of Developmental Genes to Maintain ES Cell Identity. *PLoS Genet* **8**, e1002774, (2012).
- 33 Pinato, S., Gatti, M., Scanduzzi, C., Confalonieri, S. & Penengo, L. UMI, a novel RNF168 ubiquitin binding domain involved in the DNA damage signaling pathway. *Mol Cell Biol* **31**, 118-126, (2011).
- 34 Panier, S. *et al.* Tandem Protein Interaction Modules Organize the Ubiquitin-Dependent Response to DNA Double-Strand Breaks. *Mol Cell*, (2012).
- 35 Stewart, G. S. *et al.* The RIDDLE syndrome protein mediates a ubiquitin-dependent signaling cascade at sites of DNA damage. *Cell* **136**, 420-434, (2009).
- 36 Doil, C. *et al.* RNF168 binds and amplifies ubiquitin conjugates on damaged chromosomes to allow accumulation of repair proteins. *Cell* **136**, 435-446, (2009).
- 37 Pinato, S. *et al.* RNF168, a new RING finger, MIU-containing protein that modifies chromatin by ubiquitination of histones H2A and H2AX. *BMC Mol Biol* **10**, 55, (2009).
- 38 Kalashnikova, A. A., Porter-Goff, M. E., Muthurajan, U. M., Luger, K. & Hansen, J. C. The role of the nucleosome acidic patch in modulating higher order chromatin structure. *J R Soc Interface* **10**, 20121022, (2013).
- 39 Barbera, A. J. *et al.* The nucleosomal surface as a docking station for Kaposi's sarcoma herpesvirus LANA. *Science* **311**, 856-861, (2006).
- 40 Fischer, E. S. *et al.* The molecular basis of CRL4DDB2/CSA ubiquitin ligase architecture, targeting, and activation. *Cell* **147**, 1024-1039, (2011).
- 41 Bekker-Jensen, S. *et al.* HERC2 coordinates ubiquitin-dependent assembly of DNA



- repair factors on damaged chromosomes. *Nat Cell Biol* **12**, 80-86; sup pp 81-12, (2010).
- 42 Luijsterburg, M. S. *et al.* A new non-catalytic role for ubiquitin ligase RNF8 in unfolding higher-order chromatin structure. *EMBO J* **31**, 2511-2527, (2012).
- 43 Ogiwara, H. *et al.* Histone acetylation by CBP and p300 at double-strand break sites facilitates SWI/SNF chromatin remodeling and the recruitment of non-homologous end joining factors. *Oncogene* **30**, 2135-2146, (2011).
- 44 Lans, H., Marteijn, J. A. & Vermeulen, W. ATP-dependent chromatin remodeling in the DNA-damage response. *Epigenetics Chromatin* **5**, 4, (2012).
- 45 Bensimon, A., Aebersold, R. & Shiloh, Y. Beyond ATM: the protein kinase landscape of the DNA damage response. *FEBS Lett* **585**, 1625-1639, (2011).
- 46 Smeenk, G. & van Attikum, H. The chromatin response to DNA breaks: leaving a mark on genome integrity. *Annu Rev Biochem* **82**, 55-80, (2013).
- 47 Zhou, J., Fan, J. Y., Rangasamy, D. & Tremethick, D. J. The nucleosome surface regulates chromatin compaction and couples it with transcriptional repression. *Nat Struct Mol Biol* **14**, 1070-1076, (2007).
- 48 Suto, R. K., Clarkson, M. J., Tremethick, D. J. & Luger, K. Crystal structure of a nucleosome core particle containing the variant histone H2A.Z. *Nat Struct Biol* **7**, 1121-1124, (2000).
- 49 El Oualid, F. *et al.* Chemical synthesis of ubiquitin, ubiquitin-based probes, and diubiquitin. *Angew Chem Int Ed Engl* **49**, 10149-10153, (2010).
- 50 Luger, K., Rechsteiner, T. J. & Richmond, T. J. Expression and purification of recombinant histones and nucleosome reconstitution. *Methods Mol Biol* **119**, 1-16, (1999).
- 51 Dyer, P. N. *et al.* Reconstitution of nucleosome core particles from recombinant histones and DNA. *Methods Enzymol* **375**, 23-44, (2004).
- 52 Luger, K., Rechsteiner, T. J., Flaus, A. J., Waye, M. M. & Richmond, T. J. Characterization of nucleosome core particles containing histone proteins made in bacteria. *J Mol Biol* **272**, 301-311, (1997).
- 53 Lowary, P. T. & Widom, J. New DNA sequence rules for high affinity binding to histone octamer and sequence-directed nucleosome positioning. *J Mol Biol* **276**, 19-42, (1998).
- 54 Campbell, S. J. *et al.* Molecular Insights into the Function of RING Finger (RNF)-containing Proteins hRNF8 and hRNF168 in Ubc13/Mms2-dependent Ubiquitylation. *J Biol Chem* **287**, 23900-23910, (2012).
- 55 Davey, C. A., Sargent, D. F., Luger, K., Maeder, A. W. & Richmond, T. J. Solvent mediated interactions in the structure of the nucleosome core particle at 1.9 Å resolution. *J Mol Biol* **319**, 1097-1113, (2002).



## **ACKNOWLEDGEMENTS**

We thank Tatjana Heidebrecht for help with the FP assays. Andrea Mattevi and Valentina Speranzini for useful discussions about NCP preparation. Marcello Clerici for critical reading of the manuscript. Funding was thanks to NWO-CW TOP grant 714.012.001, NWO CW Echo 700.59.009 and ERC advanced grant 249997, Ubiquitin balance.

4

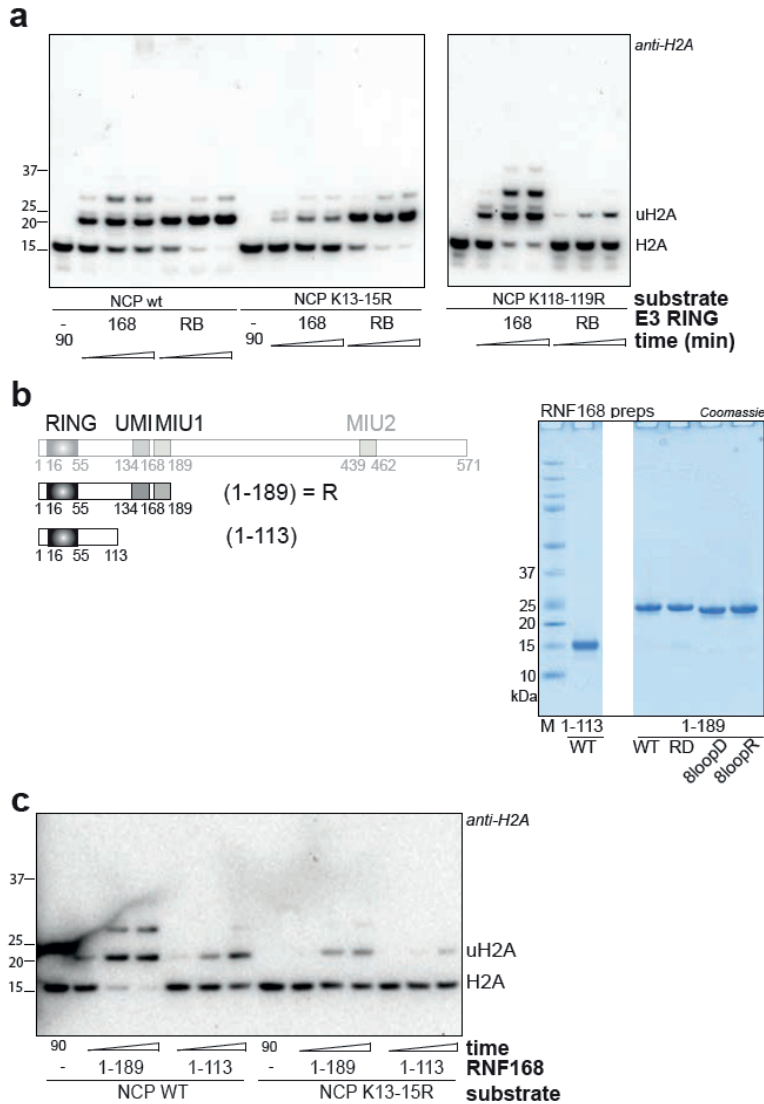
## **Author contributions**

FM and MU designed and performed the experiments. DS contributed to experiments and discussions. WJvD assisted with protein purification. TKS designed, supervised experiments. FM wrote the manuscript, with assistance from MU and TKS. All authors critically read the manuscript.

The authors have no competing financial interests.

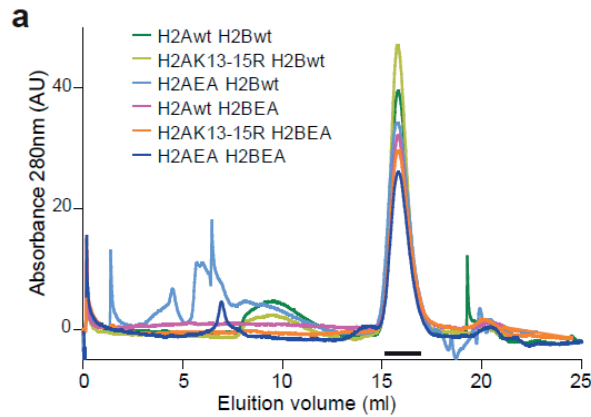
## Supplemental Material

4

**Supplementary Figure S1**

RNF168 RING domain is sufficient for specific K13-15 modification

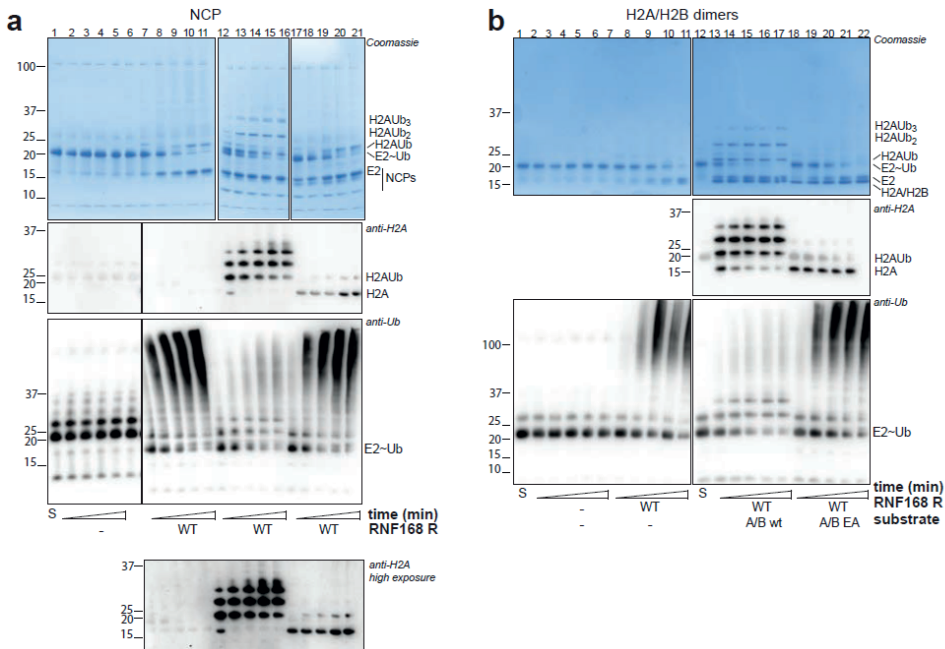
**a)** The RNF168 RING domain modifies preferentially K13-15 in H2A in NCPs whereas the PRC1 complex RING1B/BMI1 prefers K118-119. Time course (15-30-60 minutes) assay using wild-type (WT), K13-15R or K118-119R H2A assembled NCPs. **b)** Schematic representation of the RNF168 domains and constructs used. Full-length protein architecture is shown in light gray. The construct used throughout the paper is labeled as R and spans residues 1-189. The shorter RING domain spans residues 1-113, only used in Supplementary Fig. 1c as control. SDS-PAGE gel showing the samples of the RNF168 constructs used in this manuscript. **c)** RNF168 (1-113) retains K13-15 specificity on NCPs, although it is less active than RNF168 (1-189). Time course assay (10-30-90 minutes) in presence of WT and K13-15R NCPs.



**Supplementary Figure S2**

The acidic patch mutations do not affect H2A/H2B dimer formation.

**a)** Gel-filtration profiles of the different H2A/H2B dimer mutants (in 2M NaCl containing buffer) illustrate that dimer formation is not affected by mutagenesis. The horizontal black line highlights the fractions that were taken and concentrated for the assays.



**Supplementary Figure S3**

The acidic patch activates E2 dimers and is critical for K13-15 modification.

**a-b)** EA mutant NCPs **(a)** and dimers **(b)** do not redirect ubiquitin chain formation to the target lysines on H2A. Time course (1.5,3,4,6,8 minutes) experiment performed with 0.5  $\mu$ M E3. Coomassie stained SDS PAGE (12% NuPage gel, run in MOPS buffer), anti-H2A and anti-Ubiquitin (4-12% NuPage gel, run in MES buffer). Note that E91 on H2A is part of the epitope recognized by the anti-H2A antibodies, therefore there is reduced signal on western blots for this mutant, higher exposure of the anti-H2A blots are shown in panel **a**.



# Chapter 5

5

## **Strategies to stabilize RING E3 ligase-target complexes for structural analysis**

Michael Uckelmann, Herrie Winterwerp and Titia Sixma

*Division of Biochemistry*

*The Netherlands Cancer Institute,*

*Plesmanlaan 121, 1066CX Amsterdam, the Netherlands*

## Abstract

The importance of lysine-specificity of RING E3 ligases is exemplified in the DNA damage response where three different ligases, RNF168, RING1B in a PRC1 complex and BRCA1/BARD1, modify three distinct groups of lysines on H2A. The ubiquitination status eventually influences repair pathway choice and guides faithful repair. The molecular details of how specificity is achieved are not well understood, furthermore there is no generalized model put forward to explain RING E3 ligase specificity. Missing structural information on RING E3-target complexes, due to the often transient nature of these complexes, is one major limitation in understanding the basis for lysine specificity. Here we present three strategies to stabilize the RNF168-E2-Nucleosome complex for structural analysis. The strategies are generalizable and can potentially be applied to many other RING E3-E2-target complexes.

## Introduction

To maintain genomic integrity DNA lesions need to be faithfully repaired<sup>1</sup>. The cell's repair processes are in part guided by reversible histone modifications<sup>2</sup>. Specific ubiquitination of histone H2A is one such histone modification that plays an important role in the DNA damage response<sup>3</sup>. Lysine-specific monoubiquitination of target proteins is generally believed to be a crucial signaling entity in the ubiquitin system<sup>4</sup>. One family of E3 ligases that facilitate the transfer of ubiquitin to a target lysine are RING E3 ligases. These enzymes exert their function by promoting a conformation of the ubiquitin-charged E2 that is prone to aminolysis<sup>5-8</sup> while at the same time orienting the E2-active site towards the target lysine<sup>9</sup>.

Three different RING E3 ligases have been shown to modify three different groups of lysines on H2A, RNF168, RING1B (RNF2) in a PRC1 complex and BRCA1/BARD1<sup>10-12</sup>. Each of these ligases shows exclusive *in vitro* specificity for their cognate site on H2A, K13/15 for RNF168 (H2A<sup>K13/15</sup>), K118/119 for PRC1 (H2A<sup>PRC1</sup>) and K125/127/129 for BRCA1/BARD1 (H2A<sup>BRCA1</sup>). Ubiquitination on any of these sites has distinct biological outcomes.

H2A<sup>PRC1</sup> ubiquitination has a well-known role in transcriptional regulation<sup>12,13</sup>. There is accumulating evidence that this function extends to the DNA damage response, where transcriptional silencing around a break site might be necessary for faithful repair<sup>14,15</sup>. Ubiquitination on H2A<sup>BRCA1</sup> is thought to increase the extent of DNA end resection by recruiting SMARCAD1 for 53BP1 repositioning<sup>16</sup>. This long-range DNA end resection primes the cell for repair through one of the homologous recombination pathways. Ubiquitination on H2A<sup>K13/15</sup> on the other hand limits end resection by recruiting 53BP1 (TP53BP1), which establishes an early resection block that will result in repair through non-homologous end joining<sup>17,18</sup>. Though ubiquitination of the individual sites can be linked to certain biological responses,

ultimately the integration over the ubiquitination status over all three ubiquitination sites is likely a guiding factor in the DNA damage response<sup>3</sup>

The distinct contributions of the three different ubiquitination sites to the biological outcomes highlight the importance of lysine specificity of the three E3 ligases involved and thus the importance of understanding the molecular details that determine specificity. A crystal structure of a RING1B/BMI1-E2 fusion protein in complex with a nucleosome core particle (NCP) explains how specificity for H2A<sup>PRC1</sup> is achieved<sup>19</sup> but fails to explain why RNF168 and BRCA1/BARD1 modify a different group of lysines. Previous studies showed that the nucleosomal acidic patch is crucial for efficient ubiquitination of H2A by RNF168<sup>20,21</sup> but the exact molecular details remain unsolved. We aim to close this knowledge gap by providing structural information for a RNF168-E2-NCP complex.

The RNF168-E2-NCP complex is a transient, low affinity complex, which makes it difficult to analyze with current methods in structural biology. In fact, this is true for many different E3-target complexes. Sample heterogeneity of low affinity complexes poses a problem for both cryo EM and protein crystallography, thus stabilizing a transient protein-protein complex is crucial for successful structure resolution. Established ways of stabilizing transient protein complexes, which have long been used in different disciplines of structural biology, are chemical crosslinking and the genetic fusion of different complex members. Chemical crosslinking has been used in cryo-EM to address sample heterogeneity<sup>22</sup>, in mass spectroscopy to probe conformational flexibility and protein-protein interaction sites<sup>23,24</sup> and in crystallography to trap transient complexes<sup>25,26</sup>.

Crosslinking and fusion strategies have been employed successfully to stabilize multi-protein complexes in the ubiquitin/ubiquitin-like system for structural analysis. Cysteine-cysteine crosslinking was used to crystallize PCNA in complex with a SUMO-loaded E2 and the E3 ligase Siz1<sup>27</sup>. The E2 was charged by introducing a lysine close to the active site to which SUMO was readily conjugated by Siz1, leaving the active site cysteine unoccupied. The target lysine on PCNA was mutated to a cysteine, making it possible to crosslink the active site cysteine to the target ubiquitination site using ethanedithiol (EDT). In another study the structure of an E1-E2 complex was solved by activating the E2 active site cysteine for disulfide formation using 2,2-dipyridyldisulfide and then mixing with E1. The resulting disulfide linkage between the two active sites helped to stabilize the complex<sup>28</sup>.

Here we outline strategies to stabilize the RNF168-E2-NCP complex to make structural studies more feasible. We expand on and combine several different published strategies for complex stabilization and crosslinking techniques that involve E2-E3 fusion constructs<sup>29</sup>, cysteine-cysteine crosslinking<sup>27,30</sup> and E3-ubiquitin fusion proteins<sup>19</sup>. We believe the overall

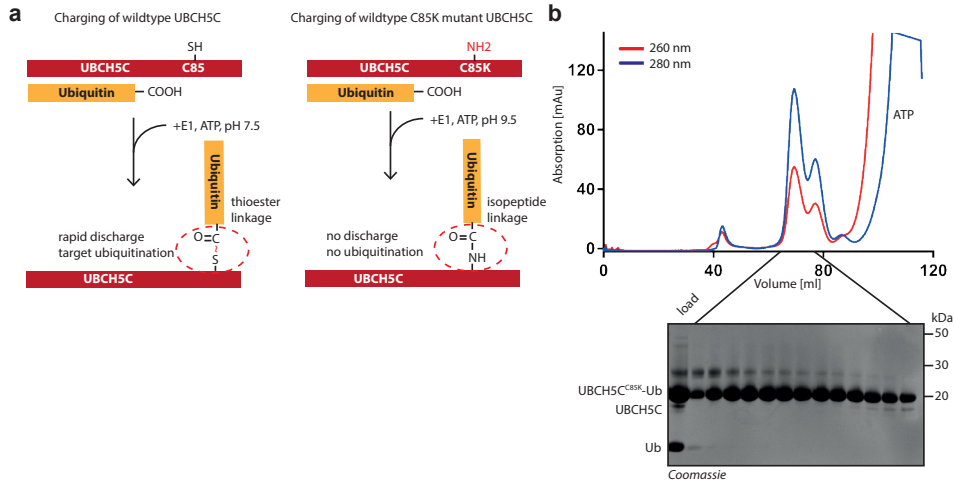


**Figure 1** Ubiquitin can be covalently linked to UBCH5C<sup>C85K</sup>.

**a** Schematic representation of wildtype UBCH5C and UBCH5C<sup>C85K</sup> being charged with ubiquitin. In the mutant UBCH5C<sup>C85K</sup>, ubiquitin will be linked covalently to the E2 active site, prohibiting discharge and target modification. **b** Purification of charged UBCH5C(C85K). Size exclusion chromatography and SDS-PAGE gel of the indicated area of the peak. Excess ATP starts to elute after 100 minutes, causing a high absorption at 260 nm.

approach can easily be generalized and could serve as a blueprint for structural studies on transient E3-target complexes in the ubiquitin field.

## Results

To obtain structural information that could inform on the unique specificity of RNF168 we set out to crystallize RNF168 in complex with its cognate E2, UBCH5C (UBE2D3), and a recombinant nucleosome core particle (NCP). We decided to use UBCH5C charged with ubiquitin to get a more complete picture of the complex in its pre-conjugation state. To stably charge UBCH5C with ubiquitin we used a published strategy<sup>5</sup> involving an E2 mutant where the active site cysteine is mutated to a lysine (UBCH5C<sup>C85K</sup>). That allows stable conjugation of ubiquitin to the E2 active site at high pH (Fig.1A). Following this approach we were able to charge UBCH5C<sup>C85K</sup> efficiently with ubiquitin and separate it from uncharged UBCH5C and free ubiquitin (Fig.1B). RNF168 (residues 1-113) and reconstituted recombinant nucleosome core particles (NCPs) were produced according to established protocols<sup>20,31</sup>, which yielded sufficient quantities and purity to start crystallographic trials. Trials were set up in molar ratios of 2:2:1 (RNF168:UBCH5C:NCP) and standard commercial screens were used.

It soon became apparent that the transient nature of the interactions prevented us from obtaining stable complexes suitable for crystallography. Diffracting crystals could be obtained but only for single components (E2, NCP), never for the whole complex. Therefore we sought to develop strategies to stabilize the complex. Analogous to a study on RING1B/BMI1<sup>19</sup>, we designed an E3-E2 fusion, i.e. RNF168-UBCH5C fusion protein to increase af-



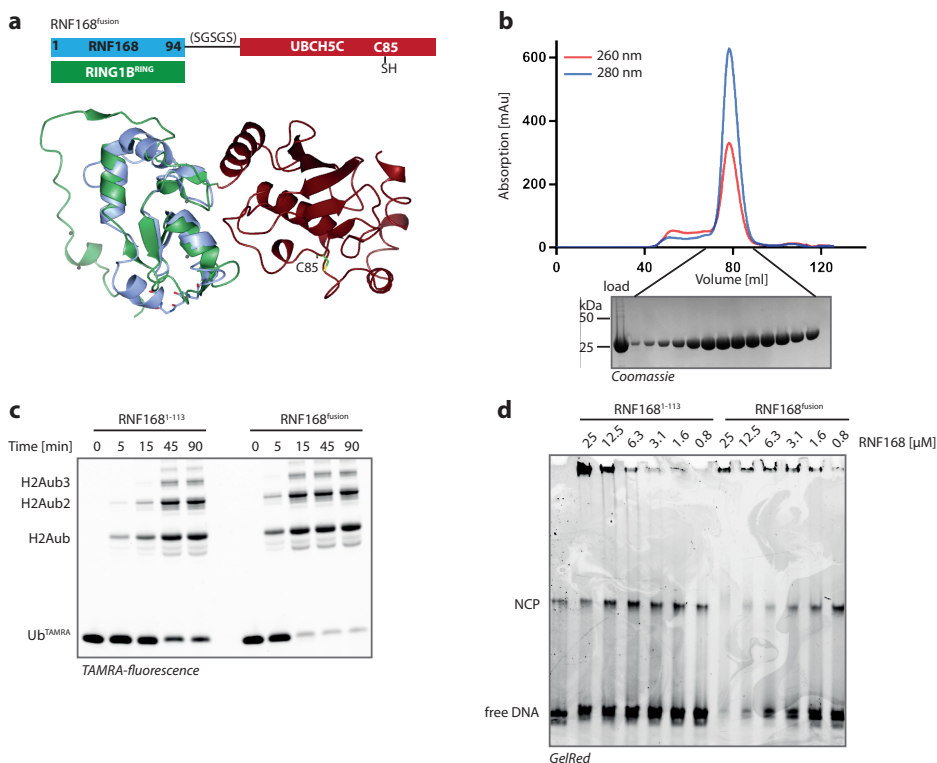


**Figure 2 RNF168<sup>fusion</sup> can be readily purified and has increased affinity for the NCP.**

**a** Structure of RNF168<sup>1-113</sup> (PDB: 4GB0) superimposed on RING1B in a RING1B-UBCH5C fusion construct (PDB: 4R8P) and schematic representation of the fusion construct used in this study. **b** Purification of the RNF168<sup>fusion</sup>. Size exclusion chromatography and SDS-PAGE gel of the indicated peak. **c** RNF168<sup>fusion</sup> is more active on NCPs than RNF168<sup>1-113</sup>. Gel based time course of H2A ubiquitination using fluorescence of TAMRA labeled ubiquitin as a readout. **d** RNF168<sup>fusion</sup> binds NCP with higher affinity compared to RNF168<sup>1-113</sup>. Gel shift assay titrating RNF168<sup>1-113</sup> or RNF168<sup>fusion</sup> to NCPs. Stained for DNA using GelRed.

finity for the nucleosome. We defined the boundaries of the construct by superimposing a structure of the RNF168 RING domain (PDB:4GB0) on the RING1B RING domain in the RING1B-UBCH5C fusion construct used for crystallizing the RING1B/BMI1-UBCH5C\_NCP complex (PDB: 4R8P)(Fig.2A). We decided to use RNF168 residues 1-94 fused to full length UBCH5C via a short linker with the amino acid sequence SGSGS to allow for a certain degree of flexibility. The RNF168-UBCH5C fusion protein (RNF168<sup>fusion</sup>) expressed well in E.coli and was readily purified (Fig.2B) to allow biochemical characterization. We tested the activity of the construct in H2A ubiquitination assays and found that it ubiquitinates H2A more efficiently than RNF168<sup>1-113</sup> (Fig.2C). Comparison of the affinities of the fusion construct vs. RNF168<sup>1-113</sup> towards the NCP by native gel-shift assays shows that RNF168<sup>fusion</sup> binds with an estimated tenfold higher affinity (Fig.2D). Activity and binding assays taken together suggest that the RNF168-E2 fusion improves complex stability. We proceeded with crystallization trials which did not yield diffracting crystals. We speculate that the RNF168<sup>fusion</sup>-NCP complex is still of a too transient nature and we searched for ways to further stabilize the complex.

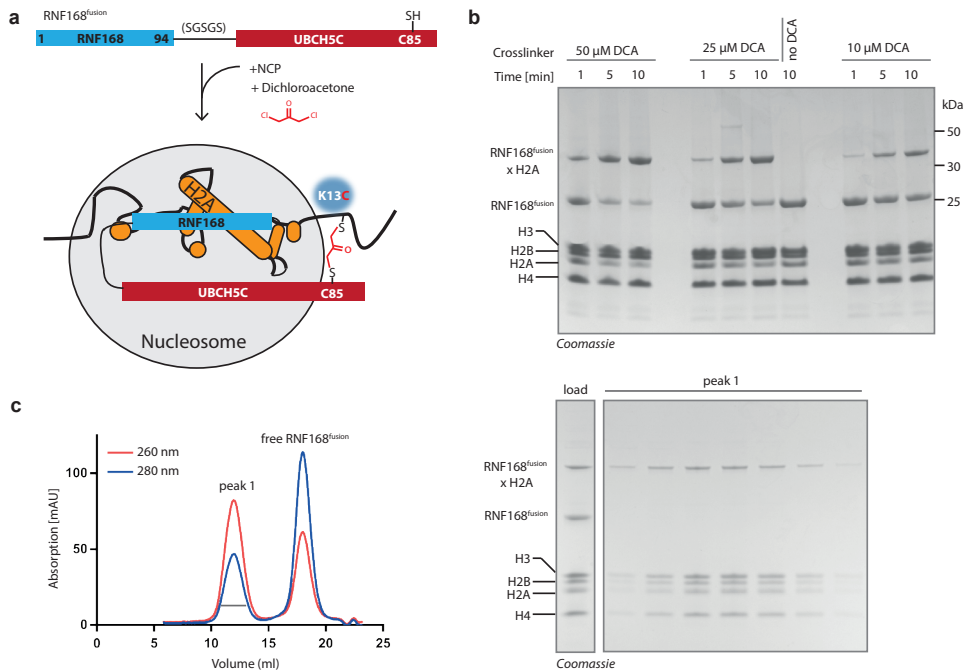


**Figure 3 RNF168<sup>fusion</sup> can be crosslinked to NCPs through a H2A K13C mutant (NCP<sup>K13C</sup>).**  
**a** Schematic overview of the crosslinking strategy. RNF168's target lysine on H2A (K13) is mutated to a cysteine and can be crosslinked to the E2 active site in RNF168<sup>fusion</sup> using DCA. **b** RNF168<sup>fusion</sup> efficiently crosslinks to NCP<sup>K13C</sup>. Crosslink time courses using different concentrations of DCA at steady concentrations of RNF168<sup>fusion</sup> and NCP analyzed by SDS-PAGE. **c** The crosslinked product can be purified for crystallization trials. Size exclusion profile of RNF168<sup>fusion</sup> and SDS-PAGE gel of the resulting fractions of the indicated peak.

We turned to crosslinking strategies to literally trap the 168-E2 fusion construct on the nucleosome. Crosslinking of cysteine residues with dichloroacetone (DCA) has been used to produce non-hydrolysable ubiquitin-histone mimics<sup>30</sup>. We adapted this strategy to produce non-hydrolysable RNF168<sup>fusion</sup>-NCP crosslinks (Fig.3A). To this end we mutated one of the RNF168 target lysines (K13) to a cysteine and reconstituted NCPs containing this mutant H2A (NCP<sup>K13C</sup>). The rationale being that the active site cysteine (C85) of the E2 in the E2-E3-target complex will be positioned in close proximity to the lysine targeted for ubiquitination (K13 or K15). By mutating K13 to cysteine we would then be able to crosslink the E2 active site to C13 on H2A using DCA (Fig.3A).

We analyzed crosslinking time courses using different concentrations of DCA (Fig.3B) to find optimal crosslinking conditions. RNF168<sup>fusion</sup> can indeed be crosslinked to H2A in nucleosomes as evident by the shifting of the RNF168<sup>fusion</sup> band towards a higher molecular weight, corresponding to the addition of one H2A molecule, and the disappearance of the band corresponding to H2A (Fig.3B). We aimed for conditions where most of the H2A is crosslinked but no unspecific byproducts are formed. The most promising conditions in this regard were 10 minutes of crosslinking with 50  $\mu$ M DCA. We scaled up the reaction under these condi-

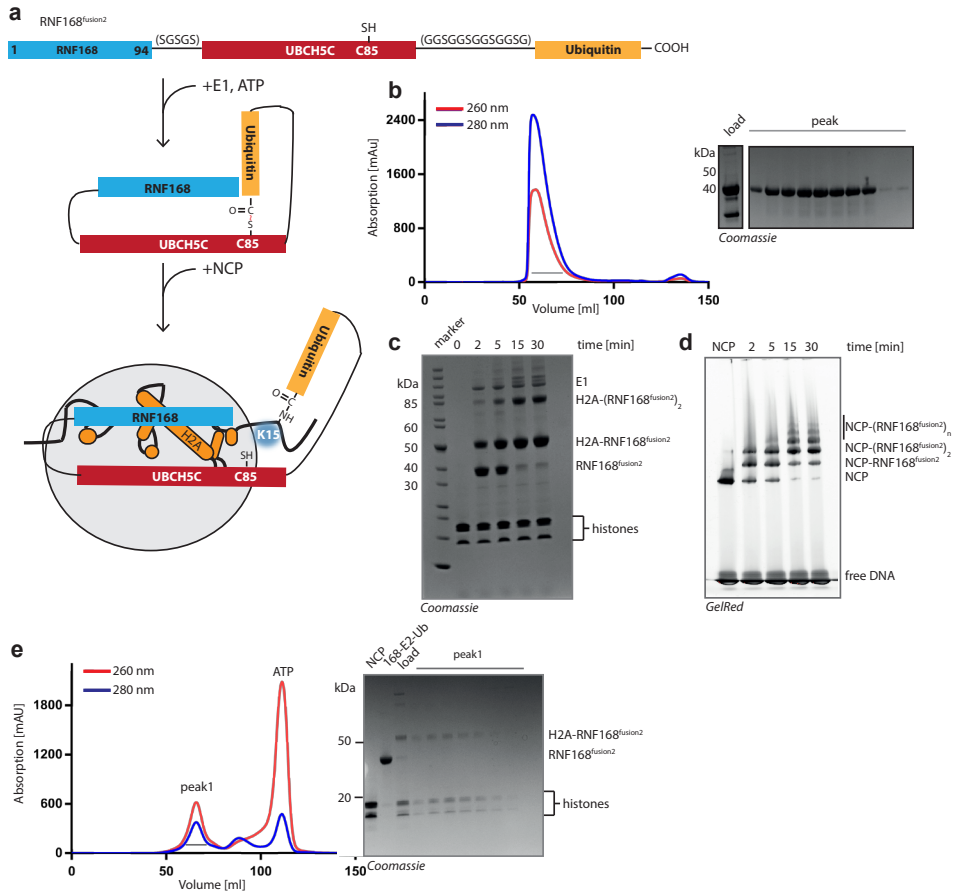


**Figure 4** RNF168<sup>fusion2</sup> can be conjugated to NCPs.

**a** Schematic representation of the RNF168<sup>fusion2</sup> conjugation strategy to stabilize the complex. The ubiquitin in RNF168<sup>fusion2</sup> will be activated by the E1, forms a thioester with UBCH5C and is then transferred to the target lysine. **b** Purification of RNF168<sup>fusion2</sup>. Size exclusion profile and SDS-PAGE gel of the indicated peak fraction. **c** RNF168<sup>fusion2</sup> gets conjugated to NCPs. Time course of the conjugation reaction analyzed on SDS-PAGE. **d** Nucleosomes stay intact upon conjugation of RNF168<sup>fusion2</sup>. Native gel of the same time course shown in C) stained for DNA with GelRed. **e** The RNF168<sup>fusion2</sup>-NCP complex can be purified for crystallographic analysis. Size exclusion profile and peak fractions of the indicated peak on SDS-PAGE.

ons and were successful in purifying the crosslinked complex from free RNF168<sup>fusion</sup> (Fig.3C). Nucleosomes crosslinked to RNF168<sup>fusion</sup> however could not be separated from unmodified nucleosomes due to the relative small difference in size. We used the purified material for crystallization trials but no diffracting crystals could be obtained so far.

Parallel to the crosslinking approach we followed another strategy to stabilize the 168-E2-NCP complex. A recent study showed that ubiquitin can be fused to E3 ligases<sup>29</sup> while retaining the enzymes functionality. This fusion protein can then be conjugated, or conjugate itself, to target protein lysines and helped to identify cellular targets of E3 ligases<sup>29</sup>. We extended this approach by including UBCH5C, creating a RNF168-UBCH5C-Ubiquitin fusion

protein (RNF168<sup>fusion2</sup>). The rationale behind this approach is that RNF168<sup>fusion2</sup> will follow the regular ubiquitination cascade (E1 activation, E2-ub thioester formation, E3 activated discharge to target lysine) and as such conjugate itself to H2A K15 via the free C-terminus of the ubiquitin within the fusion construct (Fig.4A). RNF168<sup>fusion2</sup> expressed well and was readily purified to a degree of purity suitable for crystallographic studies (Fig.4B). We tested the activity of the construct in H2A ubiquitination assays and found that RNF168<sup>fusion2</sup> is indeed conjugated to H2A, as evident by a shift of the band corresponding to RNF168<sup>fusion2</sup> towards a higher molecular weight (Fig4C). Importantly, activity is only observed in the presence of E1, showing that RNF168<sup>fusion2</sup> follows the canonical ubiquitination cascade. At longer time points a considerable amount of unspecific, higher molecular weight bands forms. These might correspond to H2A modified at several individual lysines or/and RNF168<sup>fusion2</sup> chains formed by conjugation of one RNF168<sup>fusion2</sup> to one of the available lysines on another fusion protein. Analysis on native gel (Fig.4D) shows that NCPs are still intact after conjugation of RNF168<sup>fusion2</sup>. Five minutes into the reaction most NCPs are modified with one or two molecules of RNF168<sup>fusion2</sup>. At longer time points NCPs with more than two fusion proteins are also observed.

One nucleosome is expected to be modified by two RNF168<sup>fusion2</sup> as each nucleosome is composed of two of each of the four histones and its structure resembles a symmetrical disc with two nearly identical faces. To reduce sample heterogeneity to a minimum, conditions where all of the NCPs are modified with two 168-E2-Ub molecules (i.e. one RNF168<sup>fusion2</sup> on each face of the NCP) would be most desirable for crystallographic studies. A five minute conjugation reaction seems to give the least heterogeneity under the conditions tested. Still, even under these conditions roughly one third of the NCP are unmodified, one third are modified with one 168-E2-Ub and another third carries two 168-E2-Ub. This sample heterogeneity will likely complicate the growth of diffraction grade crystals. Nonetheless we scaled up the reaction and were able to purify NCPs with 168-E2-Ub conjugated via size exclusion chromatography. Crystallographic trials are ongoing.

### Discussion

Transient, low affinity, multi-protein complexes are notoriously difficult to analyze using current methods in structural biology and structural information for many is missing. RING E3 ligase-target complexes are often of a transient nature, yet structural information of these is crucial to establish a clear picture of the molecular mechanisms of regulation of ubiquitin-driven signaling networks. Given the importance of the ubiquitin system for many cellular processes and its significance in disease and treatment<sup>32</sup> there is a need to study basic mechanisms of the enzymes involved. That establishes a necessity for tools to stabilize these complexes and make them accessible for structural analysis. Here we have described vari-

ous strategies to stabilize transient E3 ligase-target complexes for structural analysis using the RNF168-UBCH5C-NCP complex as example. We believe the approaches presented are easily transferable to other RING E3 ligase-target complexes where ubiquitination is specific for a certain lysine. Furthermore, stabilization of these complexes and reduction of sample heterogeneity in the way presented is not only crucial for crystallography but also helpful for cryo-EM.

Lysine specific RING E3 ligase stabilize the ubiquitin-charged E2 in a conformation prone for catalysis and at the same time orient the E2 active site towards the target lysine<sup>4-9</sup>. As such, the catalytic cysteine of the E2 should always be oriented towards the target lysine in the E3-E2-target complex. It follows that the presented combination of E3-E2 fusion protein and cysteine-cysteine crosslinking should, in theory, work for any E3-E2-target complex, given the target lysine is mutated to a cysteine. In practice, such an approach will be limited by the ability to produce soluble fusion proteins that retain lysine specificity and by the extent of cross reactivity of these fusion proteins with other cysteine residues on the target protein.

Similarly, the approach using a E3-E2-ub fusion protein should, in theory, work for any specific E3-E2-target pair if functional and lysine specific fusion protein can be produced. Here additional limitations are the ability of the fusion protein to participate in the canonical ubiquitination cascade and the propensity to form ubiquitin chains (i.e. chains of the fusion protein). Strong autoubiquitination activity of the E3 ligases studied is also a likely limitation.

Sample homogeneity is an important parameter for success in both, cryo-EM and crystallographic studies. For both approaches mentioned above the optimization of the reaction conditions to achieve crosslinking or conjugation of one fusion protein per target and the subsequent purification of the trapped E3-E2-target complex from the individual components will likely play an important role in successfully solving these structures.

To draw useful conclusions from the crosslinked structure and extrapolate to interpret the underlying biology of the native protein complexes it is crucial that the geometry of the native complexes is accurately reflected in the crosslinked situation. Previous studies have pointed out that the choice of the right crosslinker is important to maintain the native geometry of a E3-E2-target complex<sup>27</sup>. For the PCNA/SUMO/SIZ1/UBC9 complex the authors first used BMOE as a crosslinker to stabilize the complex but later switched to using EDT instead, as it more accurately reflects the length of the actual tetrahedral intermediate of the ubiquitination reaction. Here we use DCA which will lead to a crosslinked structure that is one atom longer than the natural tetrahedral intermediate. Compared to EDT, DCA provides the benefit of creating an irreversible crosslink. EDT crosslinks can be reduced and thus reversed. Nonetheless, the one atom in length difference might make a difference in

complex geometry and using EDT instead of DCA should be explored further.

If successful, the combination of both approaches presented here can have a powerful impact as they can be used to solve structures of different states of the ubiquitination reaction. The crosslinked complex likely resembles most closely the conformation of the E3-E2-target complex when the target lysine would attack the charged E2-ub thioester bond, just before conjugation. The E3-E2-ub fusion construct conjugated to the target lysine would likely resemble the conformation just after catalysis, which would in fact be the enzyme-product complex. Comparison of these two states will provide valuable information on subtle differences in the architecture of the enzyme-substrate and the enzyme-product complex. For enzyme-target complexes of pharmacological interest these subtle differences can be of potential use in the design of compounds to modulate either one of these two different states.

## 5

## Material and Methods

### Protein production

RNF168<sup>1-113</sup> was cloned in pGEX6p vector and purified as described before<sup>20</sup>.

hUBA1, ubiquitin and UBCH5C (wildtype and mutant) were purified as described before<sup>33</sup>.

RNF168<sup>fusion</sup> and RNF168<sup>fusion2</sup> were cloned into the petNKI-his3c-LIC-amp vector<sup>34</sup>. BL21 cells were transfected and grown in LB medium until a OD of ~0.8 was reached. Protein expression was then induced with 200  $\mu$ M IPTG and the protein was expressed overnight at 18 °C. The cells were harvested and lysed by sonication in 50 mM TRIS pH 7.5, 500 mM NaCl, 1 mM TCEP, 1  $\mu$ M ZnCl<sub>2</sub>. The lysate was cleared by spinning at 21000 x g and the supernatant was loaded on to chelating sepharose charged with Ni<sup>2+</sup>. The beads were washed with lysis buffer + 20 mM Imidazol and protein was eluted with lysis buffer + 350 mM Imidazol. The His-tag was cleaved overnight using His-tagged 3C protease while dialyzing against 50 mM TRIS pH 7.5, 250 mM NaCl, 1 mM TCEP, 1  $\mu$ M ZnCl<sub>2</sub>. After cleavage of the tag, the sample was run over Ni<sup>2+</sup>- charged chelating sepharose to remove the protease and uncleaved protein, concentrated and gel-filtered using a Superdex S75 16/60 column in 50 mM TRIS 7.5, 150 mM NaCl, 1 mM DTT, 1  $\mu$ M ZnCl<sub>2</sub>.

Histone proteins were purified as described previously<sup>31</sup> and nucleosomes were reconstituted by salt dialysis<sup>31</sup>. Briefly, refolded histone octamers containing the desired mutant (or wildtype) H2A at a concentration of 7  $\mu$ M were combined with equimolar concentration of 147 bp DNA containing the 'Widom 601' sequence<sup>35</sup> at 2 M NaCl. The sample was then dialyzed against 400 ml of a buffer containing 50 mM TRIS pH 7.5, 2 M KCl, 1 mM EDTA and 5 mM 2-mercaptoethanol for at least 3 hours. Then the salt concentration was gradually

decreased from 2 M KCl to 250 mM KCl over the course of 48 hours. The sample was then dialyzed for at least 4 hours against 50 mM TRIS pH 7.5, 150 mM KCl and 1 mM DTT, concentrated and stored at 4 °C.

### Charging of UBCH5C<sup>C85K</sup>

Charging of the UBCH5C<sup>C85K</sup> mutant with ubiquitin was done as described previously<sup>5</sup>. 200 μM of UBCH5C<sup>C85K</sup> were incubated with 1 μM hUBA1, 200 μM ubiquitin and 3 mM ATP in 30 mM TRIS pH9.5, 150 mM NaCl, 0.8 mM TCEP and 5 mM MgCl<sub>2</sub> for 20 hours at 35 °C. The charged E2 was purified using a Superdex S75 column in 50 mM TRIS pH 7.5, 150 mM NaCl, 0.5 mM TCEP.

5

### Crosslinking of RNF168<sup>fusion</sup> to NCPs

One day before the actual crosslinking experiment NCP<sup>K13C</sup> at 20 μM were reduced using 1 mM DTT and then dialyzed over night against at least two changes of 1 l of 50 mM TRIS pH 7.5, 150 mM NaCl to remove the DTT.

For small scale test reactions 10 μM reduced NCP<sup>K13C</sup> were incubated with 20 μM RNF168<sup>fusion</sup> for twenty minutes. Then 10, 25 or 50 μM of Dichloroacetone (DCA) dissolved in Dimethylformamide (DMF) were added and the reaction was stopped after 1, 5, and 10 minutes by adding 5 mM DTT. Samples were analyzed by SDS-Page.

For large scale reactions 10 μM reduced NCP<sup>K13C</sup> were incubated with 20 μM RNF168<sup>fusion</sup> for 20 minutes and then crosslinked by adding 50 μM of DCA. The crosslink reaction was stopped after 10 minutes by adding 5 mM DTT. The crosslinked sample was then purified by size exclusion chromatography on a Superdex S200 column (GE healthcare) in 50 mM TRIS pH 7.5, 150 mM NaCl and 1 mM DTT .

### NCP ubiquitination with RNF168<sup>fusion2</sup>

10 μM recombinant NCPs were mixed with 20 μM RNF168<sup>fusion2</sup> and 1 μM hUBA1. The reaction was started by adding 3 mM ATP and stopped after 2, 5, 15 and 30 minutes for small scale test reactions and after 5 minutes for large scale preparations by adding 25 mM EDTA. NCPs ubiquitinated with RNF168<sup>fusion2</sup> were purified by size-exclusion chromatography using a Superdex S200 column in 50 mM TRIS pH 7.5, 150 mM NaCl, 1 mM TCEP.



## References

1. Jackson, S. P. & Bartek, J. The DNA-damage response in human biology and disease. *Nature* **461**, 1071–8 (2009).
2. Rossetto, D., Truman, A. W., Kron, S. J. & Côté, J. Epigenetic Modifications in Double Strand Break DNA Damage Signaling and Repair. *Clin. Cancer Res.* **16**, 4543–52 (2010).
3. Uckelmann, M. & Sixma, T. K. Histone ubiquitination in the DNA damage response. *DNA Repair (Amst)*. (2017). doi:10.1016/j.dnarep.2017.06.011
4. Mattioli, F. & Sixma, T. K. Lysine-targeting specificity in ubiquitin and ubiquitin-like modification pathways. *Nat. Struct. Mol. Biol.* **21**, 308–316 (2014).
5. Plechanovová, A., Jaffray, E. G., Tatham, M. H., Naismith, J. H. & Hay, R. T. Structure of a RING E3 ligase and ubiquitin-loaded E2 primed for catalysis. *Nature* **489**, 115–120 (2012).
6. Berndsen, C. E. & Wolberger, C. New insights into ubiquitin E3 ligase mechanism. *Nat. Struct. Mol. Biol.* **21**, 301–307 (2014).
7. Pruneda, J. N. *et al.* Structure of an E3:E2-Ub Complex Reveals an Allosteric Mechanism Shared among RING/U-box Ligases. *Mol. Cell* **47**, 933–942 (2012).
8. Dou, H., Buetow, L., Sibbet, G. J., Cameron, K. & Huang, D. T. BIRC7–E2 ubiquitin conjugate structure reveals the mechanism of ubiquitin transfer by a RING dimer. *Nat. Struct. Mol. Biol.* **19**, 876–883 (2012).
9. Deshaies, R. J. & Joazeiro, C. a P. RING domain E3 ubiquitin ligases. *Annu. Rev. Biochem.* **78**, 399–434 (2009).
10. Mattioli, F. *et al.* RNF168 ubiquitinates K13–15 on H2A/H2AX to drive DNA damage signaling. *Cell* **150**, 1182–1195 (2012).
11. Kalb, R., Mallery, D. L., Larkin, C., Huang, J. T. J. & Hiom, K. BRCA1 is a histone-H2A-specific ubiquitin ligase. *Cell Rep.* **8**, 999–1005 (2014).
12. Wang, H. *et al.* Role of histone H2A ubiquitination in Polycomb silencing. *Nature* **431**, 873–8 (2004).
13. Simon, J. A. & Kingston, R. E. Occupying Chromatin: Polycomb Mechanisms for Getting to Genomic Targets, Stopping Transcriptional Traffic, and Staying Put. *Molecular Cell* **49**, 808–824 (2013).
14. Kakarougkas, A. *et al.* Requirement for PBAF in Transcriptional Repression and Repair at DNA Breaks in Actively Transcribed Regions of Chromatin. *Mol. Cell* **55**, 723–732 (2014).
15. Shanbhag, N. M., Rafalska-Metcalf, I. U., Balane-Bolivar, C., Janicki, S. M. & Green-



- berg, R. A. ATM-Dependent chromatin changes silence transcription in cis to dna double-strand breaks. *Cell* **141**, 970–981 (2010).
16. Densham, R. M. *et al.* Human BRCA1-BARD1 ubiquitin ligase activity counteracts chromatin barriers to DNA resection. *Nat. Struct. Mol. Biol.* **23**, 647–55 (2016).
  17. Chapman, J. R., Taylor, M. R. G. & Boulton, S. J. Playing the End Game: DNA Double-Strand Break Repair Pathway Choice. *Molecular Cell* **47**, 497–510 (2012).
  18. Schwertman, P., Bekker-Jensen, S. & Mailand, N. Regulation of DNA double-strand break repair by ubiquitin and ubiquitin-like modifiers. *Nat Rev Mol Cell Biol* **17**, 379–394 (2016).
  19. McGinty, R. K., Henrici, R. C. & Tan, S. Crystal structure of the PRC1 ubiquitylation module bound to the nucleosome. *Nature* **514**, 591–6 (2014).
  20. Mattioli, F., Uckelmann, M., Sahtoe, D. D., van Dijk, W. J. & Sixma, T. K. The nucleosome acidic patch plays a critical role in RNF168-dependent ubiquitination of histone H2A. *Nat. Commun.* **5**, 3291 (2014).
  21. Leung, J. W. *et al.* Nucleosome Acidic Patch Promotes RNF168- and RING1B/BMI1-Dependent H2AX and H2A Ubiquitination and DNA Damage Signaling. *PLoS Genet.* **10**, e1004178 (2014).
  22. Stark, H. in 109–126 (2010). doi:10.1016/S0076-6879(10)81005-5
  23. Xu, X. Chemical Cross-linking Mass Spectrometry for Profiling Protein Structures and Protein-Protein Interactions. *J. Proteomics Bioinform.* **8**, (2015).
  24. Schmidt, C. & Robinson, C. V. A comparative cross-linking strategy to probe conformational changes in protein complexes. *Nat. Protoc.* **9**, 2224–2236 (2014).
  25. Groothuizen, F. S. *et al.* MutS/MutL crystal structure reveals that the MutS sliding clamp loads MutL onto DNA. *Elife* **4**, e06744 (2015).
  26. Friedhoff, P. *et al.* in *Methods in enzymology* **592**, 77–101 (2017).
  27. Streich, F. C. & Lima, C. D. Capturing a substrate in an activated RING E3/E2-SUMO complex. *Nature* **536**, 304–8 (2016).
  28. Olsen, S. K. & Lima, C. D. Structure of a ubiquitin E1-E2 complex: insights to E1-E2 thioester transfer. *Mol. Cell* **49**, 884–96 (2013).
  29. O'Connor, H. F. *et al.* Ubiquitin-Activated Interaction Traps (UBAITs) identify E3 ligase binding partners. *EMBO Rep.* **16**, 1699–1712 (2015).
  30. Long, L., Furgason, M. & Yao, T. Generation of nonhydrolyzable ubiquitin-histone mimics. *Methods* **70**, 134–138 (2014).
  31. Luger, K., Rechsteiner, T. J. & Richmond, T. J. in *Chromatin Protocols* **119**, 1–16 (Hu-

mana Press, 1999).

32. Popovic, D., Vucic, D. & Dikic, I. Ubiquitination in disease pathogenesis and treatment. *Nat. Med.* **20**, 1242–1253 (2014).
33. Buchwald, G. *et al.* Structure and E3-ligase activity of the Ring-Ring complex of polycomb proteins Bmi1 and Ring1b. *EMBO J.* **25**, 2465–74 (2006).
34. Luna-Vargas, M. P. A. *et al.* Enabling high-throughput ligation-independent cloning and protein expression for the family of ubiquitin specific proteases. *J. Struct. Biol.* **175**, 113–119 (2011).
35. Lowary, P. . & Widom, J. New DNA sequence rules for high affinity binding to histone octamer and sequence-directed nucleosome positioning. *J. Mol. Biol.* **276**, 19–42 (1998).





# Chapter 6

6

General discussion

Ubiquitination is a posttranslational modification that regulates a vast array of cellular signaling pathways. Ubiquitin is attached to specific lysine residues on target proteins following an enzymatic cascade including E1, E2 and E3 enzymes. Substrates can get monoubiquitinated or modified with ubiquitin chains of different linkage types by conjugating one ubiquitin to one of the available lysine residues on another. Depending on which residues are modified with which type of modification the signaling outcome can be very different. K48 chains, for example, lead to proteasomal degradation<sup>1</sup>. In the event of a DNA double strand break different monoubiquitination events and the formation of K63-linked chains are necessary to initiate and sustain the DNA damage response<sup>2,3</sup>.

Tight regulation of the ubiquitin system is crucial to prevent short-circuiting the cell. The right lysines need to be ubiquitinated at the right time to assure that proteins are only degraded when needed and signaling cascades are only initiated and propagated when appropriate. Selective modification of lysines is not only achieved by the intrinsic substrate preferences of the enzymes involved but also by the balance that is struck between ubiquitination and deubiquitination. The main players responsible for specificity of the system are E3 ligases and deubiquitinating enzymes (DUBs). The E3 ligases facilitate lysine selection for the ubiquitin conjugation reaction, the DUBs assure selective deubiquitination. Furthermore there is competition for access to substrates with other interacting proteins and cross-regulation through PTMs other than ubiquitination. Intrinsic substrate specificity, relative protein levels and cross-talk with other PTMs thus guide the lysine specific ubiquitination response. The focus of this thesis is on ubiquitination of histone H2A (H2A) and its role in regulating the DNA damage response. Three ubiquitination sites have been identified on H2A, lysines 13/15 (K15), lysines 118/119 (K119) and lysines 125/127/129 (K127)<sup>4-6</sup>. We address how the enzymes involved in ubiquitinating and deubiquitinating these sites achieve specificity and how this affects the double strand break response.

### **Specificity of E3 ligases**

In chapter 4 we studied the specific ubiquitination of K15 on H2A by the RING E3 ligase RNF168. We were able to show that the target, the nucleosome, plays a crucial role in this reaction<sup>7</sup>. An intact acidic patch on the nucleosome surface is necessary for efficient ubiquitination of K15. Charge-neutralizing mutations of five acidic residues on the nucleosome surface abolish K15 ubiquitination but, curiously, these mutations do not interfere with binding of RNF168 to the nucleosome. This suggests a more direct involvement of the substrate in the reaction. It seems the nucleosomal acidic patch participates in a form of substrate-assisted catalysis by promoting the discharge of ubiquitin from the charged E2 to the target lysine. How is this substrate assisted catalysis achieved? An intact acidic patch might be necessary to facilitate proper orientation of the E3-E2 complex towards the target lysine to

enable the nucleophilic attack on the thioester bond in the E2 active site after initial recognition of the nucleosome.

Another explanation for the disconnect between RNF168's recruitment and activity is a direct involvement of residues of the acidic patch in catalysis. In the most generic mechanism of substrate-assisted catalysis one residue on the target acts as active site residue in the enzyme<sup>8</sup>. The acidic patch on the nucleosome could potentially activate the target lysine, a task usually fulfilled by aspartic acid 117 (D117) of the E2<sup>9</sup>. The distance from the acidic patch to the target lysine however makes this an unlikely scenario unless a major conformational change were to occur that brings the lysine closer to the acidic patch. There is also no obvious reason why D117 should be impaired in its function in the UBCH5C-RNF168 complex as E3-E2 interaction sites are conserved among RING E3s<sup>10</sup>.

It seems more likely that the substrate organizes the correct positioning of the E2-E3-complex. A similar behavior has been observed for the APC/C complex, where the degron motif on the substrate enhances the catalytic rate of ubiquitination by facilitating a productive orientation of the enzyme<sup>11</sup>. Although in this case the degron motif also enhances affinities.

Substrate-assisted catalysis has been reported for various different enzyme-substrate complexes. It plays a role in the peptide bond formation catalyzed by the ribosome<sup>12,13</sup>, in GTPases<sup>8,14</sup>, mono-ADP-ribosylation<sup>15</sup> and restriction endonucleases<sup>8</sup>, among others. It might represent an evolutionary artifact of early catalytic mechanisms that have been replaced, for most reactions, by the evolution of highly specialized enzyme active sites<sup>12</sup>. Others suggest it as a mechanism for promiscuous enzymes to achieve a certain degree of substrate specificity<sup>16</sup>. This could be an attractive model for the ubiquitin system where E3 ligases are presented with the task of choosing the right residue to modify among the vast amount of potentially available lysines. A 'licensing' residue on the correct substrate could act as a safety check, preventing ubiquitination of unlicensed sites. This licensing residue could have an active role in catalysis (e.g. acting as a general base) or a more indirect function such as inducing conformational changes in the E3-substrate complex to allow conjugation.

#### **USP48 counteracts BRCA1 signaling and is regulated by an auxiliary ubiquitin**

In chapter 3 we test a subset of DUBs for specificity towards the three different ubiquitination sites on H2A. Most of the DUBs tested show little substrate preference, but USP48 turned out to be specific for the BRCA1 site. In vitro BRCA1 ubiquitinates three adjacent lysines (K125,127 and 129) on the nucleosome core particle (NCP). Kinetic modelling using the software *KinTek explorer*<sup>17,18</sup> allowed us to dissect USP48's activity towards NCPs with one, two or three independent lysines modified.

USP48 shows a clear preference for NCPs that are modified on more than one lysine, the activity towards monoubiquitinated NCPs is very low. The affinities of USP48 towards NCPs of different ubiquitination status are basically the same. This suggests a regulatory mechanism where an additional ubiquitin close to the target site is needed to activate USP48. We termed this an 'auxiliary ubiquitin' as it aids catalysis but does not get cleaved itself. It is not clear yet how USP48 activation is achieved. Repositioning of USP48 by the auxiliary ubiquitin towards the target ubiquitination site is one possible mechanism that might enhance catalytic rates. Another possibility is the release of autoinhibition, as has been shown for OTULIN, a DUB cleaving linear ubiquitin chains. In order to release autoinhibition the proximal ubiquitin of OTULIN's substrate needs to make specific contacts with the enzyme<sup>20</sup>. A similar relief of autoinhibition would be possible for USP48. Analogous to RNF168 activation by the acidic patch, activation of USP48 by the auxiliary ubiquitin is not achieved due to a change in affinities, indicating that a direct role of the substrate in ubiquitination reactions might be a more general feature in the ubiquitin system. The substrate could function by inducing catalytically competent conformations of the enzymes involved or could have a direct role in catalysis.

Another question that remains is where on H2A the auxiliary ubiquitin needs to be placed in order to activate. It could be on one specific, or any, of the three lysines of the BRCA1 site. Future research needs to establish if one of these lysines is designated for the auxiliary ubiquitin and another one acts as the signaling entity or if it is a random process where either one of two ubiquitinated lysines can activate cleavage of the other.

The identification of the auxiliary ubiquitin adds to the growing repertoire of regulatory mechanisms to modulate DUB activity<sup>21</sup>. USPs in particular seem to be in need of regulation as most are rather promiscuous with respect to their substrate choice. The work presented in chapter 3 shows that most of the USPs tested can cleave all three ubiquitination sites on H2A. When presented with di-ubiquitins of different linkage types as a substrate USPs are also not very selective<sup>22</sup>. It should be stressed though, that unspecific cleavage of di-ubiquitins does not necessarily mean that there is no specificity towards longer chains. The topology of longer chains cannot be accurately recapitulated by only two ubiquitins. Consequently, di-ubiquitins are missing features that may be crucial for specific recognition by DUBs. Studies on linkage preference of DUBs towards longer chains are needed to address this point. For USP48 it remains to be shown if the activation by an auxiliary ubiquitin is a substrate specific mechanism that only applies to the BRCA1 site on H2A, or a broader regulatory mechanism that allows USP48 to cleave different substrates with multi-monoubiquitinated lysines. A similar mechanism has been observed for USP14, which cleaves supernumerary chains (chains on at least two lysines on one substrate) of proteasome bound



substrates<sup>23</sup>, and it will be interesting to work out similarities and differences in activity regulation between these enzymes.

### **Regulation of the DNA damage response by site specific H2A ubiquitination**

Chapter 2 discusses how ubiquitination of different sites on the nucleosome guides the double strand break response. Very generally, ubiquitination of H2A by RNF168 on lysine 15 promotes repair through NHEJ, ubiquitination by BRCA1/BARD1 triggers HR-repair and PRC1 ubiquitination of lysine 119 leads to transcriptional silencing. USP48's involvement in this regulation illustrates nicely how site specificity of a deubiquitinating enzyme directly translates to a unique biological outcome. USP48 cleaves one of the three distinct ubiquitination sites on H2A, the BRCA1 site. By doing so it regulates the extent of DNA end resection, the first step in HR repair<sup>24</sup>. Loss of USP48 causes opposite phenotypes compared to loss of BRCA1 function, indicating that both enzymes work in the same pathway but in opposite directions. The function of BRCA1 is to promote DNA end-resection<sup>25</sup> while USP48 seems to limit it.

But how does site specific ubiquitination and deubiquitination of the nucleosome translate into regulation of DNA end-resection? One important mechanism is the recruitment of downstream effectors. K15 ubiquitination on H2A serves as a binding platform for 53BP1, a protein that acts as a DNA-end resection block, which promotes repair through NHEJ<sup>26,27</sup>. H2A ubiquitination by BRCA1 on the other hand recruits the chromatin remodeler SMARCAD1<sup>25</sup>, which leads to displacement of 53BP1 away from the break site. 53BP1 displacement allows long range resection, which promotes repair by HR. If SMARCAD1 is a direct interactor of ubiquitinated nucleosomes or if SMARCAD1 recruitment is dependent on additional mediators is not known.

In the model we propose in chapter 3, USP48 and BRCA1 are competing with each other to regulate HR by defining the length of resected DNA around a break site. The length of DNA-end resection is set by the extent of H2A ubiquitination on the BRCA1 site, which is defined by the relative activities of the specific E3 and DUB. Whenever possible, the preferred way of DNA double strand break repair is through gene conversion, the error-free and least mutagenic repair pathway<sup>28</sup>. For gene conversion to take place, DNA-end resection needs to be fine-tuned to a defined length. Resection should be long enough to allow homology search, but should not exceed a certain length to avoid mutagenic single strand annealing<sup>28</sup>. BRCA1 and USP48 likely play an important role in this fine tuning mechanism. This means the activity of both enzymes needs to be restricted to a defined area around the break site. Close to the break BRCA1 needs to be active to facilitate 53BP1 displacement and drive end-resection. USP48 needs to counteract BRCA1-induced H2A ubiquitination and establish

the resection block at a distance from the break far enough to allow gene conversion, but short enough to prevent single strand annealing. To achieve this, the activity of BRCA1 and USP48 must be tightly regulated, possibly on different levels. Selective recruitment to areas at a defined distance to the break, activity modulation by interacting proteins, and relative protein levels are likely candidate mechanisms for this regulation.

## 6

Our discovery of an auxiliary ubiquitin necessary for full USP48 activity opens up an interesting possibility for an alternative regulatory mechanism. It is tempting to speculate that this auxiliary ubiquitination might be placed on the polycomb site, on K119 of H2A. H2A ubiquitinated by PRC1 would then act as an on-switch to activate USP48 for cleavage of the BRCA1 ubiquitination site. It would be an elegant mechanism, where crosstalk between two different ubiquitination sites regulates the damage response, albeit conclusive experimental evidence for this mechanism is still missing. This crosstalk would also suggest that DNA-repair through HR pathways is shut down in polycomb-silenced areas of the genome. It is possible that in these areas the maintenance of the silenced state has top priority and overwrites the need for error-free DNA repair. BRCA1-induced ubiquitination and chromatin remodeling during HR repair might disrupt the silenced state of chromatin and as such may need to be disabled by K119 ubiquitination in polycomb-silenced regions.

**Targeting the ubiquitin system**

The lysine specificity of the ubiquitin system makes it an interesting drug target for precision medicine. At the same time it is hard to exploit this specificity for therapeutic purposes, as many signaling cascades are guided by RING E3 ligases, enzymes lacking an active site. Targeting E1 or E2 enzymes through their active sites has had some success<sup>29</sup> but E1s and E2s contribute to modification of a wide range of unrelated substrates which can give rise to unwanted side effects. To enable precision targeting of the ubiquitin system the lysine-specificity of the E3 ligases needs to be leveraged, a particular challenge if the enzyme to be targeted lacks an active site. Unique enzyme-substrate interaction sites or mechanisms of allosteric regulation could be exploited to interfere with RING E3 ligase activity. This has been a successful strategy to target the p53 pathway, where the small molecule nutlin-3a disrupts the interaction of p53 and MDM2<sup>30</sup>. Outside the ubiquitin field the remarkable success of BET-inhibitors shows not only the potential of targeting protein-protein interactions but also the importance of epigenetic modification as potential drug targets<sup>31-34</sup>. BET inhibitors prevent bromodomains from binding chromatin by mimicking the shape of acetylated lysines on histone tails, the natural binding partner of bromodomains<sup>33</sup>. To identify leverage points of this kind in the ubiquitin system, high resolution structures of E3-substrate and E3-interactor complexes are crucial. The trapping strategies that are presented in chapter 5 will help to solve structures of otherwise transient E3-substrate complexes and will help to

identify unique interaction sites.

As a whole, this thesis aims to help discern the rules governing site specific ubiquitination of H2A. We have provided tools that will help to solve structures of E3-substrate complexes and uncovered an active role of the substrate in the E3-ligase reaction. Our analysis of DUB specificity has shown an intriguing mechanism of USP48 activity regulation by ubiquitin itself. Building and expanding on these early results it may at some point be possible to identify the ‘Achilles heel’ of different H2A ubiquitination and deubiquitination reactions and exploit those weaknesses for therapeutic intervention.

## References

1. Chau, V. *et al.* A multiubiquitin chain is confined to specific lysine in a targeted short-lived protein. *Science* **243**, 1576–83 (1989).
2. Schwertman, P., Bekker-Jensen, S. & Mailand, N. Regulation of DNA double-strand break repair by ubiquitin and ubiquitin-like modifiers. *Nat Rev Mol Cell Biol* **17**, 379–394 (2016).
3. Uckelmann, M. & Sixma, T. K. Histone ubiquitination in the DNA damage response. *DNA Repair (Amst)*. (2017). doi:10.1016/j.dnarep.2017.06.011
4. Kalb, R., Mallery, D. L., Larkin, C., Huang, J. T. J. & Hiom, K. BRCA1 is a histone-H2A-specific ubiquitin ligase. *Cell Rep.* **8**, 999–1005 (2014).
5. Mattioli, F. *et al.* RNF168 ubiquitinates K13-15 on H2A/H2AX to drive DNA damage signaling. *Cell* **150**, 1182–1195 (2012).
6. Wang, H. *et al.* Role of histone H2A ubiquitination in Polycomb silencing. *Nature* **431**, 873–8 (2004).
7. Mattioli, F., Uckelmann, M., Sahtoe, D. D., van Dijk, W. J. & Sixma, T. K. The nucleosome acidic patch plays a critical role in RNF168-dependent ubiquitination of histone H2A. *Nat. Commun.* **5**, 3291 (2014).
8. Dall’Acqua, W. & Carter, P. Substrate-assisted catalysis: molecular basis and biological significance. *Protein Sci.* **9**, 1–9 (2000).
9. Plechanovová, A., Jaffray, E. G., Tatham, M. H., Naismith, J. H. & Hay, R. T. Structure of a RING E3 ligase and ubiquitin-loaded E2 primed for catalysis. *Nature* **489**, 115–120 (2012).

10. Metzger, M. B., Pruneda, J. N., Klevit, R. E. & Weissman, A. M. RING-type E3 ligases: Master manipulators of E2 ubiquitin-conjugating enzymes and ubiquitination. *Biochim. Biophys. Acta - Mol. Cell Res.* **1843**, 47–60 (2014).
11. Van Voorhis, V. A. & Morgan, D. O. Activation of the APC/C Ubiquitin Ligase by Enhanced E2 Efficiency. *Curr. Biol.* **24**, 1556–1562 (2014).
12. Weinger, J. S., Parnell, K. M., Dorner, S., Green, R. & Strobel, S. A. Substrate-assisted catalysis of peptide bond formation by the ribosome. *Nat. Struct. Mol. Biol.* **11**, 1101–1106 (2004).
13. Pankaz K. Sharma, Yun Xiang, Mitsunori Kato, and & Warshel\*, A. What Are the Roles of Substrate-Assisted Catalysis and Proximity Effects in Peptide Bond Formation by the Ribosome?. (2005). doi:10.1021/BI0509806
14. Schweins, T. *et al.* Substrate-assisted catalysis as a mechanism for GTP hydrolysis of p21ras and other GTP-binding proteins. *Nat. Struct. Biol.* **2**, 36–44 (1995).
15. Kleine, H. *et al.* Substrate-Assisted Catalysis by PARP10 Limits Its Activity to Mono-ADP-Ribosylation. *Mol. Cell* **32**, 57–69 (2008).
16. Yao, J. *et al.* Substrate-Assisted Catalysis in the Reaction Catalyzed by Salicylic Acid Binding Protein 2 (SABP2), a Potential Mechanism of Substrate Discrimination for Some Promiscuous Enzymes. *Biochemistry* **54**, 5366–5375 (2015).
17. Johnson, K. A., Simpson, Z. B. & Blom, T. Global Kinetic Explorer: A new computer program for dynamic simulation and fitting of kinetic data. *Anal. Biochem.* **387**, 20–29 (2009).
18. Johnson, K. A., Simpson, Z. B. & Blom, T. FitSpace Explorer: An algorithm to evaluate multidimensional parameter space in fitting kinetic data. *Anal. Biochem.* **387**, 30–41 (2009).
19. Faesen, A. C. *et al.* Mechanism of USP7/HAUSP Activation by Its C-Terminal Ubiquitin-like Domain and Allosteric Regulation by GMP-Synthetase. *Mol. Cell* **44**, 147–159 (2011).
20. Keusekotten, K. *et al.* OTULIN antagonizes LUBAC signaling by specifically hydrolyzing Met1-linked polyubiquitin. *Cell* **153**, 1312–26 (2013).
21. Sahtoe, D. D. & Sixma, T. K. Layers of DUB regulation. *Trends in Biochemical Sciences*

- 40**, 456–467 (2015).
22. Faesen, A. C. *et al.* The Differential Modulation of USP Activity by Internal Regulatory Domains, Interactors and Eight Ubiquitin Chain Types. *Chem. Biol.* **18**, 1550–1561 (2011).
  23. Lee, B.-H. *et al.* USP14 deubiquitinates proteasome-bound substrates that are ubiquitinated at multiple sites. *Nature* **532**, 398–401 (2016).
  24. Chapman, J. R., Taylor, M. R. G. & Boulton, S. J. Playing the End Game: DNA Double-Strand Break Repair Pathway Choice. *Molecular Cell* **47**, 497–510 (2012).
  25. Densham, R. M. *et al.* Human BRCA1-BARD1 ubiquitin ligase activity counteracts chromatin barriers to DNA resection. *Nat. Struct. Mol. Biol.* **23**, 647–55 (2016).
  26. Zimmermann, M. & De Lange, T. 53BP1: Pro choice in DNA repair. *Trends in Cell Biology* **24**, 108–117 (2014).
  27. Fradet-Turcotte, A. *et al.* 53BP1 is a reader of the DNA-damage-induced H2A Lys 15 ubiquitin mark. *Nature* **499**, 50–54 (2013).
  28. Ceccaldi, R., Rondinelli, B. & D'Andrea, A. D. Repair Pathway Choices and Consequences at the Double-Strand Break. *Trends in Cell Biology* **26**, 52–64 (2016).
  29. Huang, X. & Dixit, V. M. Drugging the undruggables: exploring the ubiquitin system for drug development. *Cell Res.* **26**, 484–498 (2016).
  30. Vassilev, L. T. *et al.* In Vivo Activation of the p53 Pathway by Small-Molecule Antagonists of MDM2. *Science (80-. ).* **303**, 844–848 (2004).
  31. Dawson, M. A. *et al.* Inhibition of BET recruitment to chromatin as an effective treatment for MLL-fusion leukaemia. *Nature* **478**, 529–33 (2011).
  32. Filippakopoulos, P. & Knapp, S. Targeting bromodomains: epigenetic readers of lysine acetylation. *Nat. Rev. Drug Discov.* **13**, 337–356 (2014).
  33. Filippakopoulos, P. *et al.* Selective inhibition of BET bromodomains. *Nature* **468**, 1067–73 (2010).
  34. Picaud, S. *et al.* PFI-1, a highly selective protein interaction inhibitor, targeting BET Bromodomains. *Cancer Res.* **73**, 3336–46 (2013).



# Addendum

Summary

Samenvatting

Curriculum vitae

PhD portfolio

List of Publications



## Summary

Ubiquitination describes the conjugation of the small protein ubiquitin to a target protein lysine residue, following an enzymatic cascade involving three different groups of enzymes, ubiquitin activating enzymes (E1), ubiquitin conjugating enzymes (E2) and ubiquitin ligases (E3). Ubiquitination can be lysine specific and specificity is conferred by the E3 ligases. Ubiquitination of histone H2A is one of the many different posttranslational modifications guiding the DNA damage response. H2A can get ubiquitinated at three distinct groups of lysines by three different E3 ligases. RNF168 ubiquitinates lysine 15, RING1B/BMI1 in a PRC1 complex ubiquitinates lysine 119 and BRCA1/BARD1 ubiquitinates lysines 125/127 and 129. Which particular site is modified in a given situation will determine downstream signaling. The work presented in this thesis provides conceptual and mechanistic insights into the biology of lysine specific H2A ubiquitination and deubiquitination.

&

**Chapter 2** reviews the current understanding of the biology of H2A ubiquitination. We describe how site specificity is achieved on a molecular level and how ubiquitination on the three different sites will trigger different signaling pathways. We describe readers, writers and erasers of H2A ubiquitination and put forward a concept of signal integration, where the final biological outcome is determined through integration over the three ubiquitination sites and in crosstalk with other posttranslational modifications.

Since the E3 ligases acting on H2A show such a remarkable site specificity we decided to study lysine selective deubiquitination of DUBs acting on H2A. In **chapter 3** we tested a subset of DUBs and find USP48 to be specific for the BRCA1 site on H2A. We show that USP48 knockdown results in increased DNA end resection and increased 53BP1 foci formation, opposite phenotypes compared to the loss of BRCA1. USP48 knockdown only has an effect if BRCA1 is active, indicating that both work in the same pathway. Our accumulating evidence suggests a model where BRCA1 drives DNA end-resection by ubiquitinating H2A and USP48 counteracts this activity. On a mechanistic level we describe a novel way of regulating USP48's activity through an 'auxiliary ubiquitin'. This auxiliary ubiquitin needs to be placed adjacent to USP48's target ubiquitination site in order for the enzyme to be fully active. The auxiliary ubiquitin does not get cleaved itself.

In **chapter 4** we study ubiquitination of H2A on lysine 15 by RNF168 and describe an active role of the substrate in the ubiquitination reaction. An intact acidic patch on the nucleosome surface is necessary for efficient ubiquitination of lysine 15. Disruption of the acidic patch results in loss of RNF168 activity but does not abolish binding. This suggests a form of substrate assisted catalysis where the acidic patch on the nucleosome functions either by repositioning the enzyme after initial binding or by actively participating in catalysis.

High resolution structures of E3-substrate complexes are important to understand the molecular mechanisms that determine lysine specificity. These complexes, however, are mostly transient in nature, which makes them hard to analyze with current methods of structural biology where sample heterogeneity is a disadvantage. In **chapter 5** we describe methods to stabilize E3-substrate complexes using crosslinking strategies and fusion proteins.

**Chapter 6** discusses the results presented in this thesis, puts them in a broader perspective and points out future directions. In summary, this thesis contributes mechanistic insight into site specific ubiquitination of H2A and illustrates how modification of selective lysines can translate into regulation of the DNA damage response.



## Samenvatting

*Ubiquitination* is het koppelen van het kleine eiwit ubiquitine aan een lysine van een ander eiwit, het zogenoemde *target* eiwit. Deze ubiquitinatie wordt uitgevoerd door een enzymatisch stappensysteem met drie verschillende groepen eiwitten: ubiquitine activerende enzymen (E1), ubiquitine conjugerende enzymen (E2) en ubiquitine ligases (E3). Het koppelen of conjugeren van ubiquitine aan een bepaalde lysine kan heel precies gebeuren en deze specificiteit wordt gereguleerd door de E3 ligases.

Ubiquitinatie van het histoneiwit H2A is een van de vele verschillende, posttranslationele modificaties die de signalering bij DNA schade dirigeren. H2A kan worden ubiquitineerd op drie verschillende groepen lysines door drie verschillende E3 ligases. RNF168 ubiquitineert lysine 15 (K15), RING1B/BMI1 uit het PRC1 complex ubiquitineren lysine 119 (K119) en het complex met BRCA1 en BARD1 kunnen lysines 125, 127 en 129 van een ubiquitinmodificatie voorzien. Welke lysine er precies wordt ubiquitineerd hangt af van de situatie en is van belang voor de daaropvolgende signalering. Het werk in deze thesis geeft zowel conceptuele als mechanistische inzichten in de biologie van de lysine-specificiteit van H2A-ubiquitinatie en –deubiquitinatie.

**Hoofdstuk 2** geeft een overzicht van de huidige staat van het onderzoek naar de biologie achter H2A ubiquitinatie. We beschrijven op moleculair niveau hoe de specificiteit voor een bepaalde lysine wordt bereikt en wat de gevolgen zijn van deze ubiquitinatie voor de daaropvolgende signaleringscascades van elk van de drie mogelijke ubiquitinatieplekken. We beschrijven eiwitten die de ubiquitinatie kunnen uitlezen, aanbrengen of juist verwijderen en postuleren een model hoe deze signalen in het grote geheel passen. Dit model beschrijft hoe de biologische uitkomst wordt bepaald door samenspel van de drie ubiquitinatieplekken naast andere posttranslationele modificaties.

Aangezien de E3 ligases een opmerkelijke specificiteit hebben voor een bepaalde ubiquitinatieplek wilden we onderzoeken of het verwijderen van de ubiquitine van H2A door deubiquitinerende enzymen (DUBs) ook zo specifiek is. In **hoofdstuk 3** hebben we hiervoor een subset van verschillende DUBs getest en vonden we dat USP48 specifiek is voor de plek die door BRCA1 wordt geubiquitineerd. We laten zien dat het uitschakelen (knockdown) van USP48 in de cel zorgt voor langere resectie van het DNA einde en een verhoging in de formatie van 53BP1 *foci*: beide observaties zijn tegengesteld aan het fenotype dat wordt geobserveerd als BRCA1 is verwijderd uit de cel. Het uitschakelen van USP48 in de cel heeft alleen effect als BRCA1 actief is, iets wat aangeeft dat beide in dezelfde signaleringscascade werken. Deze observaties tezamen leiden tot een model waarin BRCA1 de resectie van DNA-eindes aanjaagt en waarin USP48 deze activiteit tegengaat. Verder hebben we ontdekt hoe de activiteit van USP48 op een mechanistisch niveau wordt gereguleerd door een extra ubiquitine als hulpmiddel. Deze ‘hulpubiquitine’ moet dichtbij de locatie van het doelwit van USP48, de BRCA1 ubiquitinatieplek, zitten om ervoor te zorgen dat USP48 volledig actief is en wordt hierbij niet zelf verwijderd van zijn lysine.

In **hoofdstuk 4** bestuderen we hoe RNF168 lysine 15 van histon H2A ubiquitineert en beschrijven we de belangrijke rol van het substraat in de ubiquitinatiereactie. Een regio op het nucleosoom met vele negatief geladen aminozuren (*acidic patch*) blijkt essentieel om de ubiquitinatie op lysine 15 efficiënt te laten verlopen. Als deze regio wordt ontworpen vernietigt dat de ubiquitinatie-activiteit van RNF168 alhoewel RNF168 nog wel kan binden. Dit suggereert een type katalyse waarbij het substraat meehelpt aan de reactie. De *acidic patch* op het nucleosoom kan hierbij helpen door het enzym goed te positioneren na de initiële binding of door actief mee te helpen aan de katalyse.



Om de moleculaire mechanismen achter de lysinespecificiteit te begrijpen zijn structuren, het liefst hoge resolutie, van complexen van E3s met substraat van groot belang. Deze complexen bestaan vaak echter maar kortstondig; dit maakt het bestuderen ervan erg lastig. Bij de huidige methoden in de structuurbiologie is heterogeniteit een groot nadeel. In **hoofdstuk 5** beschrijven we manieren om de E3-substraat complexen te stabiliseren door de eiwitten chemisch aan elkaar te conjugeren of door het creëren van fusie-eiwitten.

In **hoofdstuk 6** worden tenslotte de resultaten uit dit proefschrift bediscussieerd en bekeken in een bredere context. Dit resulteert ook in mogelijke (onderzoeks)richtingen voor de toekomst. Samenvattend: deze thesis draagt bij aan het begrip en inzicht in de mechanismen achter de specifieke ubiquitinatie van H2A en illustreert hoe deze specifieke modificatie zich vertaalt naar de regulatie van de cellulaire respons op DNA schade.

&

### **Curriculum vitae**

Michael Uckelmann was born November 28<sup>th</sup>, 1984 in Rheda-Wiedenbrück, Germany. He was awarded the Abitur from the Thomas-Morus Gymnasium in Oelde in 2004 and started to study biology at the Justus-Liebig University of Giessen in 2005. In 2008 he was awarded the Bachelor degree in biology and enrolled in the Master of Biology program of the Justus-Liebig University in Giessen. He was awarded the Master degree in 2010. During his Bachelor and Master studies Michael did research internships in the group of Prof. Peter Friedhoff where he worked on the biochemical characterization of enzymes of the mismatch repair pathway. In 2011 he joined the group of Prof. Titia Sixma at the Netherlands Cancer Institute in Amsterdam for his doctoral studies where he combined structural and biochemical methods to study lysine specificity of E3 ligases and deubiquitinating enzymes in the ubiquitin system. The results of this research are presented in this thesis.



## PhD portfolio

Name of the PhD student: Michael Uckelmann  
Erasmus MC Dept.: Genetics  
Graduate School: Onderzoekschool Oncologie Amsterdam  
PhD period: 2011 – 2017  
Promotor: Prof.dr. Titia K. Sixma

### 1. PhD training

#### *Courses*

2011 OOA experimental oncology, Amsterdam

2014 Replication stress and chromosomal instability, Amsterdam  
2014 English writing and presenting, Amsterdam

2015 Epigenetics and non-coding RNA, Amsterdam

#### *Seminars and workshops*

2011 – 2013 OOA PhD student retreat (Poster/oral presentation)  
2011 – 2017 NKI research club meeting (oral presentation)  
2011 – 2017 Weekly division research meeting (oral presentations)  
2011 – 2017 International NKI seminar, lunch meetings with speakers  
2017 Cancer Genomics Centre, annual meeting (oral presentation)

#### *(Inter-)national conferences*

2011 Rubicon, Malta (Poster)  
2011 CHAINS2011, Maarssen  
2012 ZOMESVII, Munich (Poster)  
2012 CW “Chemistry in relation to Biology”, Veldhoven (Poster)  
2013 CW “Chemistry in relation to Biology”, Veldhoven (oral presentation)  
2014 Benzon foundation ubiquitin meeting, Copenhagen (Poster)  
2016 GRC Chromatin Structure and Function, Les Diableretes (Poster)

### 2. Teaching

2012 Supervision Bachelor student  
2013 Supervision Master student

&

**List of Publications**

**M Uckelmann\***, RM Densham\*, R Baas, HHK Winterwerp, A Fish, TK Sixma, JR Morris *USP48 restrains resection by site specific cleavage of the BRCA1 ubiquitin mark from H2A*. Manuscript in revision, Nature Communications, \*Authors contributed equally

**Uckelmann M**, Sixma TK. *Histone ubiquitination in the DNA damage response*. DNA Repair (Amst). 2017 Aug;56:92-101.

Thorslund T, Ripplinger A, Hoffmann S, Wild T, **Uckelmann M**, Villumsen B, Narita T, Sixma TK, Choudhary C, Bekker-Jensen S, Mailand N. *Histone H1 couples initiation and amplification of ubiquitin signaling after DNA-damage*. Nature. 2015 Nov 19;527(7578):389-93.

Mattiroli F\*, **Uckelmann M\***, Sahtoe DD, van Dijk WJ, Sixma TK. *The nucleosome acidic patch plays a critical role in RNF168-dependent ubiquitination of histone H2A*. Nat Commun. 2014;5:3291. \*Authors contributed equally

Pillon MC, Lorenowicz JJ, **Uckelmann M**, Klocko AD, Mitchell RR, Chung YS, Modrich P, Walker GC, Simmons LA, Friedhoff P, Guarné A. *Structure of the endonuclease domain of MutL: unlicensed to cut*. Mol Cell. 2010 Jul 9;39(1):145-51.



## Acknowledgements

This thesis would not have been possible without the help, directly or indirectly, of many different people.

First of all thank you very much Titia. Thanks for taking a chance on that slightly strange guy with a degree from the prestigious university of Giessen. Thank you for being an excellent supervisor along the way, giving guidance when needed, for valuable advice and for allowing me the freedom to follow up on my own ideas. I learned a lot in the last couple of years and in no small part thanks to you. Also, thanks for those English grammar lessons...

&

Thanks to Peter, my supervisor during my MSc thesis, for laying the foundations of my scientific education and part of my life, I suppose. After all, I would not be in Amsterdam without you. Thanks also to the members of my PhD committee Fred and Jacques for helpful advice.

Most of this work would have been impossible without great collaborators. A big thanks to Ruth and Jo over in Birmingham for the massive amount of work you did on the USP48 project, you made it possible. Also thanks to Hugo and Velten for our great collaboration on the RNF168 project.

By making this such a great department to work for the people of B8 played a big part in the success of this work. A special thanks to Sasha, whom I knew before I even came to Amsterdam and who is a constant source of encyclopedic knowledge of biophysics. I will miss our constant discussions, even those about science. What am I supposed to do if there is no one to wind me up anymore at my next job? Thanks Tassos for good advice and new ideas from a (sometimes) different angle and enjoyable conversations over a beer. Thanks Pim for running the lab so smoothly and good luck to Yvette for continuing that in the future. Thanks Herrie for all the help in the last few years and for tackling those nasty nucleosome preps. Again, good luck to John with continuing it. And thanks to Patrick for great advice on anything protein.

Some special thanks to former lab members/friends that have moved on but are not forgotten. Thanks Marcello and Danny for our good times together, I sincerely hope us three will never work in the same place again. Fra, I learned so much from you over the years, thanks for everything and welcome back to the Netherlands. Mariano, Jens, Florian, Anas, Nicholas and Christophe, thanks for great times in and outside the lab. Thanks Judith and Rick for giving me an introduction to the lab some seven years ago, Kash, Elli and Flora for being a great source of crystallographic knowledge. Thanks Tati for taking care of pretty much everyone and everything without ever losing your temper or your cheerful nature.

Thanks also to the people who joined after me. Andrea, I hope you won't be haunted by too many cryo-nightmares in the future. Robbert, it's almost your turn so just hang in there and special thanks for being my paranimf. Shreya, all the best to you and keep your head up high. A special mention to Roy for spotting the USP48 isoform issue. Xiaohu, our time working together so far has been a real joy. Hans, thanks for the help with the EM. Thanks to all the rest of the Sixma/Perrakis gang, Willem, Bart, Doreth, Susanne, Fernando, Luca, Nassos, George, Robbie, Yoshi, Misbha, Torben, Ismael, Mirna for the enjoyable work atmosphere and fun times at the borrel. Thijn and the crew, Jacqueline, Vincent, Joppe, Markus, Lisa, Lucas, Abdelghani, Elmer, Astrid, it's a real pleasure to see your projects taking shape. Thanks for the good advice and great company.



Many thanks to all my friends outside work who helped me preserve my sanity and made this experience in Amsterdam so much more enjoyable. Thanks Cesare for being such a good friend and roommate. Thanks Santi for being a great friend, best man, paranimf and business partner (a man of many talents). Thanks Anais, Alessandra, Petrit, Alvaro, Jacobien, Kong, Sedef, Judith, Flo, Renato, Lorenzo and Pavel, I'd find something nice to say about each of you but space is limited and it is getting late. Rest assured you're all awesome. Same goes for the old friends from Germany, Christian (the other great witness) and Steffie, Moritz, Monja, Lilly, Sonja, Paddy, Jo, Mathis, Verena, Thomas. I'm fortunate to call all of you my friends.

Thanks also to those equally awesome new friends and family members I gained through marriage. Femke (not only a great friend but also a great master of ceremony) and Michel, no matter where, Amsterdam, Singapore or even Merenberg, we'll always have a good time. Thanks Merel, Leonie and Ramon for many relaxed dinners with that occasional bottle of wine (Ramon, if all goes downhill we'll still have that alternative business plan). Lora and Thomas, we see you guys too little really but if we do it's always a pleasure. Tesse, please write your book already. Loes and Eric, Annemien, Wessel and Marloes, I am glad to have met you all. A massive special thanks to Yme for throwing a party and to Aniek for remembering.

Thanks to my parents, Dank an meine Eltern für den unermüdlichen Einsatz und grenzenloses Vertrauen. Ohne euch wäre ich nicht da wo ich heute bin.

Saving the best for last, thanks to the most important person of all, Jitske, without whom I'm not sure where I would be right now. Thanks for tolerating a scientist (in opleiding) in your life. Thanks for supporting me all the way. Thanks for believing in me no matter what and thanks for enduring me constantly changing the plans for our future. Can't wait to spend the rest of my life with you. Until a coconut will end it all.

&